Understanding and improving thermosensitive smart drug delivery system

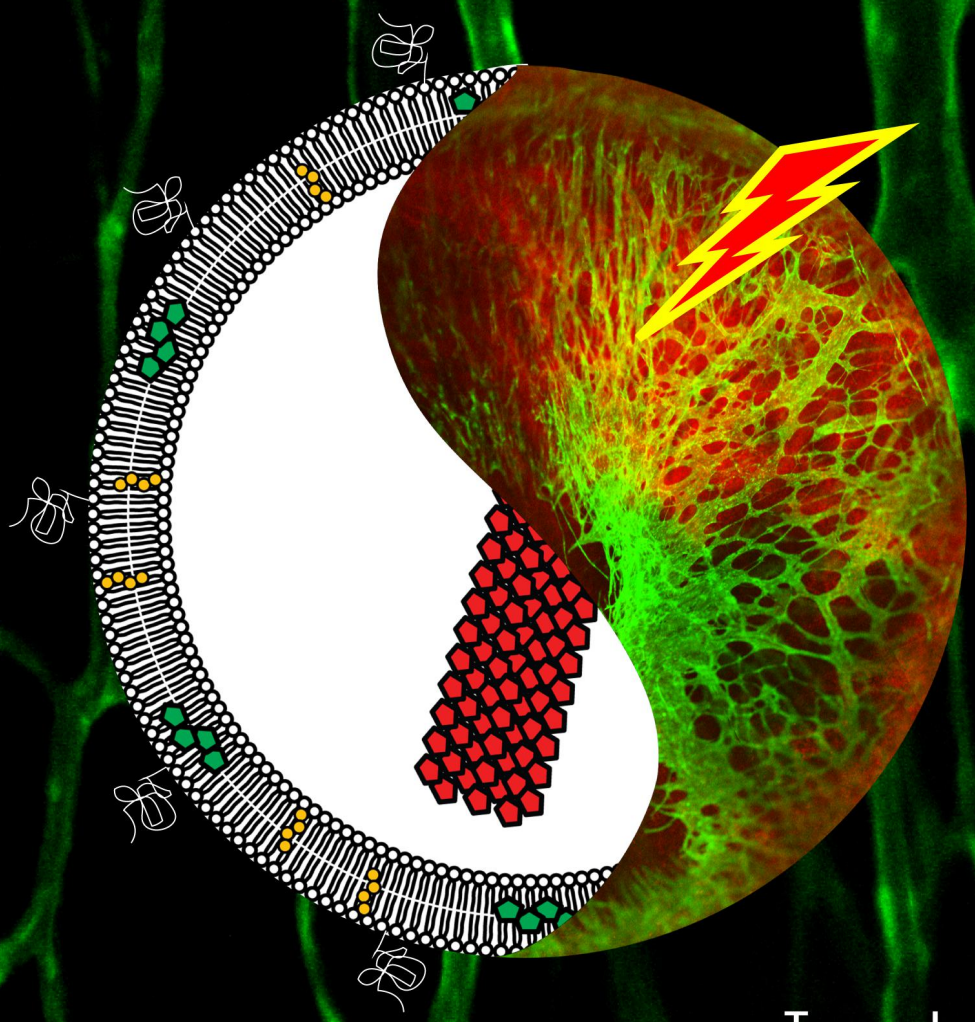

Tao Lu
鲁涛 著

Understanding and improving thermosensitive smart drug delivery systems

Tao Lu

The author appreciates the kind support for printing this thesis from:

Lipoid

Erasmus University Rotterdam

The research for this thesis was performed in the Department of Surgical Oncology, Erasmus MC, Rotterdam, the Netherlands.

Layout, Cover and Bookmark design by Tao Lu

Cover information:

Front page: Liposomal drug (cartoon) combined with microscopic tumor vessel for hyperthermia triggered release.
Background: Before hyperthermia, no drug (red) is released in tumor vessel (green).
Back page: After hyperthermia, drug (red) is released from liposome and taken up by tumor vessel and cells.

Copyright © 2019 by Tao Lu. All rights reserved. No part of this publication may be reproduced or transmitted in any form or by any means, electronic or mechanical, including photocopy, recording, or any information storage and retrieval system, without permission in writing from the author.

ISBN: 978-94-028-1550-4

Printed by Ipskamp Printing

Understanding and improving thermosensitive smart drug delivery systems

Het begrijpen en verbeteren van temperatuurgevoelige slimme drug delivery systemen

Thesis

To obtain the degree of Doctor from the
Erasmus University Rotterdam
by command of the rector magnificus
Prof. dr R.C.M.E. Engels
and in accordance with the decision of the Doctoral Board.

The public defence shall be held on

Friday 14th June 2019 at 13:30 hrs

By

Tao Lu

born in Hefei, Anhui, China

Erasmus University Rotterdam

Doctoral Committee

Promotor:	Prof. dr A.B. Houtsmuller
Copromotor:	Dr. T.L.M. Ten Hagen
Other members:	Prof. dr C.W.G.M. Löwik
	Prof. dr G. Storm
	Prof. dr N. de Jong

To my family

Contents

Chapter 1	General introduction	1
Chapter 2	Formulation and optimization of idarubicin thermosensitive liposomes provides ultrafast triggered release at mild hyperthermia and improves tumor response	21
Chapter 3	Thinking out of nanoparticle: Externally triggered smart drug delivery systems demand chemotherapeutics with kinetics superior for local delivery	61
Chapter 4	Inhomogeneous crystal grain formation in DPPC-DSPC based thermosensitive liposomes determines content release kinetics	91
Chapter 5	A novel kinetic model to describe the release of trigger-responsive drug delivery systems	121
Chapter 6	Discussion and Summary	141
Chapter 7	Samenvatting / Dutch summary	169
	Dankwoord / Acknowledgements	174
	List of publications	178
	PhD portfolio	180
	Curriculum Vitae	183

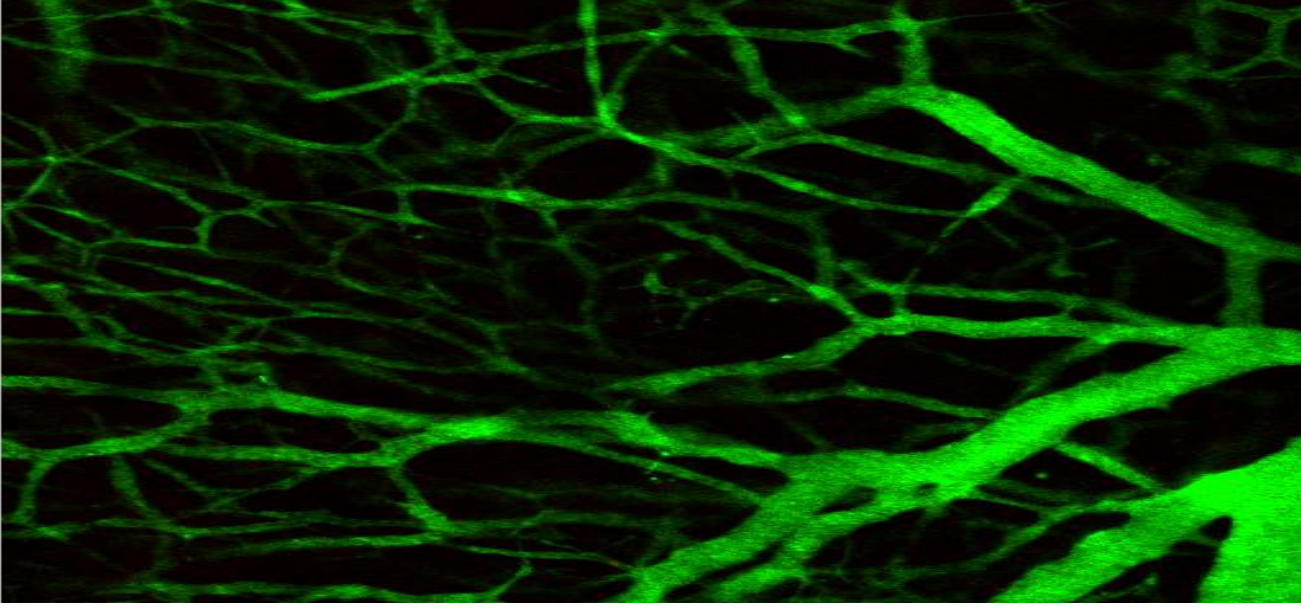

Chapter 1

Introduction

Solid cancers and treatment

Cancer is becoming the leading cause of death in the world and gaining impact fast in developing countries [1, 2], of which solid tumors are a significant part. Unlike normal tissue or organs, solid tumors are poorly structured as a result of fast proliferation of cancer cells, leading to an abnormal vasculature system. Tumor-associated vasculature exhibits a lack of hierarchical branching in which the recognizable features of arterioles, venules and capillaries are lost. The vessels are tortuous and unevenly dilated. Therefore, tumor blood flow is chaotic, can be stationary and even change direction of flow [3]. This results in interstitial hypertension, hypoxia, hypoperfusion and acidosis in solid tumors. Together, the factors cause solid tumor to have a complex microenvironment and provide unique biochemical and physiological properties, which cause barriers to treatment of solid cancers.

Classical cancer therapies widely used in the clinic include surgical intervention, radiotherapy and chemotherapy or a combination of these options. Surgery, used to prevent or lower the risk of developing certain types of cancer, is a common option in cancer treatment. Surgery is most effective when completely removing cancerous tissues that are at an early stage and have not spread to other parts of the body. However, in some cases, cancer tissue are not possible to be removed by surgery because of patient's health state or vital organs involved [4, 5]. Often radiotherapy or/and chemotherapy are given when surgery is not applicable or not necessary. Radiotherapy relies on the high doses of radiation to damage the DNA, thereby killing cancer cells. The cancer cells are less capable of recovering from the damage induced by radiation compared to healthy cells. But the side effects induced by radiation can limit the dose and may induce a secondary cancer. Besides, the lack of enough oxygen in solid tumors also affect the efficacy of radiotherapy as molecular oxygen is a potent radiosensitizer [6]. Chemotherapy is another important treatment option for cancer (Table 1). It makes use of cytotoxic agents to attack rapidly proliferating cells such cancerous cells, thus suppressing cancer

development [7]. However, some healthy cell types have fast proliferating rates as well, including bone marrow cells, intestinal cells and hair follicles, hence these toxic agents can cause severe side effects in those healthy tissues. In addition, due to that most cytotoxic compounds are not that selective and administrated in a free form, conventional chemotherapy requires a high dose to reach a therapeutic concentration at tumors. Together with the often large volume of distribution, meaning that the drug ends up in most parts of the body, leads to dose-limiting and possibly life-threatening systemic toxicity. For instance, doxorubicin (DXR), an anthracycline, has a wide antitumor spectrum which is one of the most widely used chemotherapeutic drugs for cancer treatment [8]. DXR can effectively kill cancer cells by intercalating with DNA, but its severe myelosuppression and cardiotoxicity limits the clinical use when giving in a free form. Idarubicin, another anthracycline drug, has been reported with the same antitumor mechanism but less cardiotoxicity and higher cytotoxicity compared to DXR [9, 10]. However, the short circulation time of IDA in blood hardly leads to effectiveness in most solid tumors but induces side effects in healthy tissues [11], which is used only as a second-line chemotherapeutic drug for leukemia in the clinic at present [12, 13].

Another hot therapy for cancer nowadays is immunotherapy, including the application of immune checkpoint inhibitor (e.g. PD 1/PD-L1 inhibitor) and adoptive T cell transfer (e.g. Car-T and TCR-T) [14, 15]. Cancer immunotherapy aims to activate or enhance the ability of the host immune cells against tumor (e.g. blocking the immunosuppression in tumor or modifying T cells), thus specifically killing cancer cells. This is expected to reduce side-effects resulted from conventional radio-/chemotherapy. Immunotherapies showed promising efficacy on some patients, however the extremely high cost (over $200,000/year per patient [16, 17]) and limited cancer type that can be beneficial from immunotherapy, make cancer immunotherapy difficult before it can be widely applied in the clinic.

These conventional therapies are not cancer specific and expose a risk to patients because of the side effects on healthy tissues. Because of these reasons, novel and more targeted therapies on cancer treatment are necessary to be investigated.

Table 1. Examples of commonly used chemotherapeutics in the clinic

Types of commonly used chemotherapeutics	Examples
Alkylating agents	Cisplatin, Melphalan, Ifosfamide
Alkaloids	Vincristine, Paclitaxel, Tenisopide
Antitumor antibiotics	Doxorubicin, Mitomycin, Idarubicin
Antimetabolites	Methotrexate, 5-Fluorouracil, Gemcitabine

Liposomal chemotherapy for solid cancers treatment

Due to the severe systemic toxicity induced by traditional chemotherapeutic drugs to healthy tissues, nano-sized drug carriers are developed to encapsulate cytotoxic compounds. Liposomes have been one of the best studied drug delivery systems used in cancer treatment since the1970s [18]. Liposomes are potent biocompatible nano-sized carriers, composed of different phospholipids with or without cholesterol, forming hollow vesicles with aqueous core and hydrophobic bilayer (Figure 1), which can load chemical compounds, genetic materials and contrast agents for delivery [19]. Nowadays there have been many liposomal products with size at around 100 nm either commercially available or under clinical trials [20]. After encapsulation by these liposomes, cytotoxic compounds avoid the direct contact with healthy tissue during delivery and circulate longer when liposomes are coated with a polyethyleneglycol (PEG). It is believed, although quite under debate,

that chemotherapeutic compounds accumulate more in tumors based on the enhanced permeability and retention (EPR) effects [21, 22] as a result of the loose and chaotic structure of tumor vasculature, which leads to gaps between endothelial cells that allow these nanoparticles to passively accumulate in tumoral interstitial space [23].

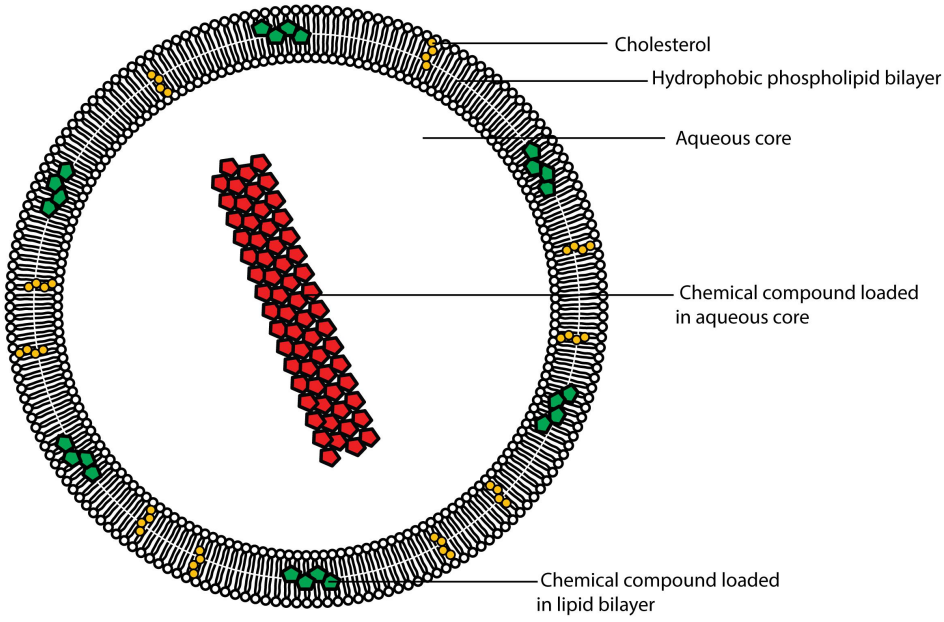

Figure 1. schematic representation of a liposome. The liposome is a hollow vesicle with aqueous core and hydrophobic phospholipid bilayer. The liposomal bilayer consists of different phospholipids and cholesterol can be added. Hydrophilic drugs can be encapsulated inside aqueous compartment and hydrophobic compounds can be loaded in the bilayer.

A well-known and most widely used liposomal chemotherapeutic is Doxil® (Caelyx® in Europe), a pegylated liposome with size at 90 nm encapsulating DXR approved by the FDA in 1995 [24]. DXR is loaded into liposomes by a pH or ion gradient [25, 26], which is also called active loading or remote loading. Here the liposome aqueous core has an excess of protons relative to the external media that makes DXR

protonate when entering the liposome. Exceeding a certain interior concentration, protonated DXR will precipitate and crystallized with anions inside the core liposomes (Figure 1). This DXR liposome formulation reduces the systemic side effects and prominently prolongs the circulation half-life of DXR from minutes when given in free form to 21-54 hours after administered in patients [27, 28], which leads to an increased accumulation in tumors compared to free drugs [29, 30]. However, Doxil® causes new dose limiting side effects, including palmar-plantar erythrodysesthesia and stomatitis, which are related to the passive accumulation of pegylated liposomes in the skin especially at hands and feet during the prolonged blood circulation time, where DXR is slowly released resulting in local toxicity [24]. Besides, Doxil® shows slow DXR release from liposomes to cause a limited bioavailable drug concentration exposed to tumor cells due to the stable liposome carrier, which impedes the anti-cancer activity [30, 31]. Though the liposomal product shows improved efficacy in some solid tumors such as Kaposi sarcoma and ovarian cancer [24], due to the complex microenvironment and chaotic vasculature between tumor types and within patient populations the extravasation level of nanoparticles from tumor vessels can be significantly different and limited [23, 32, 33]. More importantly, the majority of tumor vasculature is not desirably developed, causing limited perfusion and even blocked vessels in tumor. Together, these result in insufficient drug level in tumor when applying these conventional liposomes for solid tumor treatment. Therefore, to improve treatment in solid tumors, strategies that can elevate drug delivery and facilitate drug uptake by tumor cells more site-specifically and efficiently is required.

Mild hyperthermia

Hyperthermia has been used alone or as a combination to treat tumors in the clinic for years [34-37]. For example, RFA (radio frequency ablation), a solid tumor treatment strategy used in the clinic, causes cell death by

inducing a local high temperature up to 100°C in tumor tissue [38]. In a combination therapy, mild hyperthermia (40-44°C) can be clinically utilized as an adjuvant to the radiotherapy or chemotherapy, generating synergistic effects and enhancing therapeutic effect of these treatments [34]. Mild hyperthermia (HT) benefits the chemotherapy in multiple ways. HT can increase blood flow, thus facilitating the perfusion of chemotherapeutic compounds inside tumor [39, 40]. Furthermore, mild hyperthermia improves the permeability of tumor vessels to small molecules and nanoparticles by broadening the gaps between the endothelial cells in tumor vessels, which improves drug accumulation in tumor tissues [41-43]. Li and colleagues have shown that extravasation of liposomes from tumor vessels was increased under mild hyperthermia, compared to non-tumor vessels at which HT hardly showed improved extravasation [44, 45]. And also HT can inhibit DNA repairs and sensitize cancer cells to chemotherapy [34, 46, 47]. Krawczyk et al. reported that using local mild hyperthermia at 41-42.5°C inhibits homologous recombination – one major pathway for DNA double strand breaks repairing which reduces the effectiveness of chemotherapy and radiotherapy [48].

Another function of mild hyperthermia in combination treatment is used a trigger for heating responsive release drug delivery systems. Local heat-triggered drug carries can produce a site-specific release and a high drug concentration at heated areas, e.g. tumor, thus facilitating drug molecules infusion and penetration in tumor tissue, and increasing the tumor cell uptake and reducing drug level in non-heated sites. At present, several methods have been reported to generate local hyperthermia, including using alternating magnetic field (AMF) [49], near-infrared laser [50] and high-intensity focused ultrasound (HIFU) to trigger drug release locally [51].

Thermosensitive liposomes

Designing drug delivery carriers which are able to controllably release content by environmental stimuli is of great significance for achieving a high drug level at disease sites. Thermosensitive liposomes (TSL) receive more attentions due to the advantages that it is relatively easy to set up external heating equipment facilitating drug release at mild hyperthermic temperatures, and obtain a timely and rapid release only at the heated area (e.g. tumor), thus providing enhanced drug delivery to tumor. When designing a thermosensitive liposome, the selection of phospholipids is crucially important as it determines the preferred temperature for drug release [52]. The liposome membrane consisted of ideally mixed phospholipids has a melting temperature (Tm) at which the lipid bilayer undergoes a phase transition from a solid gel phase to a liquid crystalline phase and thus improves the permeability of liposomal membrane (Figure 2). When temperature below Tm, the bilayer is in solid gel state and phospholipid molecules arrange orderly and tightly, forming an immobile and impermeable membrane. When heating the liposomal membrane around Tm, the lipid molecules at grain boundary regions of membrane begin to melt into liquid state but others remain in solid gel phase [53, 54], which creates many "gaps" resulted from disordered arrangement of lipid molecules between two phases, thereby leading to rapid and massive drug release from aqueous core of liposomes. When further increasing temperature to greatly exceed Tm, the whole liposome membrane is into liquid crystalline state and the "gap" between solid and liquid phase is not presented anymore, which causes reduced permeability of membrane and thus drug release is decreased [55].

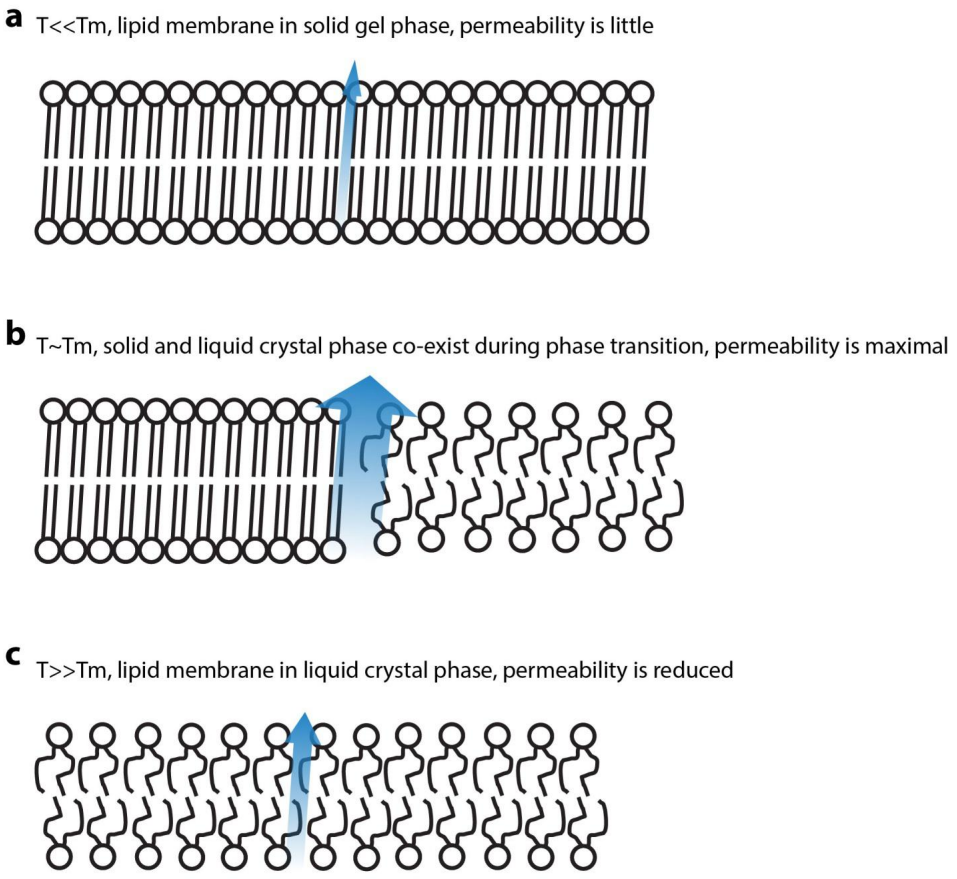

Figure 2. Schematic representation of liposomal membrane permeability states at different temperatures. (a) When below Tm, liposomal membrane is in solid gel phase and lipid molecules stand orderly and tightly, leading to minimal space lipid molecules for content release. (b) When approaching Tm, liposomal membrane undergoes a phase transition generating co-existence of solid phase and liquid phase, which causes disordered arrangement of lipid molecules between these two phases and results in maximum space for release drug. (c) When T beyond Tm, liposomal membrane is in liquid phase and all lipid molecules are more ordered standing than state at Tm, space between lipid molecules is decreased and membrane permeability to drug is reduced.

Thermosensitive liposomes were first proposed by Yatvin in 1978 [56], who demonstrated the heat-triggered release of carboxyfluorescein or neomycin when using DPPC (1,2-dipalmitoyl-sn-glycero-3-phosphocholine; Tm 41°C) and DSPC (1,2-distearoyl-sn-glycero-3-phosphocholine; Tm 55°C) at 3:1 molar ratio to form TSL. However, the release rate was slow and stability was poor due to the immatural formulation at that time, leading to the suboptimal effectiveness. In the decades that followed, thermosensitive liposomes have been further developed and used for cancer chemotherapy, showing and improved cancer cell killing. Pegylation and cholesterol were introduced into thermosensitive liposomes which is termed traditional thermosensitive liposomes (TTSL), showing enhanced circulation time and stability at body temperature [57, 58]. However, considering the short transition time of liposomes passing the heated tumor areas, the release from TTSL was still not fast enough and the overall Tm of liposome was too high. Needham and Dewhirst proposed a new formulation, namely ThermoDox®, which applied lysolipid instead of cholesterol and DSPC in their thermosensitive liposome composition [59]. Lysolipids form micelle and generate pores in liposomal membrane at Tm, thus leading to a higher content release [60, 61]. Yet lysolipid also reduces the liposome stability, which causes higher drug leakage at body temperature during delivery [62, 63]. Tagami et al. applied Brij surfactants to replace lysolipid and PEG-lipid in liposomes which maintain the fast release kinetics but increase liposome stability [64]. Similarly, Lindner et al. reported a novel phospholipid, $DPPG_2$ (1,2-dipalmitoyl-sn-glycero-3-phosphoglyceroglycerol) added in TSL composition, showing improved stability without affecting thermosensitivity for drug release [65]. Li et al. reported thermosensitive liposomes consisted of DPPC, DSPC and 5 mol% PEG-lipids can perform similarly rapid drug release and keep the improved stability at physiological temperature when tested in serum medium [66].

These above developed thermosensitive liposomes all have shown significantly improved chemotherapy efficacy due to the locally effective

release of cytotoxic compounds in tumor areas compared to non-thermosensitive liposomes in several tumor models. Interestingly, to date it seems that doxorubicin has been used as the only drug candidate for thermosensitive liposome encapsulation in most literature reports. Apart from the fluorescent and easy loading properties of doxorubicin, doxorubicin shows effectiveness in several cancers when used in free form before, which probably makes people assume that DXR should still be the best option for thermosensitive liposomes encapsulation when treating these tumors. Despite thermosensitive liposomes offering a fast release of doxorubicin in tumor sites, the uptake rate of DXR by tumor cells may be not optimal due to its hydrophilicity, which may limit efficacy of DXR-TSL. For a successful thermosensitive liposome as a drug delivery system, besides desired stability at body temperature and rapid release under hyperthermia, the fast cellular uptake of released drug molecules is also crucially important. Therefore, selection of proper drugs and thermosensitive liposomes to reach the optimal release performance and treatment effectiveness will be investigated in this thesis.

Aim of the thesis

This thesis aims to describe the use of DPPC-DSPC based thermosensitive liposome in combination with local mild hyperthermia to improve better chemotherapy efficacy from 2 parts: 1) what is the proper drug to be encapsulated in TSL, 2) what is the mechanism of our TSL rapid release and how to reach optimal release formulation.

Topics of the thesis

Chapter 2 describes the development of a novel thermosensitive liposome formulation loading with a new drug – Idarubicin (IDA), an anthracycline similar to doxorubicin but more hydrophobic. This IDA-TSL was optimized and tested in vitro and in vivo. Its stability at body temperature, triggered release at mild hyperthermia and efficacy in tumor response were investigated.

Chapter 3 further investigates IDA and DXR as loaded drugs, which are different in hydrophobicity, encapsulated in TSL. Deep and quantitative comparison of IDA-TSL and DXR-TSL were performed with regard to their in vitro release kinetics and cellular uptake and retention, in vivo circulation and distribution, real time release profiles inside tumor during HT and post HT, intratumoral distribution and accumulation of released IDA and DXR, and efficacy in tumors. This work is to understand how to choose the best drug for thermosensitive liposome-mediated delivery systems.

Chapter 4 deeper describes the mechanism of rapid release at Tm of DPPC-DSPC based thermosensitive liposome. Carboxyfluorescein was used as a model drug loaded inside TSL composited of different ratios of DPPC and DSPC, indicating the proper composition generates a maximal grain boundary density, thus leading to a maximum release.

Chapter 5 searches for a proper release equation to describe release profiles of thermosensitive liposomes, especially at Tm. Several commonly used mathematic models were tested and a new empirical equation was established, which shows the better fitting effect for release at Tm and non-Tm.

Chapter 6 discusses the results of the studies and reviews the current status of thermosensitive liposome mediated drug delivery with HT.

References

[1] P. Boyle, B. Levin, World cancer report 2008, IARC Press, International Agency for Research on Cancer, 2008.
[2] S. Chakraborty, T. Rahman, The difficulties in cancer treatment, ecancermedicalscience, 6 (2012).
[3] M.W. Dewhirst, T.W. Secomb, Transport of drugs from blood vessels to tumour tissue, Nature Reviews Cancer, 17 (2017) 738.
[4] L.E. Quint, Lung cancer: assessing resectability, Cancer Imaging, 4 (2004) 15.
[5] J.C. Wong, S. Raman, Surgical resectability of pancreatic adenocarcinoma: CTA, Abdominal imaging, 35 (2010) 471-480.
[6] S. Rockwell, I.T. Dobrucki, E.Y. Kim, S.T. Marrison, V.T. Vu, Hypoxia and radiation therapy: past history, ongoing research, and future promise, Current molecular medicine, 9 (2009) 442-458.
[7] K. Cheung-Ong, G. Giaever, C. Nislow, DNA-damaging agents in cancer chemotherapy: serendipity and chemical biology, Chemistry & biology, 20 (2013) 648-659.
[8] G. Bonadonna, S. Monfardini, M. de Lena, F. Fossati-Bellani, Clinical evaluation of adriamycin, a new antitumour antibiotic, Br Med J, 3 (1969) 503-506.
[9] L.M. Hollingshead, D. Faulds, Idarubicin, Drugs, 42 (1991) 690-719.
[10] D. Crivellari, D. Lombardi, S. Spazzapan, A. Veronesi, G. Toffoli, New oral drugs in older patients: a review of idarubicin in elderly patients, Critical reviews in oncology/hematology, 49 (2004) 153-163.
[11] C.J. Twelves, Oral idarubicin in solid tumour chemotherapy, Clinical Drug Investigation, 9 (1995) 39-54.
[12] E. Berman, G. Heller, J. Santorsa, S. McKenzie, T. Gee, S. Kempin, S. Gulati, M. Andreeff, J. Kolitz, J. Gabrilove, Results of a randomized trial comparing idarubicin and cytosine arabinoside with daunorubicin and cytosine arabinoside in adult patients with newly diagnosed acute myelogenous leukemia, Blood, 77 (1991) 1666-1674.
[13] P.H. Wiernik, P.L. Banks, D.C. Case, Jr., Z.A. Arlin, P.O. Periman, M.B. Todd, P.S. Ritch, R.E. Enck, A.B. Weitberg, Cytarabine plus idarubicin or daunorubicin as induction and consolidation therapy for previously untreated adult patients with acute myeloid leukemia, Blood, 79 (1992) 313-319.

[14] D.M. Pardoll, The blockade of immune checkpoints in cancer immunotherapy, Nature Reviews Cancer, 12 (2012) 252.
[15] N.P. Restifo, M.E. Dudley, S.A. Rosenberg, Adoptive immunotherapy for cancer: harnessing the T cell response, Nature Reviews Immunology, 12 (2012) 269.
[16] I. Hernandez, V. Prasad, W.F. Gellad, Total Costs of Chimeric Antigen Receptor T-Cell Immunotherapy, JAMA oncology, (2018).
[17] B.F. Incollingo, Considering Cost: What's an Immunotherapy Worth?(2015), in, 2015.
[18] S.B. Kaye, V.J. Richardson, Potential of liposomes as drug-carriers in cancer chemotherapy: a review, Cancer chemotherapy and pharmacology, 3 (1979) 81-85.
[19] V.P. Torchilin, Recent advances with liposomes as pharmaceutical carriers, Nature reviews Drug discovery, 4 (2005) 145.
[20] T.M. Allen, P.R. Cullis, Liposomal drug delivery systems: from concept to clinical applications, Advanced drug delivery reviews, 65 (2013) 36-48.
[21] R.K. Jain, T. Stylianopoulos, Delivering nanomedicine to solid tumors, Nature reviews Clinical oncology, 7 (2010) 653.
[22] Y. Matsumura, H. Maeda, A new concept for macromolecular therapeutics in cancer chemotherapy: mechanism of tumoritropic accumulation of proteins and the antitumor agent smancs, Cancer research, 46 (1986) 6387-6392.
[23] F. Yuan, M. Leunig, S.K. Huang, D.A. Berk, D. Papahadjopoulos, R.K. Jain, Mirovascular permeability and interstitial penetration of sterically stabilized (stealth) liposomes in a human tumor xenograft, Cancer research, 54 (1994) 3352-3356.
[24] Y.C. Barenholz, Doxil®—the first FDA-approved nano-drug: lessons learned, Journal of controlled release, 160 (2012) 117-134.
[25] G. Haran, R. Cohen, L.K. Bar, Y. Barenholz, Transmembrane ammonium sulfate gradients in liposomes produce efficient and stable entrapment of amphipathic weak bases, Biochimica et Biophysica Acta (BBA)-Biomembranes, 1151 (1993) 201-215.
[26] L.D. Mayer, M.B. Bally, P.R. Cullis, Uptake of adriamycin into large unilamellar vesicles in response to a pH gradient, Biochimica Et Biophysica Acta (BBA)-Biomembranes, 857 (1986) 123-126.
[27] A. Gabizon, R. Catane, B. Uziely, B. Kaufman, T. Safra, R. Cohen, F. Martin, A. Huang, Y. Barenholz, Prolonged circulation time and

enhanced accumulation in malignant exudates of doxorubicin encapsulated in polyethylene-glycol coated liposomes, Cancer research, 54 (1994) 987-992.
[28] N.Z. Wu, D. Da, T.L. Rudoll, D. Needham, A.R. Whorton, M.W. Dewhirst, Increased microvascular permeability contributes to preferential accumulation of Stealth liposomes in tumor tissue, Cancer research, 53 (1993) 3765-3770.
[29] R.-L. Hong, C.-J. Huang, Y.-L. Tseng, V.F. Pang, S.-T. Chen, J.-J. Liu, F.-H. Chang, Direct comparison of liposomal doxorubicin with or without polyethylene glycol coating in C-26 tumor-bearing mice: is surface coating with polyethylene glycol beneficial?, Clinical Cancer Research, 5 (1999) 3645-3652.
[30] A.L.B. Seynhaeve, B.M. Dicheva, S. Hoving, G.A. Koning, T.L.M. ten Hagen, Intact Doxil is taken up intracellularly and released doxorubicin sequesters in the lysosome: evaluated by in vitro/in vivo live cell imaging, Journal of controlled release, 172 (2013) 330-340.
[31] K.M. Laginha, S. Verwoert, G.J.R. Charrois, T.M. Allen, Determination of doxorubicin levels in whole tumor and tumor nuclei in murine breast cancer tumors, Clinical cancer research, 11 (2005) 6944-6949.
[32] P. Vaupel, F. Kallinowski, P. Okunieff, Blood flow, oxygen and nutrient supply, and metabolic microenvironment of human tumors: a review, Cancer research, 49 (1989) 6449-6465.
[33] K.J. Harrington, S. Mohammadtaghi, P.S. Uster, D. Glass, A.M. Peters, R.G. Vile, J.S.W. Stewart, Effective targeting of solid tumors in patients with locally advanced cancers by radiolabeled pegylated liposomes, Clinical Cancer Research, 7 (2001) 243-254.
[34] R.D. Issels, L.H. Lindner, J. Verweij, P. Wust, P. Reichardt, B.-C. Schem, S. Abdel-Rahman, S. Daugaard, C. Salat, C.-M. Wendtner, Neo-adjuvant chemotherapy alone or with regional hyperthermia for localised high-risk soft-tissue sarcoma: a randomised phase 3 multicentre study, The lancet oncology, 11 (2010) 561-570.
[35] J. van der Zee, D. González, G.C. van Rhoon, J.D.P. van Dijk, W.L.J. van Putten, A.A.M. Hart, Comparison of radiotherapy alone with radiotherapy plus hyperthermia in locally advanced pelvic tumours: a prospective, randomised, multicentre trial, The Lancet, 355 (2000) 1119-1125.

[36] E. Vorotnikova, R. Ivkov, A. Foreman, M. Tries, S.J. Braunhut, The magnitude and time-dependence of the apoptotic response of normal and malignant cells subjected to ionizing radiation versus hyperthermia, International journal of radiation biology, 82 (2006) 549-559.
[37] B. Hildebrandt, P. Wust, O. Ahlers, A. Dieing, G. Sreenivasa, T. Kerner, R. Felix, H. Riess, The cellular and molecular basis of hyperthermia, Critical reviews in oncology/hematology, 43 (2002) 33-56.
[38] B.J. Wood, J.R. Ramkaransingh, T. Fojo, M.M. Walther, S.K. Libutti, Percutaneous tumor ablation with radiofrequency, Cancer, 94 (2002) 443-451.
[39] C.W. Song, H.J. Park, C.K. Lee, R. Griffin, Implications of increased tumor blood flow and oxygenation caused by mild temperature hyperthermia in tumor treatment, International Journal of Hyperthermia, 21 (2005) 761-767.
[40] C.W. Song, Effect of local hyperthermia on blood flow and microenvironment: a review, Cancer research, 44 (1984) 4721s-4730s.
[41] G. Kong, R.D. Braun, M.W. Dewhirst, Characterization of the effect of hyperthermia on nanoparticle extravasation from tumor vasculature, Cancer research, 61 (2001) 3027-3032.
[42] M. de Smet, S. Langereis, S. van den Bosch, K. Bitter, N.M. Hijnen, E. Heijman, H. Grüll, SPECT/CT imaging of temperature-sensitive liposomes for MR-image guided drug delivery with high intensity focused ultrasound, Journal of controlled release, 169 (2013) 82-90.
[43] G. Kong, R.D. Braun, M.W. Dewhirst, Hyperthermia enables tumor-specific nanoparticle delivery: effect of particle size, Cancer research, 60 (2000) 4440-4445.
[44] L. Li, T.L.M. ten Hagen, M. Bolkestein, A. Gasselhuber, J. Yatvin, G.C. van Rhoon, A.M.M. Eggermont, D. Haemmerich, G.A. Koning, Improved intratumoral nanoparticle extravasation and penetration by mild hyperthermia, Journal of controlled release, 167 (2013) 130-137.
[45] L. Li, T.L.M. ten Hagen, M. Hossann, R. Süss, G.C. van Rhoon, A.M.M. Eggermont, D. Haemmerich, G.A. Koning, Mild hyperthermia triggered doxorubicin release from optimized stealth thermosensitive liposomes improves intratumoral drug delivery and efficacy, Journal of Controlled Release, 168 (2013) 142-150.
[46] A.L. Oei, L.E.M. Vriend, J. Crezee, N.A.P. Franken, P.M. Krawczyk, Effects of hyperthermia on DNA repair pathways: one treatment to inhibit them all, Radiation Oncology, 10 (2015) 165.

[47] H.H. Kampinga, E. Dikomey, Hyperthermic radiosensitization: mode of action and clinical relevance, International journal of radiation biology, 77 (2001) 399-408.
[48] P.M. Krawczyk, B. Eppink, J. Essers, J. Stap, H. Rodermond, H. Odijk, A. Zelensky, C. van Bree, L.J. Stalpers, M.R. Buist, Mild hyperthermia inhibits homologous recombination, induces BRCA2 degradation, and sensitizes cancer cells to poly (ADP-ribose) polymerase-1 inhibition, Proceedings of the National Academy of Sciences, 108 (2011) 9851-9856.
[49] S. Nappini, F.B. Bombelli, M. Bonini, B. Nordèn, P. Baglioni, Magnetoliposomes for controlled drug release in the presence of low-frequency magnetic field, Soft Matter, 6 (2010) 154-162.
[50] A. Agarwal, M.A. Mackey, M.A. El-Sayed, R.V. Bellamkonda, Remote triggered release of doxorubicin in tumors by synergistic application of thermosensitive liposomes and gold nanorods, ACS nano, 5 (2011) 4919-4926.
[51] N. Hijnen, S. Langereis, H. Grüll, Magnetic resonance guided high-intensity focused ultrasound for image-guided temperature-induced drug delivery, Advanced drug delivery reviews, 72 (2014) 65-81.
[52] Z. Al-Ahmady, K. Kostarelos, Chemical components for the design of temperature-responsive vesicles as cancer therapeutics, Chemical reviews, 116 (2016) 3883-3918.
[53] T. Kaasgaard, C. Leidy, J.H. Crowe, O.G. Mouritsen, K. Jørgensen, Temperature-controlled structure and kinetics of ripple phases in one-and two-component supported lipid bilayers, Biophysical journal, 85 (2003) 350-360.
[54] D.H. Kim, M.J. Costello, P.B. Duncan, D. Needham, Mechanical properties and microstructure of polycrystalline phospholipid monolayer shells: Novel solid microparticles, Langmuir, 19 (2003) 8455-8466.
[55] D. Papahadjopoulos, K. Jacobson, S. Nir, I. Isac, Phase transitions in phospholipid vesicles fluorescence polarization and permeability measurements concerning the effect of temperature and cholesterol, Biochimica et Biophysica Acta (BBA)-Biomembranes, 311 (1973) 330-348.
[56] M.B. Yatvin, J.N. Weinstein, W.H. Dennis, R. Blumenthal, Design of liposomes for enhanced local release of drugs by hyperthermia, Science, 202 (1978) 1290-1293.

[57] M.H. Gaber, K. Hong, S.K. Huang, D. Papahadjopoulos, Thermosensitive sterically stabilized liposomes: formulation and in vitro studies on mechanism of doxorubicin release by bovine serum and human plasma, Pharmaceutical research, 12 (1995) 1407-1416.
[58] S. Unezaki, K. Maruyama, N. Takahashi, M. Koyama, T. Yuda, A. Suginaka, M. Iwatsuru, Enhanced delivery and antitumor activity of doxorubicin using long-circulating thermosensitive liposomes containing amphipathic polyethylene glycol in combination with local hyperthermia, Pharmaceutical research, 11 (1994) 1180-1185.
[59] D. Needham, G. Anyarambhatla, G. Kong, M.W. Dewhirst, A new temperature-sensitive liposome for use with mild hyperthermia: characterization and testing in a human tumor xenograft model, Cancer research, 60 (2000) 1197-1201.
[60] J.K. Mills, D. Needham, Lysolipid incorporation in dipalmitoylphosphatidylcholine bilayer membranes enhances the ion permeability and drug release rates at the membrane phase transition, Biochimica et Biophysica Acta (BBA)-Biomembranes, 1716 (2005) 77-96.
[61] D. Needham, J.-Y. Park, A.M. Wright, J. Tong, Materials characterization of the low temperature sensitive liposome (LTSL): effects of the lipid composition (lysolipid and DSPE–PEG2000) on the thermal transition and release of doxorubicin, Faraday discussions, 161 (2013) 515-534.
[62] M.C. Sandström, L.M. Ickenstein, L.D. Mayer, K. Edwards, Effects of lipid segregation and lysolipid dissociation on drug release from thermosensitive liposomes, Journal of controlled release, 107 (2005) 131-142.
[63] B. Banno, L.M. Ickenstein, G.N.C. Chiu, M.B. Bally, J. Thewalt, E. Brief, E.K. Wasan, The functional roles of poly (ethylene glycol)-lipid and lysolipid in the drug retention and release from lysolipid-containing thermosensitive liposomes in vitro and in vivo, Journal of pharmaceutical sciences, 99 (2010) 2295-2308.
[64] T. Tagami, M.J. Ernsting, S.-D. Li, Optimization of a novel and improved thermosensitive liposome formulated with DPPC and a Brij surfactant using a robust in vitro system, Journal of controlled release, 154 (2011) 290-297.
[65] L.H. Lindner, M.E. Eichhorn, H. Eibl, N. Teichert, M. Schmitt-Sody, R.D. Issels, M. Dellian, Novel temperature-sensitive liposomes with

prolonged circulation time, Clinical Cancer Research, 10 (2004) 2168-2178.
[66] L. Li, T.L.M. ten Hagen, D. Schipper, T.M. Wijnberg, G.C. van Rhoon, A.M.M. Eggermont, L.H. Lindner, G.A. Koning, Triggered content release from optimized stealth thermosensitive liposomes using mild hyperthermia, Journal of Controlled Release, 143 (2010) 274-279.

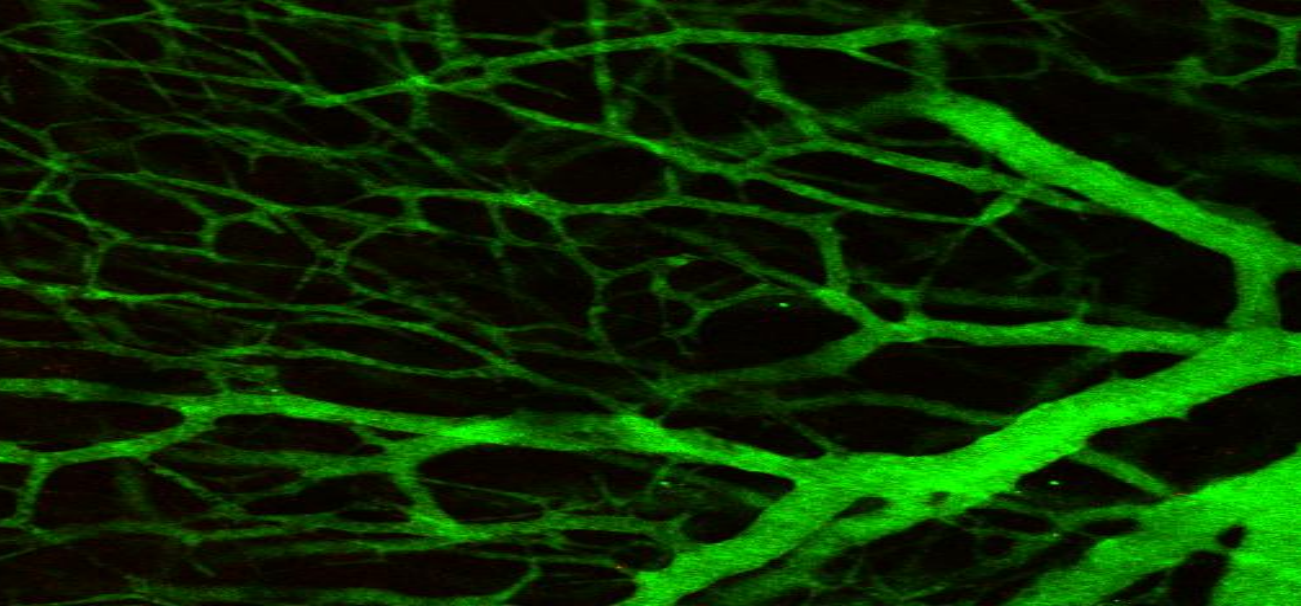

Chapter 2

Formulation and optimization of idarubicin thermosensitive liposomes provides ultrafast triggered release at mild hyperthermia and improves tumor response

Tao Lu, Wouter J.M. Lokerse, Ann L.B. Seynhaeve, Gerben A. Koning, Timo L.M. ten Hagen*

Journal of Controlled Release, 2015, 220(A), 425-437

Abstract

Drug delivery through thermosensitive liposomes (TSL) in combination with hyperthermia (HT) has shown great potential. HT can be applied locally forcing TSL to release their content in the heated tumor resulting in high peak concentrations. To perform optimally the drug is ideally released fast (seconds) and taken up rapidly by tumor cells. The aim of this study was to develop a novel thermosensitive liposome formulation of the anthracycline idarubicin (IDA-TSL). The hydrophobicity of idarubicin may improve its release from liposomes and subsequently rapid cellular uptake when combined mild hyperthermia. Here, we investigated a series of parameters to optimize IDA-TSL formulation. The results show that the optimal formulation for IDA-TSL is DPPC/DSPC/DSPE-PEG (6/3.5/0.5 mol%), with ammonium EDTA of 6.5 pH as loading buffer and a size of ~85 nm. *In vitro* studies demonstrated minimal leakage of ~20% in FCS at 37°C for 1 h, while an ultrafast and complete triggered release of IDA was observed at 42°C. On tumor cells IDA-TSL showed comparable cytotoxicity to free IDA at 42°C, but low cytotoxicity at 37°C. Intravital microscopy imaging demonstrated an efficient *in vivo* intravascular triggered drug release of IDA-TSL under mild hyperthermia, and a subsequent massive IDA uptake by tumor cells. In animal efficacy studies, IDA-TSL plus mild HT demonstrated prominent tumor growth inhibition and superior survival rate over free IDA with HT or a clinically used Doxil treatment. These results suggest beneficial potential of IDA-TSL combined with local mild HT.

Keywords:

Thermosensitive liposome, idarubicin, triggered drug release, mild hyperthermia

1. Introduction

One of the major challenges of current available chemotherapeutic agents used in conventional or combination therapy for cancer is reducing considerable side effects while improving intratumoral delivery [1-2]. For instance, anthracycline antibiotics, especially doxorubicin (DXR), represent one of the most widely used anticancer drugs, but also are of limited benefit to cancer patients because of severe cardiotoxicity and myelosuppression [3,4]. Nanosized liposomes receive increasing interest due to their ability to reduce drug side effects on normal tissues and prolong its retention in circulation. Besides, high intratumoral accumulation of these drug-loaded liposomes also improves antitumor activity because of the EPR (enhanced permeability and retention) effect [5]. Several liposomal formulations have been approved [6-9], among which Doxil® (Caelyx® in Europe) is the most well-known and widely used chemotherapeutic liposome. This DXR-loaded liposome exhibits reduced side effects and prolonged half-life *in vivo*. However, Doxil® does not show much improvements in efficacy mainly attributed to the slow drug release and the lack of tumor specific targeting, which hinders its therapeutic efficacy [10].

In 1978, Yatvin *et al*. proposed the concept of temperature-sensitive liposomes which could generate content release at phase transition temperature (T_m) by using mild hyperthermia (HT) [11]. The initial thermosensitive liposomes were composed of dipalmitoylphosphatidylcholine (DPPC) alone or with distearoylphosphatidylcholine (DSPC) with a T_m range from 42.5-44.5°C [11,12]. However, slow release rate of encapsulated drug, and at that time difficulty to apply hyperthermia locally, limited its application [11,13]. To improve release kinetics Needham *et al*. used lysolipids which have low T_m (e.g. monopalmtoylphophatidylcholine (MPPC) or monostearoylphosphatidylcholine (MSPC)), lipid-grafted PEG and DPPC, to create a new, low temperature sensitive liposomal DXR formulation (DXR-LTSL) [14-16]. This formulation, commercially named ThermoDox® (currently in phase III clinical trials [17]), demonstrates substantial drug release in a matter of seconds at around 39-41 °C. Nevertheless, DXR-LTSL is less stable at physiological temperature,

exhibiting high leakage of ~50% within 1 h [18-20]. Recently, a series of further optimized doxorubicin thermosensitive liposome (DXR-TSL) formulations have been reported, showing desired triggered release by mild HT and favorable stability at physiological temperature [18, 21-23].

In contrast to classic liposomes, which are believed to rely on the EPR effect to accumulate in tumor tissue, TSL can also be used to achieve so-called intravascular release [24]. As soon as a TSL enters the heated region rapid release is enforced resulting in a high local peak concentration. To enable maximum performance the released drug should rapidly enter tumor cells before washout. In this application TSL stability is of lesser importance compared to passive accumulation, while rapid release is crucial, indicating that other chemotherapeutics with more favorable kinetics than doxorubicin could be used. The intravascular release also enables the treatment of mircometastasis surrounded by non-leaky vessels. With the integration of imaging technologies such as MRI and hyperthermia smaller and multiple tumors can be heated and treated [24], which makes this approach more useful for metastatic disease creating possibilities for new drug-TSL formulations.

DXR has been investigated in various liposomal formulations owing to its wide antitumor activity and active loading ability, and handy fluorescence detection property [25]. By contrast, idarubicin (IDA), another anthracycline anticancer drug, which is more hydrophobic and structurally similar to DXR [26,27], receives lesser attention in liposomal nanoparticles. However, IDA has less cardiotoxicity than doxorubicin [26]. Although currently this drug is approved primarily for the treatment of acute and chronic myelogenous leukemia, and acute lymphoblastic leukemia, etc. [28,29], IDA also displays anti-tumor activity in melanoma, sarcoma, lung, ovarian and breast cancers [30]. IDA has a similar anticancer mechanism of action to other anthracycline drugs, by interfering with DNA synthesis [31]. It is worth to note that IDA is five to ten times more potent than daunorubicin and doxorubicin in some studies [32-34]. Additionally, idarubicinol, the metabolite of IDA, exhibits antitumor effects comparable to IDA [34,35]. More importantly, IDA shows less sensitivity to the activities of P-gp and multidrug resistant proteins [36,37]. These reports indicate the potential of an improved

effectiveness compared to DXR-liposome when IDA is encapsulated in liposomes.

Nevertheless, a few IDA liposomal formulations have been reported to date [30,38-40]. Dos Santos *et al*. show rapid leakage of IDA when encapsulated in cholesterol-containing liposomes [40]. They thought that for IDA-like hydrophobic drugs, decreasing the interactions between the drug and liposomal membrane is more important, suggesting that using cholesterol-free liposomes is beneficial to decrease leakage of IDA [30]. While, Gubernator *et al*. recently developed a new method to load IDA by applying EDTA ion gradient instead of conventional sulfate and citrate gradients, forming a more stable drug precipitate in liposomes, which exhibited desirable stability in plasma even if cholesterol-containing liposomes are used [39]. The authors concluded that the formation of stably insoluble drug precipitates inside liposomes can lead to increased drug retention equally [39].

However, the above IDA formulations are conventional liposomes, and there is no thermosensitive liposome formulation for IDA so far. In previous work, we have attained several favorable DXR-TSL formulations which revealed minimal leakage at 37 °C and fast release at 42 °C in 100% FCS in *in vitro* tests [18,41,42]. Therefore, in this study, we developed and optimized a novel IDA-TSL formulation to improve IDA retention at 37 °C and rapid release at 42 °C. The IDA-TSLs were characterized from *in vitro* and *in vivo*.

2. Materials and methods

2.1. Materials

1,2-dipalmitoyl-sn-glycero-3-phosphcholine (DPPC), 1,2-distearoyl-sn-glycero-3-phosphocholine (DSPC) and 1,2-distearoyl-sn-glycero-3-phosphoethanolamine-N-PEG_{2000} (DSPE-PEG) were provided by Lipoid (Ludwigshafen, Germany). PD-10 columns were obtained from GE Healthcare (UK). Idarubicin hydrochloride, cholesterol and other chemicals were purchased from Sigma Aldrich unless otherwise specified.

2.2. Preparation of TSLs

TSLs were mainly composed of DPPC/DSPC/DSPE-PEG in various molar ratios (see Table 1.) by using the thin lipid film hydration method, followed by heated extrusion [18]. Briefly, 100 μmol of lipids was dissolved in methanol/chloroform (1/9 v/v) mixed solvent which was then evaporated at 40°C, followed by nitrogen flush for 30 min to remove residual solvent. The resulting dried lipid film was hydrated with appropriate solutions of sodium citrate (300 mM, pH 4.0), ammonium sulfate (250 mM, pH 5.5), ammonium oxalate (250 mM, pH 5.5) or ammonium EDTA (300 mM, pH 4.5-6.5) at 60°C (see Table 1.). Additionally, thermostable liposomes (DSPC/DSPE-PEG: 9.5/0.5) were prepared as comparison with TSLs. Small unilamellar vesicles were obtained by extrusion through Nuclepore® (Whatman Inc., USA) filters with pore sizes from 50-200 nm on a Thermo barrel extruder at 65°C (Northern Lipids, Canada). Diameter and polydispersity index (PDI), as well as zeta potential were measured by using Zetasizer Nano-ZS (Malvern Instruments Ltd., UK).

2.3. Preparation of ion gradients for IDA encapsulation into TSLs

PD-10 column was used to change the external solution of TSLs to HEPES buffer (150 mM NaCl, 20 mM HEPES, pH 7.4) in order to produce the ion gradients. Lipid concentration was then measured by phosphate assay [43] for subsequent quantitative IDA encapsulation. Loading IDA into TSLs was performed similar to DXR-loading process [18]. Briefly, TSLs with low pH or high ammonium concentration inside were mixed with HEPES buffer (pH 8.5 or 9.5) and IDA according to a molar drug/lipid ratio of 0.15/1 (0.3/1 or 0.45/1 for individual formulations), followed by co-incubation at 37°C for 40 min at a speed of 800 rpm in a thermal shaker (Eppendorf Thermomixer, the Netherlands). As anthracyclines are relatively unstable at high pH IDA loading should be performed within the time-frame given, during which we observed no reduction in IDA activity [44]. The IDA-loaded TSLs were collected by ultracentrifugation (Beckman Coulter, US) at 40,000 rpm for 2 h at 4°C, following by resuspension in HEPES buffer (pH 6.5) overnight at 4°C. Phosphate assay was performed again to quantify the drug to lipid ratio.

2.4. Cryo-TEM images of IDA-TSLs

IDA-TSL consisting of DPPC/DSPC/DSPE-PEG (60/35/5, mol/mol) by using ammonium EDTA gradient (pH 6.5) with a drug/lipid ratio of 30 mol% was prepared. Cryo-transmission electron microscopy (cryo-TEM) images of IDA-TSL were captured via a Fei Tecnai F30ST microscope (Philips, the Netherlands) according to the methods described previously [42]. Briefly, 3 µl of IDA-TSL suspension was dropped on a lacy carbon film and subsequently snap-frozen in liquid ethane by a Vitro bot. An amorphous ice film was created, containing particles of interest.

2.5.*In vitro* IDA-TSL stability and release kinetics in 100% FCS

2.5.1. Time-dependent release

To determine the *in vitro* stability of IDA-TSL, 50 µl of 8 mM [lipid] IDA-TSL suspension was added into 2.95 ml 100% fetal calf serum (FCS) in a quartz cuvette at 37°C for 1h. Real-time leakage of IDA was detected with a water bath combined spectrofluorometry (Ex. 485 nm/Em. 571 nm, Ex. slit 5 nm/Em. slit 10 nm) (Hitachi F-4500 Fluorescence Spectrophotometer, Japan).The average fluorescence intensity of the initial 5 seconds was recorded as I_0 of IDA-TSL leakage, while fluorescence was measured as I_t at a certain time point. After 1h, detergent (10% Triton X-100) was used to disrupt all liposomes to measure maximal IDA fluorescence, which was recorded as I_{max}. Leakage (%) = $(I_t - I_0)/(I_{max} - I_0) \times 100$. Release of IDA-TSL at 42°C was performed similarly.

2.5.2. Temperature-dependent release

Temperature-dependent release was performed by adding 50 µl of 8 mM [lipid] IDA-TSL suspension into pre-heated 2.95 ml of 100% FCS in a quartz cuvette. This cuvette was then incubated for 5 min at temperature ranges (from 25°C, 30-45°C), followed by adding detergent to obtain maximal fluorescence. The temperature-dependent release (%) was calculated in the same way described above (2.5.1.), but using the fluorescence intensity measured at 25°C for calibration.

2.6. *In vitro* IDA-TSL cytotoxicity assay

Murine B16BL6 melanoma and human BLM melanoma cells were cultured in DMEM medium (containing 4500 mg glucose/L, L-alanyl-L-

glutamine) with 10% FCS, and murine C26 colon carcinoma cells were cultured in RPMI-1640 medium (containing L-alanyl-L-glutamine) with 10% FCS. Based on the results in 2.5, cytotoxicity assays were performed with the optimal IDA-TSL formulation. B16BL6, C26 and BLM cells were seeded in 96 well-plates at a density of 1500 cells/well, and placed in an incubator (37°C, 5% CO_2) for 24 h. IDA-TSL, free IDA and empty TSL were diluted from stock solutions in cell culture medium and filtered through 0.45 µm filters. These three resulting solutions, subsequently, were exposed to heating at 37 or 42°C for 15 min in a water bath, followed by 5-times dilution with cell medium into 9 continuous concentrations. After adding samples to the cells, the 96 well-plates were incubated for 72 h directly, or for 1 h followed by 3-times wash and treated with fresh medium for an additional incubation of 72 h. Cell survival rates were measured by using the colorimetric SRB assay described by Vichai *et al.* [45]. IC_{50} (50% cellular growth inhibition) was calculated and presented.

2.7. Flow cytometry and *in vitro* live cell imaging

To confirm *in vitro* activity of IDA-TSL systems on live cells, several IDA-TSL formulations were tested: IDA-TSL with 80, 70, 60, or 50% DPPC, loaded with citrate buffer, and compared to free IDA and cell medium. BLM cells in full FCS were exposed to the different formulations for 30 min at 37 or 42°C, at an IDA concentration of 20 µg/ml (3 ml for flow cytometry, cells growing in T25 flask; 1 ml for cell confocal imaging, cells growing in 12-well-glass-bottom-plate). Thereafter cells were washed and harvested by trypsinization, followed by flow cytometry. For each sample 50,000 cells were analyzed by flow cytometer on a BD FACS Canto™. For confocal laser scanning microscope (CLSM) cells were washed and fresh medium added, followed by confocal imaging (Zeiss LSM 510 META, Germany) using a helium-neon laser (Ex. 543 nm, Em. LP 560 nm). Images with higher magnifications were captured to visualize IDA uptake by cells.

2.8. Mouse tumor models

NMRI *nu/nu* mice were purchased from Harlan and housed at 20-22°C, humidity of 50-60%, and 12 h light-dark cycles. Sterile rodent food and acidified vitamin C-fortified water were offered *ad libitum*. Eight-week

old mice with weight of 40-45 g (NMRI *nu/nu*) were chosen for experiments. Mice (C57BL/6) with constitutive vascular endothelial cell expression of an eNOS-Tag-GFP fusion protein were developed by Dr. R. de Crom and R. van Haperen, Department of Cell Biology, Erasmus MC, Rotterdam, the Netherlands, bred in house and used for intravital microscopy experiments. All animal studies were performed according to protocols approved by the committee of Animal Research of the Erasmus MC, Rotterdam, the Netherlands.

B16BL6 cells (~10^6) were injected subcutaneously in the flank of a C57BL/6 mouse to grow a tumor bulk with a diameter of circa 1 cm. A small piece of this tumor (~1 mm^3) was then transplanted into the fascia of a dorsal skin flap placed in a window chamber on the mouse [18]. These window chambers-bearing mice were housed individually at 30°C with 70% humidity. Experiments commenced when diameters of tumors reached approximately 5 mm in the dorsal skin flap window chamber.

For *in vivo* efficacy study, a tumor piece (~3 mm^3) of BLM melanoma (6 mice/group) were transplanted subcutaneously in the hind leg of NMRI *nu/nu* mice. When tumors reached around 100 mm^3 in size, mice were used for efficacy experiments.

2.9. *In vivo* IDA-TSL release by intravital microscopy

In vivo IDA-TSL release was observed by intravital fluorescence microscopy. Mice were anesthetized with isofluorane (Nicholas Piramal, UK) on a thermal plate at 37°C during the whole experimental process. An external circular conductive heating coil was attached to the glass at the back side of window chamber to provide homogenous local HT [18]. Thermocouples (point-welded thin manganese and constantan wires from Thesso®, Amsterdam) were imbedded in the window chamber for online monitoring of temperature in the tumor tissue. IDA-TSL (4 mg/kg) was injected intravenously through the tail vein.

Regions of interest were observed by CLSM. Image acquisition of background was handled before IDA-TSL injection. Initial images were captured as before mild HT within 10 min post-injection, and then the window chamber tissues were heated to 42°C and maintained for 1 h.

Release of IDA-TSL was monitored online by a helium-neon laser (Ex. 543 nm, Em. LP 560 nm), and endothelial cells were visualized by an argon laser (Ex. 488 nm, Em. BP 505-550 nm). Intermittent images were taken every 10 seconds during heating at 42°C. Images with higher magnifications were captured at the end of experiments to visualize IDA uptake by tumor cells. CLSM image software (Zeiss, Germany) was then used to analyze these collected images.

2.10. Therapeutic efficacy

Mice bearing subcutaneously tumor size of around 100 mm^3 (Length × Width × Depth × 0.4) in their right hind legs were anesthetized and prepared for local mild HT [18]. Briefly, the skin and foot surrounding tumor in right legs were covered in Vaseline cream to protect normal tissue from heating damage. The hind tumor-bearing legs were placed inside a water bath (tumor temperature at 42°C) and kept at a steady position during the HT treatment. When tumor temperature reached 42°C, IDA-TSL, free IDA and saline were administered at 1.5 mg/kg (IDA) through i.v. injection. The tumor temperature was maintained at 42°C for 1 h. Normothermia (NT) mice treated with IDA-TSL, free IDA and saline at the same doses were maintained at 37°C for 1 h as comparison. Doxil was used here to mimic clinic application as comparison by giving a first dose of 4.5 mg/kg and 3 times a dose of 1 mg/kg at an interval of 4 days. Tumor size was measured every day after treatment. Mice were euthanized when tumor reached ~15x15x15 mm^3 in size or based on human endpoint.

2.11. Statistical analysis

In vitro and *in vivo* data were analyzed using Mann Whitney U test or Kruskal Wallis test when appropriate. P values below 0.05 were considered significant.

3. Results

3.1. *In vitro* characterization of IDA-TSLs

The IDA-TSLs described here were of uniform diameter of ~85 or ~130 nm (respectively designated small and large) with PDI values below 0.1. IDA could be encapsulated with an efficiency of around 100% (Table 1).

3.1.1. The influence of loading buffers on IDA-TSL stability

Several buffers are used in the literature to load doxorubicin or idarubicin in liposomes. Here sodium citrate, ammonium sulfate, ammonium oxalate and ammonium EDTA salt solutions, were selected to load IDA (formulation 1-4 in Table 1). When sodium citrate or ammonium sulfate was applied, leakage up to ~43% to ~50% was observed within 1 h-incubation in 100% FCS at 37°C. Maximal release at 42°C was reached within a few seconds (Figure 1A,B). Also using ammonium oxalate as loading buffer resulted in instable liposomal formulation of IDA with a leakage of circa 40% at 37°C. Rapid heat triggered drug release was observed at 42°C, similar to ammonium sulfate IDA-TSL (Figure 1C). By contrast, loading IDA using ammonium EDTA showed a significantly lowered leakage to ~23% at 37°C. Rapid and maximum release was maintained at 42°C (Figure 1D). Hence, ammonium EDTA solution was selected as the optimal loading buffer for the following IDA-TSL formulations.

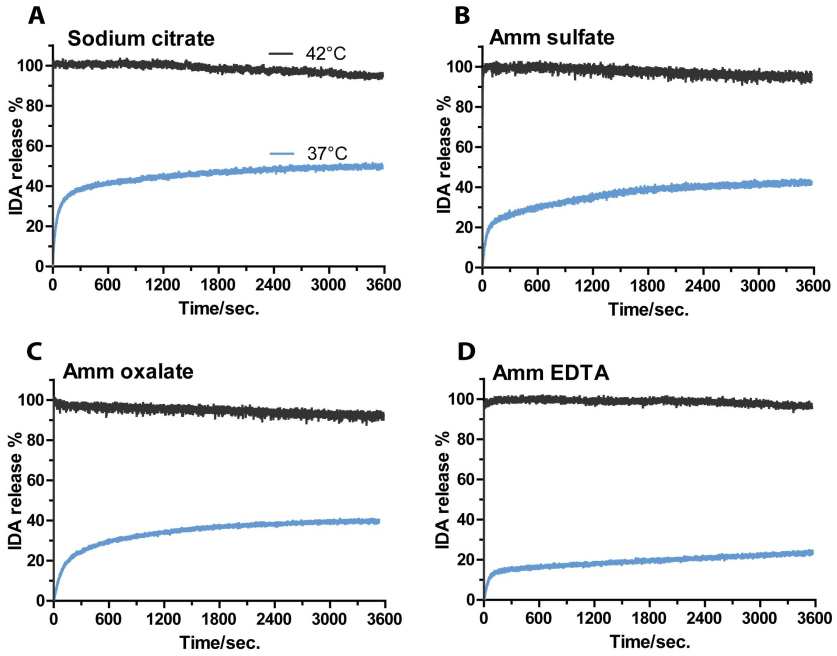

Figure 1. The influence of loading buffer on idarubicin (IDA) release from 85 nm IDA-TSL at 37°C (blue) and 42°C (black) in FCS for 1 h. The loading buffer was sodium citrate pH 4.0 (A), ammonium sulfate pH 5.5 (B), ammonium oxalate pH 5.5 (C) or ammonium EDTA pH 5.5 (D). Liposome composition was DPPC/DSPC/DSPE-PEG: 7/2.5/0.5. (Three independent tests were performed. A representative release profile is shown.)

3.1.2. The influence of liposome compositions on IDA-TSL stability

Cholesterol is used to increase stability of liposomal membranes and improve enclosure of contents [46]. Therefore we added cholesterol to IDA-TSL formulation for further optimization (formulation 5 in Table 1). For the same purpose, paraffin, the most lipophilic molecule, was used to formulate IDA-TSL (formulation 6 in Table 1). Nevertheless, both cholesterol and paraffin did not improve IDA-TSL stability showing around 30% leakage at 37°C (Figure 2A). Interestingly, these two

formulations demonstrated decreased release rates at 42°C, reaching maximum release after ~10 min (Figure 2A).

Table 1. Characterization parameters of IDA-TSL used in this study. Mean±SD, N=3.

Liposomes composition (mole)	Ion gradient	Particle size (nm)		Polydispersity index		Drug/lipid (mole/mole)		Leakage (%) at 37°C in 100% FCS		Release (%) at 42°C in 100% FCS				Zeta potential after loading (mV)
		Before loading	After loading	Before loading	After loading	Before loading	After loading	5min	1h	20sec	1min	10min	1h	
1) DPPC/DSPC/DSPE-PEG 7/2.5/0.5	Citrate-Na (pH 4.0)	84±2	85±1	0.03±0.01	0.04±0.02	0.15/1	0.167/1	38±5	49±5	99±1	99±1	98±2	90±6	-6.7±0.3
2) DPPC/DSPC/DSPE-PEG 7/2.5/0.5	$(NH_4)_2SO_4$ (pH 5.5)	83±1	82±1	0.04±0.02	0.04±0.02	0.15/1	0.158/1	29±4	43±2	99±1	99±1	99±1	92±2	-7.7±0.2
3) DPPC/DSPC/DSPE-PEG 7/2.5/0.5	Oxalate-NH_4 (pH 5.5)	86±1	84±2	0.03±0.01	0.03±0.01	0.15/1	0.143/1	25±3	41±4	99±1	99±1	96±1	91±3	-7.2±0.5
4) DPPC/DSPC/DSPE-PEG 7/2.5/0.5	EDTA-NH_4 (pH 5.5)	86±3	85±2	0.06±0.03	0.07±0.01	0.15/1	0.152/1	14±2	23±2	99±1	99±1	99±1	93±3	-7.6±0.6
5) DPPC/DSPC/ Cholesterol/DSPE-PEG 7/2/0.5/0.5	EDTA-NH_4 (pH 5.5)	87±2	86±2	0.04±0.03	0.05±0.02	0.15/1	0.151/1	16±2	27±1	71±1	80±2	99±1	99±1	-6.5±0.2

6) DPPC/DSPC/Paraffin/DSPE-PEG 7/2/0.5/0.5	EDTA-NH_4 (pH 5.5)	83±2	81±3	0.05±0.02	0.04±0.02	0.15/1	0.17/1	13±1	28±2	72±2	84±1	99±1	99±1	-6.8±0.6
7) DPPC/DSPC/DSPE-PEG 8/1.5/0.5	EDTA-NH_4 (pH 5.5)	85±0	84±1	0.06±0.02	0.07±0.02	0.15/1	0.164/1	19±2	26±1	87±4	93±5	99±1	94±1	-7.2±0.4
8) DPPC/DSPC/DSPE-PEG 6/3.5/0.5	EDTA-NH_4 (pH 5.5)	87±2	86±2	0.06±0.01	0.04±0.02	0.15/1	0.147/1	16±0	21±1	99±1	97±1	92±1	90±4	-7.2±0.6
9) DPPC/DSPC/DSPE-PEG 5/4.5/0.5	EDTA-NH_4 (pH 5.5)	86±3	87±1	0.05±0.02	0.06±0.01	0.15/1	0.162/1	14±0	19±2	66±5	80±6	79±5	77±3	-8.4±0.3
10) DPPC/DSPC/DSPE-PEG 6/3.5/0.5	EDTA-NH_4 (pH 4.5)	88±2	88±1	0.05±0.01	0.06±0.01	0.15/1	0.139/1	15±1	21±1	99±1	97±2	94±2	89±3	-8.0±0.2
11) DPPC/DSPC/DSPE-PEG 6/3.5/0.5	EDTA-NH_4 (pH 6.5)	85±2	85±1	0.08+0.01	0.07±0.01	0.15/1	0.155/1	13±1	21±2	99±1	99±1	96±2	93±1	-8.4±0.3
12) DPPC/DSPC/DSPE-PEG 6/3.5/0.5	EDTA-NH_4 (pH 6.5)	131±4	130±5	0.07±0.01	0.07±0.02	0.15/1	0.172/1	14±2	20±3	96±1	91±2	83±5	91±2	-8.5±0.6
13) DPPC/DSPC/DSPE	EDTA-NH_4	84±2	80±1	0.06±0.01	0.05±0.02	0.30/1	0.302/1	13±1	20±2	99±1	99±1	97±1	91±3	-7.5±0.2

-PEG 6/3.5/0.5	(pH 6.5)													
14) DPPC/DSPC/DSPE -PEG 6/3.5/0.5	EDTA-NH_4 (pH 6.5)	86±2	81±2	0.05±0.02	0.04±0.02	0.45/1	0.488/1	15±2	27±1	99±1	99±1	97±2	88±3	-5.8±0.3
15) DSPC/DSPE-PEG 9.5/0.5	EDTA-NH_4 (pH 6.5)	87±3	85±2	0.07±0.02	0.05±0.02	0.30/1	0.289/1	2±1	10±3	1±1	3±1	11±5	17±3	-7.3±0.6

To investigate the effects of different DPPC percentages on IDA-TSL stability, a series of IDA-TSL formulations were prepared by using 80%, 70%, 60% and 50% DPPC with matching percentage of DSPC and 5% DSPE-PEG (formulation 7 = TSL80, formulation 4 = TSL70, formulation 8 = TSL60 and formulation 9 = TSL50 in Table 1). As seen in Figure 2B, IDA-TSL exhibited a decline in leakage at 37°C from TSL80 of ~26%, to TSL70 of ~23%, to TSL60 of ~21% and to TSL50 of ~19%. Besides, the release rates of these four formulations at 42 °C were also different, among which TSL80 showed maximum release after ~2 min, and TSL70 need approximately ~10 seconds, whereas TSL60 exhibited a complete release within 1-2 seconds. By contrast, around 1-2 min of delay was observed in TSL50 to reach the maximum release, which was ~80% of IDA at that time point when exposed to 42°C. Based on these results, we selected the IDA-TSL60 formulation (DPPC/DSPC/DSPE-PEG: 6/3.5/0.5) for the following optimization.

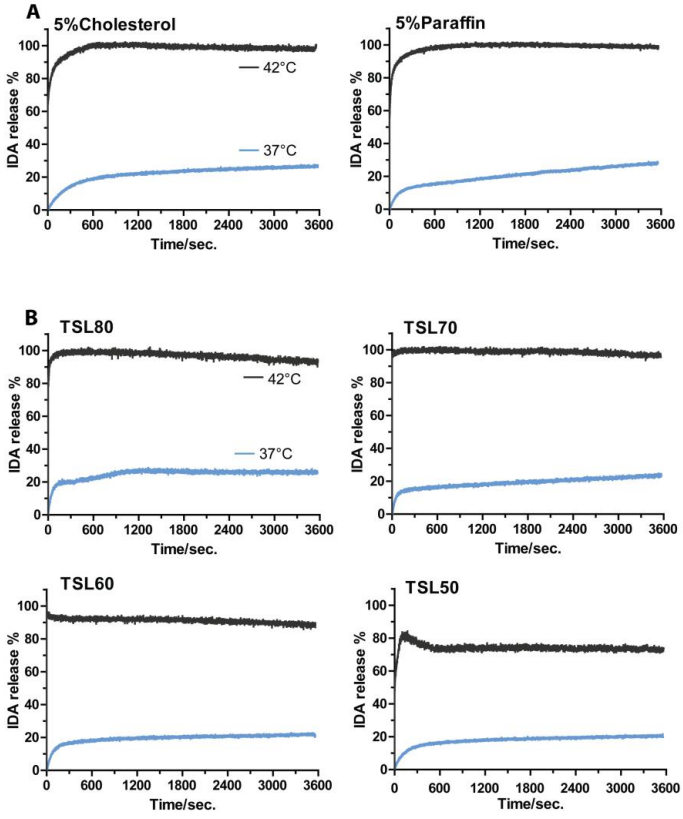

Figure 2. The influence of adding cholesterol or paraffin (A) and changing DPPC percentage (B) in liposome composition on idarubicin (IDA) release from 85 nm IDA-TSL at 37°C (blue) and 42°C (black) in FCS for 1 h. Loading buffer was ammonium EDTA with pH 5.5. (Three independent tests were performed. A representative release profile is shown.)

3.1.3. The influence of internal EDTA pH on IDA-TSL stability

To access the effects of electrostatic attraction on IDA-TSL stability, we prepared a series of internal pH of 4.5, 5.5 and 6.5 by adding ammonia to EDTA solutions to load IDA, while an external pH of 8.5 (for pH 4.5/5.5 inside) or 9.5 (for pH 6.5 inside) was maintained, respectively (formulation 8, 10, 11 in Table 1). Complete encapsulation was obtained for these three formulations (Table 1). As shown in Figure 3, these formulations had comparable stability, which exhibited a leakage of ~20% at 37°C after 1 h. Likewise, immediately maximum release at 42°C was observed in all three formulations. By comparison, IDA-TSL with pH 6.5 inside seemed to have 1-2% less leakage than the other two formulations, therefore, ammonium EDTA solution with pH of 6.5 (external pH 9.5) was applied in subsequent formulations.

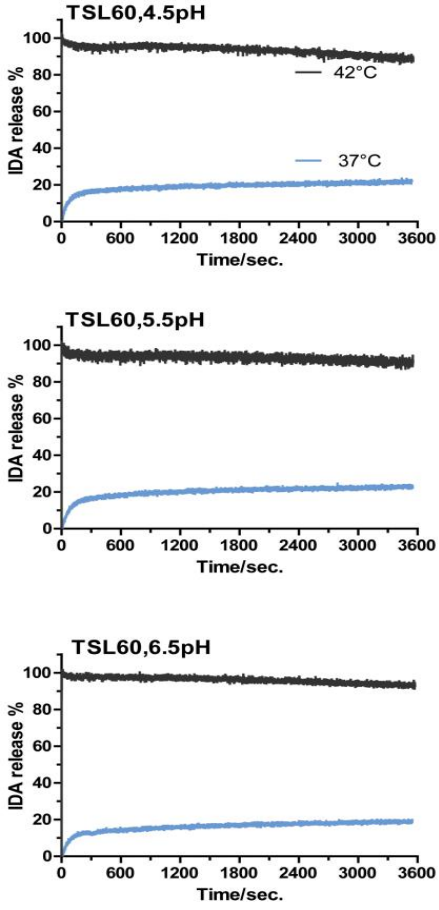

Figure 3. The influence of ammonium EDTA pH on idarubicin (IDA) release from 85 nm IDA-TSL at 37°C (blue) and 42°C (black) in FCS for 1 h. IDA-TSL was composed of DPPC/DSPC/DSPE-PEG:6/3.5/0.5. (Three independent tests were performed. A representative release profile is shown.)

3.1.4. The influence of liposome sizes on IDA-TSL stability

Liposomes with different sizes exhibit various extents of curvature, which can affect their contents release profiles [47,48]. Hence, we formulated IDA-TSLs with diameters of ~85 nm and ~130 nm (formulation 11-12 in Table 1). We observed that IDA-TSL of ~130 nm did not demonstrate any improvement on stability (leakage of ~20%) at 37°C compared with IDA-TSL ~85 nm (Figure 4A). Interestingly, at 42°C, large IDA-TSL showed an immediate and maximum release followed by a sudden drop down to ~90%; whereas we did not observe this with small sized IDA-TSLs. The same trend was observed with IDA-TSL with a diameter of ~180 nm at 42°C, also showing a low leakage of ~20% at 37 °C (data not shown). Therefore, we continued to use liposomes with a diameter of ~85 nm.

3.1.5. The influence of drug to lipid ratios on IDA-TSL stability

To evaluate the effects of drug/lipid ratios on IDA-TSL release, three IDA-TSL formulations with drug to lipid molar ratios of 15%, 30% and 45% were prepared, respectively (formulation 11, 13-14 in Table 1). As Figure 4B illustrates, increasing the drug/lipid ratio to 30% did not further improve IDA retention in liposomes, presenting almost the same release profiles as drug/lipid ratio of 15%, with leakage of ~20% at 37 °C and ultrafast maximal release within 1-2 seconds at 42°C in 100% FCS. By comparison, 45%-drug-loaded IDA-TSL was less stable by showing an increased leakage of ~27% at 37°C for 1 h-incubation, although it revealed a complete encapsulation of IDA (Table 1) and had an immediate release at 42°C as well. Therefore, both drug/lipid ratios of 15% and 30% were determined to be suitable for optimized IDA-TSL formulations.

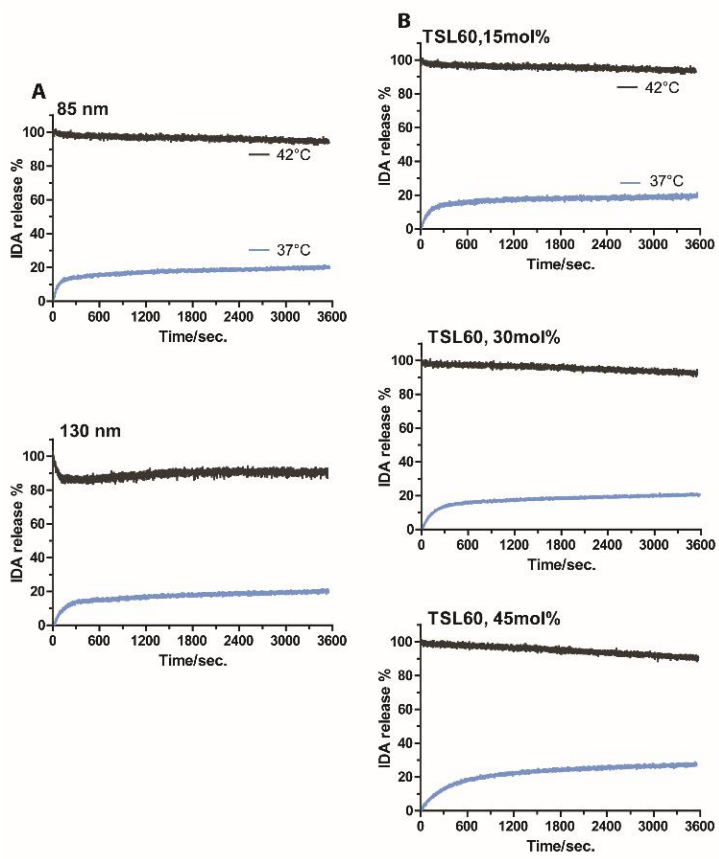

Figure 4. The influence of liposome size (A) and drug/lipid ratio (B) on idarubicin (IDA) release from IDA-TSL at 37°C (blue) and 42°C (black) in FCS for 1 h. IDA-TSL was composed of DPPC/DSPC/DSPE-PEG:6/3.5/0.5, loaded by ammonium EDTA pH 6.5. (Three independent tests were performed. A representative release profile is shown.)

3.1.6. The temperature-dependent release of IDA-TSLs

In the temperature-dependent release test, we compared IDA-TSL60 with IDA-TSL70 and IDA-TSL50, at a molar drug-to-lipid ratio of 15% loaded by EDTA with pH 6.5, from 30 °C to 45°C at an interval of 1°C. As shown in Figure 5, all these three formulations displayed leakage

beginning at 30-31°C followed by gradual increase until 38°C after 5 min incubation in 100% FCS. However, IDA-TSL70 revealed a significant release of ~60% at 39°C to almost complete release at 40°C; while IDA-TSL60 exhibited a drug-release of only 35% at 40°C but a massive release of ~75% at 41°C, following by reaching maximum IDA release at 42°C. As expected, the release of IDA-TSL50 was incomplete at 42°C and reached its maximum at 44°C.

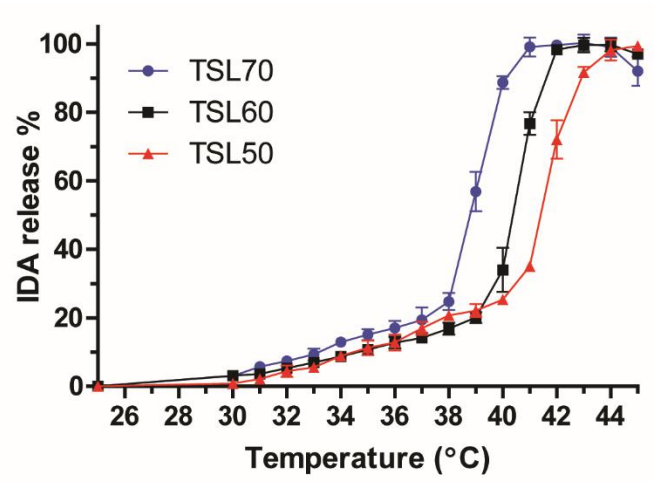

Figure 5. Temperature-dependent idarubicin (IDA) release from IDA-TSL with decreasing percentage of DPPC (respectively 70, 60 or 50%) during 5 min incubation in FCS at different temperatures. IDA-TSL70 (blue circle), IDA-TSL60 (black square) and IDA-TSL50 (red triangle). N=3.

3.1.7. Cryo-TEM imaging

Figure 6 shows IDA-EDTA precipitates inside IDA-TSLs with drug/lipid ratios of 30 mol% by cryo-TEM analysis. Less rounded liposomes were observed after IDA loading. IDA-EDTA precipitates presented as irregular appearance in the interior of TSLs.

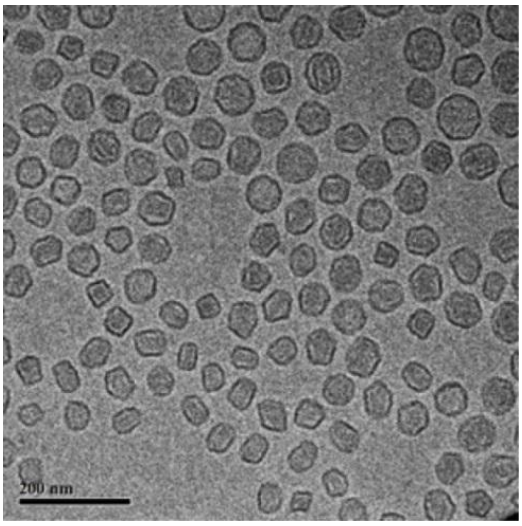

Figure 6. Cryo-TEM image of idarubicin containing thermosensitive liposomes (IDA-TSL) composed of DPPC/DSPC/DSPE-PEG (6/3.5/0.5) with 30 mol% IDA loading by ammonium EDTA pH 6.5. Bar, 200 nm.

3.2. *In vitro* cytotoxicity of IDA-TSLs

IDA-TSL (DPPC/DSPC/DSPE-PEG: 6/3.5/0.5) with 30% of drug loading formulation was used for the cytotoxicity tests in B16BL6, C26 and BLM tumor cell lines. As illustrated in Figure 7, empty liposomes had negligible cytotoxicity on all tested cell lines. Table 2 presents IC_{50} values with/without mild hyperthermia that were calculated based on fitting curves calculated with GraphPad Prism. The cytotoxicity of IDA-TSL under HT (42°C) indicated nearly equivalent cytotoxicity to free IDA (at 37 and 42°C) in these three cell lines; while IDA-TSL at NT (37°C) exhibited reduced cytotoxicity to cells leading to significantly increased IC_{50} on B16BL6, C26 and BLM cell lines (Table 2, Figure 7). IDA-TSL revealed an 11-fold decrease in IC_{50} when combined with HT compared to NT on C26 cells after 1 h treatment; while for B16BL6 and BLM cell lines, IDA-TSL showed 6-fold and 3-fold reduction, respectively (Table 2, Figure 7A-C). The same conclusion was evidenced by exposure of cell lines to drugs for 3 days. (Table 2, Figure 7D-F).

Table 2. IC_{50} (nM) of IDA-TSL in comparison with free IDA.

	Co-incubation for 1 h			Co-incubation for 3 days		
	B16BL6	C26	BLM	B16BL6	C26	BLM
		HT/NT			HT/NT	
IDA-TSL	8/46*	8/91*	14/44*	5/9*	0.37/4*	1/6*
IDA Free	7/7	7/7	10/15	4/4	0.31/0.34	1/1

*Nonparametric Mann–Whitney test, *p* value < 0.05. Data are represented as Mean, N=3. HT: hyperthermia (42°C), NT: normothermia (37°C).

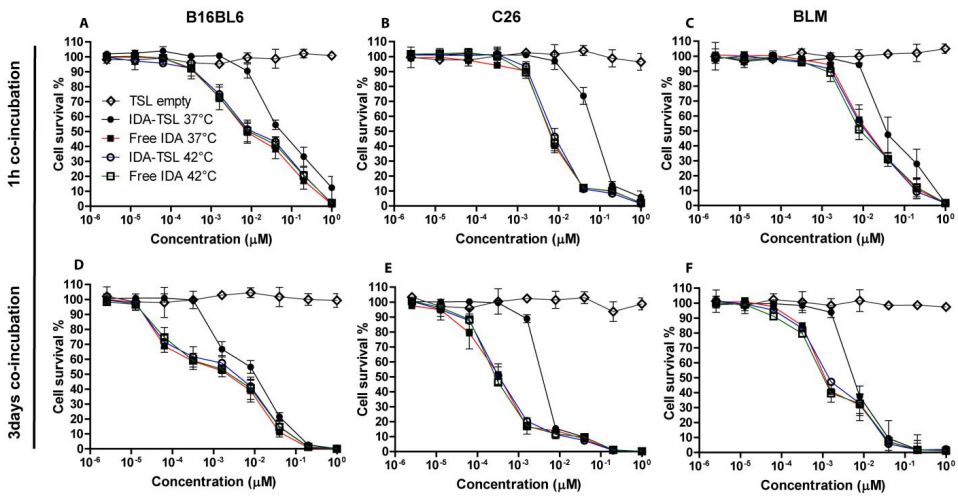

Figure 7. *In vitro* cytotoxicity of idarubicin containing thermosensitive liposomes (IDA-TSL) on B16BL6 murine melanoma cell line (A,D), C26 murine carcinoma cell line (B,E) and BLM human melanoma cell line (C,F) at 37°C and 42°C for 1 h or 3 days co-incubation. TSL empty (diamond), IDA-TSL at 37°C (filled circle), IDA-TSL at 42°C (empty

circle), free IDA at 37°C (filled square) and free IDA at 42°C (empty square). Liposome composition was DPPC/DSPC/DSPE-PEG:6/3.5/0.5. N=3.

3.4. Flow cytometry and *in vitro* imaging

Flow cytometry studies (Figure 8A,B), show overlapping peaks when tumor cells were exposed to IDA-TSL 80, 70, 60, 50 (% DPPC), IDA-TSL citrate (loaded by citrate buffer) and free IDA at 42°C, indicating complete IDA release from TSL system. At 37°C, only minor differences of leaked IDA were found from TSL 80 to 50, except that IDA-TSL loaded with citrate buffer showed higher leakage, which was consistent with above formulation optimization results. The peak fluorescence at 37°C, which represents IDA leaked from TSL 60 (at 20 μg/ml), corresponds with the peak fluorescence observed with the same amount of free IDA (at 5 μg/ml), confirming the stability of the TSL (data not shown). Confocal imaging confirms that IDA-TSL released massive IDA at 42°C and less IDA leaked at 37°C, resulting in less evident cellular uptake (Figure 8C), though no obvious IDA leakage differences can be seen among these TSLs. The confocal images show slightly reduced idarubicin accumulation with TSL 50 compared to the others at 42°C. Interestingly, more IDA accumulated in the cytoplasm (Figure 8C).

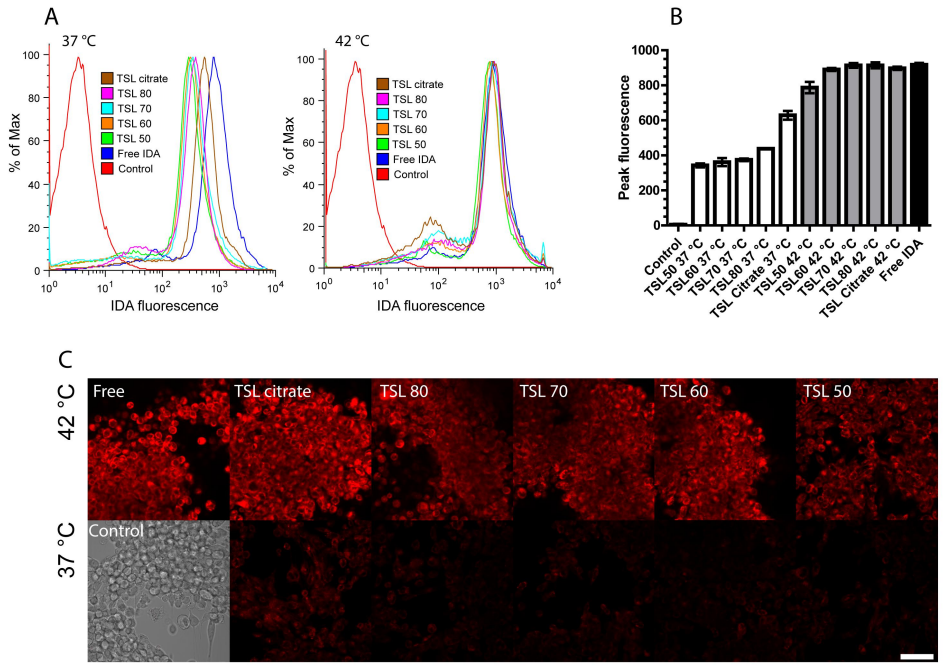

Figure 8. A. *In vitro* activity of idarubicin (IDA) loaded in different formulations was measured by flow cytometry at 37 and 42°C in BLM cell. B. Based on A, peak fluorescence of each sample at 37 or 42°C was calculated. C. Confocal imaging of cellular uptake of IDA released from different TSL formulations at 37 and 42°C. Settings: IDA gain=500, dimension=512 x 512. Bar applies for all images, 50 µm.

3.4. *In vivo* IDA-TSL release under local mild HT

In vivo IDA release from IDA-TSL was monitored by intravital fluorescence microscopy using mice implanted with the murine B16BL6 melanoma in the dorsal skin flap window chamber (Figure 9 and Supplementary video). As shown in Figure 9, at 37°C before applying HT, there was no obvious leakage of IDA observed in the vessels after injecting IDA-TSL at a dosage of 4 mg/kg (Figure 9A). IDA-TSL began to release intravascularly when mild hyperthermia was started from 37°C to 42°C which was reached within 4 min (Figure 9B,C). IDA release

continued and extravasated towards the interstitial space, showing massive release and penetration approximately within 15 min post-HT (Figure 9D-F). Subsequently, released IDA in the interstitial space was taken up by tumor cells. From 30 min post-HT, no apparent change on IDA release and penetration can be seen. The IDA fluorescent signal in vessels decreased as a consequence of wash-out by blood flow (Figure 9G,H). In agreement with the *in vitro* confocal images more IDA was observed to accumulate in the cytoplasm; while nuclear accumulation was less evident (see the white arrows in Figure 9I,J).

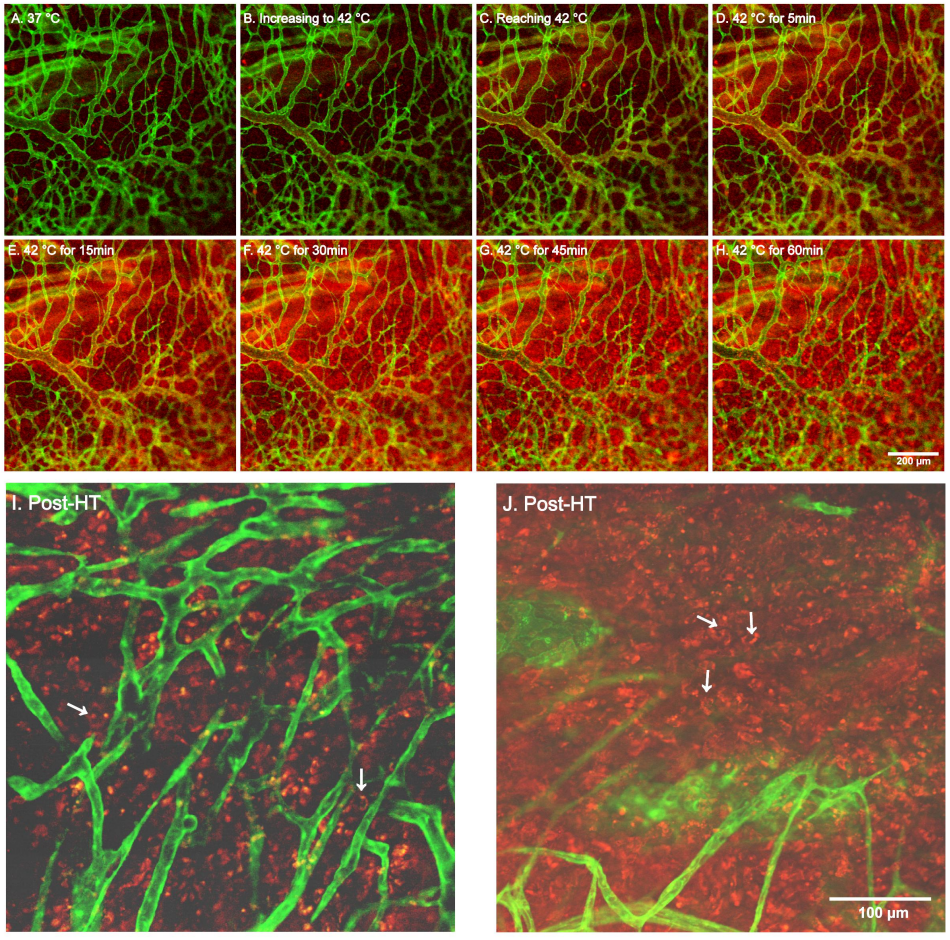

Figure 9. *In vivo* idarubicin (IDA) release from IDA-TSL in murine B16BL6 melanoma at 37 °C (A) and mild hyperthermia for 1 h (B-H).

Cellular uptake of IDA after treatment with mild hyperthermia (I,J). Bar, 200 µm (A-H), 100 µm (I,J).

3.5. Tumor growth control

In human BLM melanoma-bearing NMRI *nu/nu* mice a dose escalation study was performed starting with 1, 1.5 and 2 mg/kg in combination with HT. At 2 mg/kg foot swelling and weight loss were encountered which were outside of the set ethical boundaries. Therefore, a single low dose of 1.5 mg/kg IDA-TSL, which was accompanied by transient limited weight loss, was used for further experiments. Clearly, free IDA was not sufficient to produce a tumor response at this dose. However, IDA-TSL at a dose of 1.5 mg/kg with local mild HT induced significantly suppressed tumor growth over a time course of at least 20 days compared to free IDA and saline with mild HT after a single dose treatment ($p<0.002$ for both). Moreover, the efficacy of IDA-TSL with HT was superior to Doxil, even though the latter was used at a cumulative dose of 7.5 mg/kg ($p<0.005$). Yet IDA-TSL with NT hardly produced tumor suppression comparable to free IDA and saline with or without HT (Figure 10A). By day 20, all mice treated with IDA-TSL plus HT survived (Figure 10B), with an average tumor size below 400 mm^3; while other groups of mice had to be euthanized before day 20 due to large tumor volume. In IDA-TSL plus HT group, 4 out of 6 mice had a complete abrogation of tumor growth during 30 days (IDA-TSL HT *vs* Doxil, $p<0.05$). Mice presented acceptable body weight loss, maximally 15% on day 8-9 after IDA-TSL plus HT treatment, followed by gradual recovery (Figure 10C).

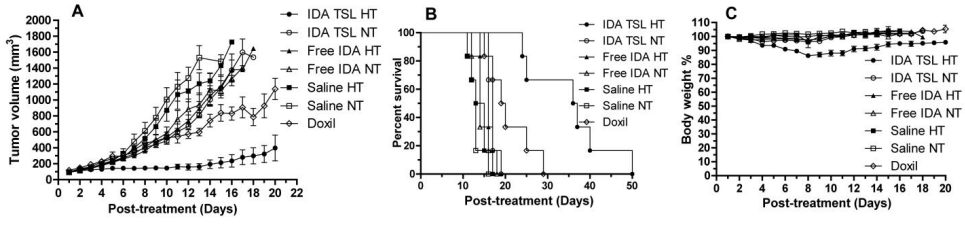

Figure 10. Tumor response in mice treated idarubicin containing thermosensitive liposomes IDA-TSL (circle), free IDA (triangle) and saline (square) in combination with local mild hyperthermia (HT, closed) or normothermia (NT, open), Doxil was used as a standard clinic

comparison (A). Comparison of mice survival rate (B, $p<0.05$ for IDA-TSL HT compared to Doxil) and body weight after treatment (C). Data are represented as mean±SEM, N=6.

4. Discussion

In this study we developed a novel, well-defined idarubicin thermosensitive liposome formulation, which was prepared by applying DPPC/DSPC/DSPE-PEG (6/3.5/0.5 mol%) and using the approach of ammonium EDTA remote drug loading. Approximately 100% of encapsulation efficiency is obtained. This IDA-TSL possesses an ultrafast, triggered release of IDA by applying mild HT (42°C), while a low leakage was observed at body temperature.

Classic liposomal remote loading approaches (such as sodium citrate and ammonium sulfate gradients) induced higher leakage when used to load the hydrophobic anthracycline idarubicin. Ammonium EDTA loading approach, developed by Gubernator *et al*. [39], showed less IDA leakage from liposomes due to the lower water-solubility of IDA-EDTA precipitate compared to other IDA precipitates at pH 4.0-6.5, thus promoting IDA retention inside thermosensitive liposomes.

Cholesterol and paraffin, the highly lipophilic small molecules cholesterol and paraffin, were added in TSL formulation to increase the rigidity of liposomal membrane [48,49], which we speculated may decrease leakage of IDA-TSLs at 37°C. However, the leakage was not diminished but slightly increased at 37°C and retarded release at 42°C, which are probably due to the presence of cholesterol molecules that can increase the liposomal membrane fluidity at temperature below T_m and decrease the membrane fluidity above T_m [50]. Additionally, interaction between IDA and cholesterol by forming complexes also possibly limits IDA release at 42°C [40,51].

Changing the DPPC percentage of the liposomal composition affected two features of IDA-TSL: IDA leakage at 37°C and IDA triggered-release rate at 42°C. Increasing DPPC decreases T_m of liposome membranes. Li *et al*. [41] demonstrated a reduced drug leakage with increasing T_m with DXR-TSLs, which was consistent with the IDA-TSL results at 37°C

shown here (Figure 2B). At 42°C, the release rate in our IDA-TSL formulation is thought to be determined by the boundary density between gel phase and liquid phase. Liposomes with different T_m cause different densities of gel-liquid boundaries at a given temperature. TSL60 is supposed to produce the highest gel-liquid boundary densities for IDA efflux at 42°C, which exhibited the fastest release rate in the four formulations. TSL70, due to a relatively low T_m, is believed to possess excessive liquid phase in the membrane at 42°C, leading to relatively less boundary density for drug release. From the temperature-release, TSL70 showed complete release at 41°C (Figure 5), suggesting that at 41°C the optimal density of gel-liquid boundary for IDA ultrafast release is achieved. Similarly, the trend can be explained in the same way for TSL80 with a lower T_m. For the same reason, relatively slow release of TSL50 is due to insufficient liquid phase to yield enough gel-liquid boundaries at 42°C. Increasing lipophilic DSPC also explains the incomplete IDA release at 42°C in TSL50, owing to the more incorporation of IDA in bilayer. TSL50 showing almost 100% release when temperature was raised to 45°C (see Figure 5), can be attributed to further enhanced densities of gel-liquid boundary, which was also confirmed by our previous work on DXR [41].

We suspected that IDA-TSL stability is proportional to the ability to form IDA precipitate by EDTA anions. In other words, if more stages of ionization of EDTA are generated by increasing internal liposomal pH (EDTA pK_{a1}=2.07, pK_{a2}=2.75, pK_{a3}=6.24, and pK_{a4}=10.34), then EDTA anions could produce stronger electrostatic forces to IDA cations, thereby forming more stable IDA precipitate. However, we observed no obvious improvement, which might be because the solubility of IDA-EDTA precipitation was also increased by higher pH [39], thus “neutralizing” the benefit of enhanced electrostatic force.

Many investigators pointed out that decreasing liposomal size increases the membrane curvature and causes looser packing of bilayer, thus leading to faster content release [47,48]. According to the molecular dynamics simulation study on lipid bilayer, Tieleman *et al*. found that lipids escaping from a monolayer (termed as hydrophobic defect) caused lateral diffusion of lipids and membrane fusion, consequently leading to thinning of the bilayer in defect regions [52]. Based on this, we believe

that more lipid loss occurs in smaller liposome as a result of increased curvature, thus resulting in stronger membrane fusion. We speculate these thinning membranes in defect regions are beneficial to penetration of hydrophilic molecules, which is also concluded by Hossann *et al* [47]. Hence, IDA-TSLs with various sizes exhibited more or less the same leakage at 37 °C possibly because of the high hydrophobicity of IDA. It is not clear why 130 nm-IDA-TSL demonstrated a little drop after maximum release at 42°C, however, based on the conclusion of Tieleman *et al*. [52], small liposomes exhibit more contracted acyl chains than the large ones in defect regions (which are also the drug release regions). We speculate that the released IDA is more prone to adsorb back to the lipophilic acyl tails in the larger liposome bilayer, resulting in drop on fluorescent density.

Most of the IDA-TSL formulations exhibited a property in common: ultrafast release at 42°C. Though underlying reason is currently not clear, the release profiles of IDA-TSLs are comparable to DXR-LTSL which incorporates lysolipids. We speculate that IDA-TSL is likely to have similar ultrafast release mechanism. It is believed that lysolipids, surfactant-like lipids, can form nano pores (~10 nm [16]) at T_m allowing rapid release [15,16,53,54]. The hydrophobic nature of IDA enhances interaction with the liposomal membrane and as such may affect triggered release. Gallois *et al*. found IDA was prone to form self-association of 2-3 molecules in lipid bilayer [51]. According to the size measurement of DXR molecule of ~2.5 nm [54], the IDA di-/trimers are therefore considered as ~5-7.5 nm in size because of their similar structures. The large vacancies left by released IDA di-/trimers will probably be used as pores to facilitate the ultrafast and massive release of IDA from liposomal interior. The grain boundaries as a result of lipid chain mismatches have a pre-phase transition at $<T_m$ [53,54], we believe the incorporation of IDA in the membrane increases these boundary defects, possibly causing a further pre-phase transition at these grain boundaries. Hence, an initial release can be observed in all IDA-TSL formulations at 37°C. For the same reason, the gradually growing leakage of IDA from ~31°C, demonstrated by the temperature-dependent release assay (Figure 5), can be explained by the pre-phase transition happening at these grain boundaries as well. We hypothesize that the release of IDA from TSL at 37°C is a feature of hydrophobic IDA. Liposomes of a relative non-

thermosensitive nature (DSPC/DSPE-PEG:9.5/0.5, Table1 formulation 15 and Supplementary Figure 1), released around 10% after 1 h incubation in FCS at 37 and around 20% at 42°C. we speculate that IDA associated with the liposomal membrane is released instantly when exposed to full FCS, while IDA contained as a crystal in the liposomal core is released at transition temperature. Hydrophobic drugs tend to accumulate more in the lipophilic membrane during drug loading process, this, at least in full FCS environment, will give rise to a relatively higher release from liposomal formulations, which is also seen with for instance vincristine [55].

As TSL have a higher propensity of instability preparation and storage have a more profound impact on product quality. General precautions which improve liposome stability are storage under nitrogen or inert gas such as argon to prevent oxidation. Also antioxidants can be used for this. Coating of liposomes with PEG or applying a charge can prevent liposome aggregation and fusion. Addition of cholesterol may increase stability but this will affect the thermosensitive nature of the particle (such as the results in IDA-TSL). To stabilize TSL storage at 4°C is recommended. We observed less than 1% release of IDA from TSL over a 8-week period in HEPES buffer at 4°C.

Uptake of IDA by tumor cells was affected by DPPC content and loading buffer used. Although most of the formulations showed fast to ultrafast release at 42°C and comparable leakage at 37°C, cells accumulated less idarubicin from IDA-TSL50 compared to others at 42°C (Figure 8C, which is supported by the flow cytometry results (Figure 8A,B)). However, when applied *in vivo* performance of TSL seem to be less influenced by small differences in stability and release rate, as we observed with doxorubicin-based TSL, which is most likely due to the more complex nature of the *in vivo* setting. Increased stability and limited release of content at 37°C reduces side-effects and improve efficacy. Moreover, fast local triggered release and rapid cellular uptake augments tumor response. Optimization of IDA-TSL will therefore improve performance *in vivo*. Systemic leakage at 37°C of all formulations is within a range which is not likely to cause a difference in tumor response, although systemic toxicity may vary. Additionally, IDA is released maximally and within a very short time frame from all formulations when HT is applied. As IDA is released by HT this quick and high local levels

can therefore be expected the drug needs to act also quickly on the cells. We hypothesize that these particular drug kinetics may therefore be a more dominant determinant in *in vivo* efficacy.

The *in vitro* studies (cytotoxicity, flow cytometry and confocal imaging) display a more striking and significant reduction in activity of IDA-TSL exposed to 37°C compared to 42°C. These findings suggest that IDA-TSL releases less at body temperature, leading to reduced toxicity in absence of mild HT. When mild HT induced complete drug release from IDA-TSL, comparable chemotherapeutic efficacy was observed *in vitro* to free IDA (Figure 7, Table 2). As expected, *in vivo* drug release was negligible before mild HT. However, with increasing temperature to 42°C, IDA-TSL showed a triggered, intravascular IDA release, followed by IDA penetration toward interstitial space and tumor cell uptake (Figure 9). Rapid and profound release in the heated region explains the strong tumor response to IDA-TSL in combination with HT, while no objective tumor response was observed when no HT was applied [Figure 10]. IDA-TSL also performed better than a dosing schedule with Doxil, of which the later inflicted only some tumor growth delay. This is most likely due to the intrinsic higher stability of Doxil resulting in slow release of its contents and therefore poor intratumoral concentrations of bioavailable drug [10]. Albeit the reason of IDA accumulation in extra-nuclei instead of intra-nuclei is not clear yet [Figure 8,9], the same observation was confirmed by Ma *et al* [33]. The work of Zohreh *et al*. [56], who found IDA had low binding affinity to chromatin, indicated that less aggregation of IDA with chromatin occurs inside cells compared with DXR. Therefore, we surmise the extra-nuclei accumulation of IDA can be ascribed to its high hydrophobicity.

Conclusion

In this study we successfully developed a novel and well-designed idarubicin temperature-sensitive liposome formulation, which demonstrates low leakage at physiological temperature and ultrafast triggered drug release under mild HT. The significant difference in *in vitro* studies between IDA-TSL with or without mild HT and desirable *in vivo* intravascular drug release by local mild HT explains the profound

tumor response found in BLM tumor-bearing mice compared to the free drug and Doxil treated mice. These results indicate the potential of IDA-TSL for further development in combination with HT. Further investigation is currently performed to unravel the underlying ultrafast release mechanism at 42°C and on the optimal therapeutic efficacy of IDA-TSL in different solid tumors.

Acknowledgement

We thank Joost Rens and Cindy Vermeulen for their kind help in our animal work and appreciate Prof. Holger Gruell and his team with the cryo-TEM imaging.

Supporting data

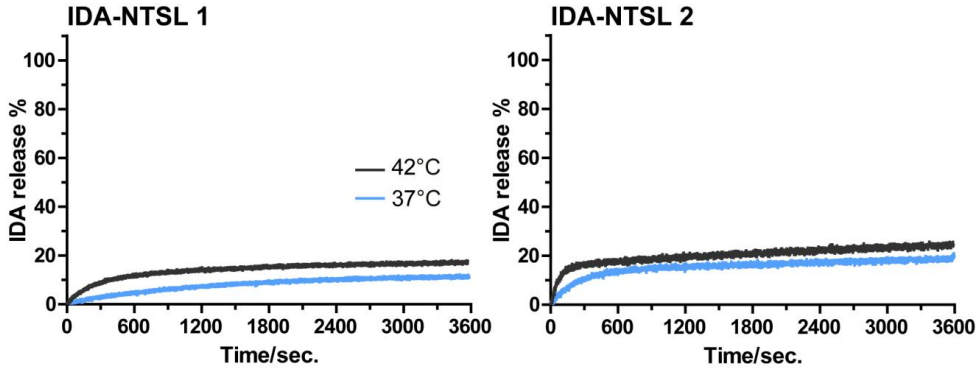

Supplementary Figure 1. The release profiles of idarubicin (IDA) containing non-thermosensitive liposomal formulations at 37°C (blue) and 42°C (black) in FCS for 1 h. IDA-NTSL 1 (left) was composed of DSPC/DSPE-PEG: 9.5/0.5. IDA-NTSL 2 (right) was composed of HSPC/Cholesterol/DSPE-PEG: 5.5/4/0.5. (Three independent tests were performed. A representative release profile is shown.)

Reference

[1] T.S. Hauck, T.L. Jennings, T. Yatsenko, J. C. Kumaradas, W.C.W. Chan, Enhancing the toxicity of cancer chemotherapeutics with gold nanorod hyperthermia, Adv. Mater. 20 (2008) 3832-3838.
[2] P. E. Kintzel, R.T. Dorr, Anticancer drug renal toxicity and elimination: dosing guidelines for altered renal function, Cancer Treat. Rev. 21 (1995) 33-64.
[3] P.K. Singal, N. Iliskovic, Doxorubicin-induced cardiomyopathy, N. Engl. J. Med. 339 (1998) 900-905.
[4] K.N. Bhinge, V. Gupta, S.B. Hosain, S.D. Satyanarayanajois, S.A. Meyer, B. Blaylock, Q.J. Zhang, Y.Y. Liu, The opposite effects of doxorubicin on bone marrow stem cells versus breast cancer stem cells depend on glucosylceramide synthase, Int. J. Biochem. Cell Biol. 44 (2012) 1770–1778.
[5] Y. Matsumura, H. Maeda, A new concept for macromolecular therapeutics in cancer chemotherapy; mechanism of tumoritropic accumulation of proteins and the antitumor agent SMANCS, Cancer Res. 46 (1986) 6387-6392.
[6] T.M. Allen, P.R. Cullis, Liposomal drug delivery systems: From concept to clinical applications, Adv. Drug Deliv. Rev. 65 (2013) 36-48.
[7] Y. Barenholz, Doxil®- the first FDA-approved nano-drug: lessons learned, J. Control. Release 160 (2012) 117-134.
[8] C. E. Petre, D.P. Dittmer, Liposomal daunorubicin as treatment for Kaposi's sarcoma, Int. J. Nanomedicine 2 (2007) 277-288.
[9] G. Batist, G. Ramakrishnan, C.S. Rao, A. Chandrasekharan, J. Gutheil, T. Guthrie, P. Shah, A. Khojasteh, M.K. Nair, K. Hoelzer, K. Tkaczuk, Y.C. Park, L.W. Lee, Reduced cardiotoxicity and preserved antitumor efficacy pf liposome-encapsulated doxorubicin and cyclophosphamide compared with conventional doxorubicin and cyclophosphamide in a randomized , multicenter trial of metastatic breast cancer, J. Clin. Oncol. 19 (2001) 1444-1454.
[10] A.L.B. Seynhaeve, B.M. Dicheva, S. Hoving, G.A. Koning, T.L.M. ten Hagen, Intact Doxil is taken up intracellularly and released doxorubicin sequesters in the lysosome: evaluated by in vitro/ in vivo cell imaging, J. Control. Release. 172 (2013) 330-340.

[11] M. B. Yatvin, J. N. Weinstein, W. H. Dennis, R. Blumenthal, Design of liposomes for enhanced local release of drugs by hyperthermia, Science 202 (1978) 1290-1293.
[12] M. B. Yatvin, H. Muhlensiepen, W. Forschen, J. N. Weinstein, L. E. Feinendegen, Selective delivery of liposome-asociated cis-dichlorodiammine platinum (II) by heat and its influence on tumor drug uptake and growth, Cancer Res. 41 (1981) 1602-1607.
[13] G. Kong, M.W. Dewhirst, Hyperthermia and liposomes, Int. J. Hyperthermia 15 (1999) 345-370.
[14] D. Needham, G. Anyarambhatla, G. Kong, M.W. Dewhirst, A new temperature-sensitive liposome for use with mild hyperthermia: characterization and testing in a human tumor xenograft model, Cancer Res. 60 (2000)1197–1201.
[15] J.K. Mills, D. Needham, Lysolipid incorporation in dipalmitoylphosphatidylcholine bilayer membranes enhances the ion permeability and drug release rates at the membrane phase transition, Biochim. Biophys. Acta 1716 (2005) 77-96.
[16] D. Needham, J.Y. Park, A.M. Wright, J.H. Tong, Materials characterization of the low temperature sensitive liposome (LTSL): effects of the lipid composition (lysolipid and DSPE–PEG2000) on the thermal transition and release of doxorubicin, Faraday Discuss. 161 (2013) 515-534.
[17] http://clinicaltrials.gov/ct2/results?term=thermodox.
[18] L. Li, T.L.M. ten Hagen, M. Hossann, R. Suss, G.C. van Rhoon, A.M.M. Eggermont, D. Haemmerich, G.A. Koning, Mild hyperthermia triggered doxorubicin release from optimized stealth thermosensitive liposomes improves intratumoral drug delivery and efficacy, J. Control. Release 168 (2013) 142-150.
[19] G.N. Chiu, S.A. Abraham, L.M. Lckenstein, G. Karlsson, K. Edwards, E.K. Wasan, M.B. Bally, Encapsulatuon of doxorubicin into thermosensitive liposomes via complexation with transition metal manganese, J. Control. Release 104 (2005) 271-288.
[20] B. Banno, L.M. Lckenstein, G.N. Chiu, M.B. Bally, J. Thewalt, E. Brief, E.K. Wasan, The functional roles of poly-(ethylene glycol)-lipid and lysolipid in the drug retention and release from lysolipid-containing thermosensitive liposomes *in vitro* and *in vivo*, J. Pharm. Sci. 99 (2010) 2295-2308.

[21] S.M. Park, M.S. Kim, S.J. Park, E.S. Park, K.S. Choi, Y.S. Kim, H.R. Kim, Novel temperature-triggered liposome with high stability: Formulation, *in vitro* evaluation, and *in vivo* study combined with high-intensity focused ultrasound (HIFU), J. Control. Release 170 (2013) 373-379.
[22] M. de Smet, S. Langereis, S. van den Bosch, H. Grull, Temperature-sensitive liposomes for doxorubicin delivery under MRI guidance, J. Control. Release 143 (2010) 120-127.
[23] K.J. Chen, H.F. Liang, H.L. Chen, Y.C. Wang, P.Y. Cheng, H.L. Liu, Y.N. Xia, H.W. Sung, A thermoresponsive bubble-generating liposomal system for triggering localized extracellular drug delivery, ACS Nano 7 (2013) 438-446.
[24] A.A. Manzoor, L.H. Lindner, C.D Landon, J. Park, A.J. Simnick, M.R. Dreher, S. Das, G.A. Koning, T.L.M. tenhagen, D. Needham, M.W. Dewhirst, Overcoming limitations in nanoparticle drug delivery: triggered, intravascular release to improve drug penetration into tumors, Cancer Res. 72 (2012) 5566-5575.
[25] J.K. Mills, D. Needham, The materials enginnering of temperature-sensitive liposomes, Methods Enzymol. 387 (2004) 82-113.
[26] D. Crivellari, D. Lombardi, S. Spazzapan, A. Veronesi, G. Toffoli, new oral drugs in older patients: a review of idarubicin in elderly patients, Crit. Rev. Oncol. Hematol. 49 (2004) 153-163.
[27] A. Casazza, A. Di Marco, G. Bonadonna, V. Bonfante, C. Bertazzoli, O Bellini, G. Pratesi, L. Sala, L. Ballerini, Effects of modifictions in position 4 of the chromophore or in position 4' of the aminosugar, on the antitumor activity and toxicity of daunorubicin and doxorubicin, Anthracyclines: Current status and New Developments, Academic Press Inc., New York, 1980, pp. 403-430.
[28] P.H. Wiernik, P.L. Banks, D.C. Case Jr., Z.A. Arlin, P.O. Periman, M.B. Todd, P.S. Ritch, R.E. Enck, A.B. Weitberg, Cytarabine plus idarubicin or daunorubicin as induction and consolidation therapy for previously untreated adult patients with acute myeloid leukemia, Blood 79 (1992) 313-319.
[29] E. Berman, G. Heller, J. Santorsa, S. McKenzie, T. Gee, S. Kempin, S. Gulati, M. Andreeff, J. Kolitz, J. Gabrilove, et al., Results of a randomized trial comparing idarubicin and cytosine arabinoside with daunorubicin and cytosine arabinoside in adult patients with newly diagnosed acute myelogenous leukemia, Blood 77 (1991) 1666-1674.

[30] N. Dos Santos, D. Waterhouse, D. Masin, P.G. Tardi, G. Karlsson, K. Edwards, M.B. Bally, Substantial increases in idarubicin plasma concentration by liposome encapsulation mediates improved antitumor activity, J. Control. Release 105 (2005) 89-105.
[31] E. Willmore, F. Errington, M.J. Tilby, C.A. Austin, Formation and longevity of idarubicin-induced DNA topoisomerase II cleavable complexes in K562 human leukaemia cells, Biochem. Pharmacol. 63 (2002) 1807-1815.
[32] W.R. Vogler, E. Velez-Garcia, R.S. Weiner, M.A. Flaum, A.A. Bartolucci, G.A. Omura, M.C. Gerber, P.L. Banks, A phase III trial comparing idarubicin and daunorubicin in combination with cytarabine in acute myelogenous leukemia: a Southeastern Cancer Study Group, J. Clin. Oncol. 10 (1992) 1103-1111.
[33] P. Ma, X.W. Dong, C.L. Swadley, A. Gupte, M. Leggaas, H.C. Ledebur, R.J. Mumper, Development of idarubicin and doxorubicn solid lipid nanoparticles to overcome Pgp-mediated multiple drug resistance in leukemia, J. Biomed. Nanototechnol. 5 (2009) 151-161.
[34] M.M. Ames, F. Spreafico, Selected pharmacologic charachteristics of idarubicin and idarubicinol, Leukemia 6 (1992) 70-75.
[35] M. Limonta, A. Biondi, G. Giudici, G. Specchia, C. Catapano, G. Masera, T. Barbui, M. D'Incalci, Cytotoxicity and DNA damage caused by 4-demethoxydaunorubicin and its metabolite 4-demethoxy-13-hydroxydaunorubicin in human acute myeloid leukemia cells Cancer Chemother. Pharmacol. 26 (1990) 340–342.
[36] D.J. Roovers, M. van Vliet, A.C. Bloem, H.M. Lokhorst, Idarubicin overcomes *P*-glycoprotein-related multidrug resistance: comparison with doxorubicin and daunorubicin in human multiple myeloma cell lines, Leuk. Res. 23 (1999) 539–548.
[37] R. Testi, L. Mattii, D. Di Simone, L. Zaccaro, G. Malvaldi, B. Grassi, M. Petrini,Evaluation of resistance index of several anticancer agents on parental and resistant P-388 cell lines,Leuk. Res. 19 (1995) 257–261.
[38] P. Slifirski, W. Szelejewski, G. Grynkiewicz, J. Gubernator, A. Kozubek, Liposomal formulation of idarubicin, Acta Pol. Pharm. 60 (2003) 138-140.
[39] J. Gubernator, G. Chwastek, M. Korycinska, M. Stasiuk, G. Grynkiewicz, F. Lewrick, R. Suss, A. Kozubek, The encapsulation of idarubicin within liposomes using the novel EDTA ion gradient method

ensures improved drug retention *in vitro* and *in vivo*, J. Control. Release 146 (2010) 68-75.
[40] N. Dos Santos, L.D. Mayer, S.A. Abraham, R.C. Gallagher, K.A. Cox, P.G. Tardi, M.B. Bally, Improved retention of idarubicin after intravenous injection obtained for cholesterol-free liposomes, Biochim. Biophys. Acta 1561 (2002) 188-201.
[41] L. Li, T.L.M. ten Hagen, A. Haeri, T. Soullie, C. Scholten, A.L.B. Seynhaeve, A.M.M. Eggermont, G.A. Koning, A novel two-step mild hyperthermia for advanced liposomal chemotherapy, J. Control. Release 174 (2014) 202-208.
[42] B.M. Dicheva, T.L.M. ten Hagen, D. Schipper, A.L.B. Seynhaeve, G.C. van Rhoon, A.M.M. Eggermont, G.A. Koning, Targeted and heat-triggered doxorubicin delivery to tumors by dual targeted cationic thermosensitive liposomes, J. Control. Release, 195 (2014) 37-48.
[43] G. Rouser, S. Fkeischer, A. Yamamoto, Two dimentional thin layer chromatographic separation of polar lipids and determination of phospholipids by phosphorus analysis of stops, Lipids 5 (1970) 2491-2499.
[44] P.K. Gupta, F.C. Lam, C.T. Hung, Investigation of the stability of Doxorubicin hydrochloride using factorial design, Drug Dev. Ind. Pharm. 14 (1988) 1657-1671.
[45] V. Vichai, K. Kirtikara, Sulforhodamine B colorimetric assay for cytotoxicity screening, Nat. Protoc. 3(2006) 1112-1116.
[46] J.V. Natarajan, C. Nugraha, X.W. Ng, S. Venkatraman, Sustained-release from nanocarriers: a review, J. Control. Release, in press.
[47] M. Hossann, T. Wang, M. Wiggenhorn, R. Schmidt, A. Zengerle, G. Winter, H. Eibl, M. Peller, M. Reiser, R. D. Issels, L. H. Lindner, Size of thermosensitive liposomes influences content release, J. Control. Release 147 (2010) 436-443.
[48] A. Nagayasu, K. Uchiyama, H. Kiwada, The size of liposomes: a factor which affects their targeting efficiency to tumors and therapeutic activity of liposomal antitumor drugs, Adv. Drug Deliv. Rev. 40 (1999) 75-87.
[49] C. Kirby, J. Clarke, G. Greoriadis, Effect of cholesterol content of smallunilamellar liposomes on their stability in vivo and iv vitro, Biochem. J. 186 (1980) 591-598.
[50] L. Coderch, J. Fonollosa, M. De Pera, J. Estelrich, A. De La Maza, J.L. Parra, Influence of cholesterol on liposome fluidity by EPR

relationship with percutaneous absorption, J. Control. Release 68 (2000) 85-95.
[51] L. Gallois, M. Fiallo, A. Garnier-Suillerot, Comparison of the interaction of doxorubicin, daunorubicin, idarubicin and idarubicinol with large unilamellar vesicles: Circular dichroismstudy, Biochim. Biophys. Acta 1370 (1998) 31-40.
[52] D.P. Tieleman, J. Bentz, Molecular dynamics simulation of the evolution of hydrophobic defects in one monolayer if a phosphatidylcholine bilayer: Relevance for membrane fusion mechanisms, Biophys. J. 83 (2002) 1501-1510.
[53] D. Needham, M.W. Dewhirst, The development and testing of a new temperature-sensitive drug delivery system for the treatment of solid tumors, Adv. Drug Deliv. Rev. 53 (2001) 285-305.
[54] C.D. Landon, J.Y. Park, D. Needham, M.W. Dewhirst, Nanoscale drug delivery and hyperthermia: The materials design and preclinical and clinical testing of low temperature-sensitive liposomes used in combination with mild hyperthermia in the treatment of local cancer, Open Nanomed. J. 3(2011) 38-64.
[55] J.X. Cui, C.L. Li, C.X. Wang, Y.H. Li, L. Zhang, L. Zhang, X. Xiu, Y.F. Li, N. Wei, Development of pegylated liposomal vincristine using novel sulfobutyl ether cyclodextrin gradient: is improved drug retention sufficient to surpass DSPE-PEG-induced drug leakage, J. Pharm. Sci. 100 (2011) 2835-2848.
[56] Z. Zahraei, A. R. Chadegani, A comparison of the effect of anticancer drugs, idarubicin and adriamycin, on soluble chromatin, Eur. J. Pharmacol. 575 (2007) 28–33.

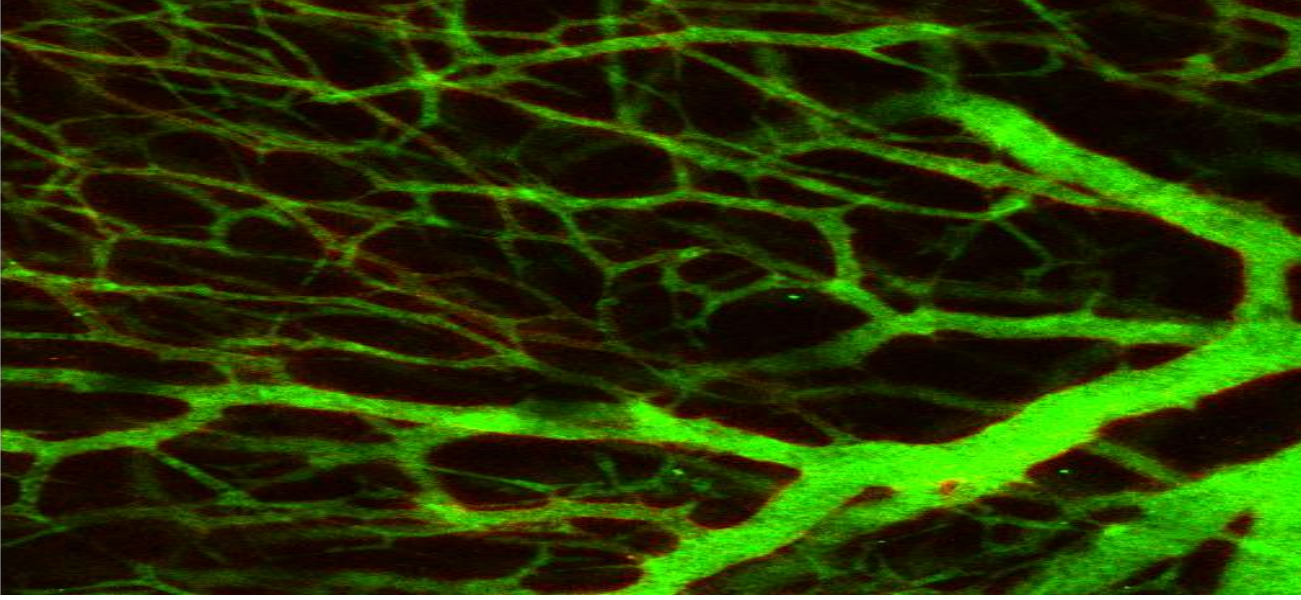

Chapter 3

Thinking out of nanoparticle: Externally triggered smart drug delivery systems demand chemotherapeutics with kinetics superior for local delivery

Tao Lu, Dieter Haemmerich, Hui Liu, Ann L.B. Seynhaeve, Gerard van Rhoon, Adriaan B. Houtsmuller, Timo L.M. ten Hagen*

Under revision

Abstract

Increasing the bioavailable drug level in a tumor is key to enhance efficacy of chemotherapy. Heat-sensitive smart drug delivery systems (SDDS) in combination with local hyperthermia facilitate high local drug levels, thus improving uptake in the tumor. However, inability to rapidly and efficiently absorb the locally released drug results in reduced efficacy, as well as undesired redistribution of the drug away from the tumor to the system. Based on this paradigm we replaced doxorubicin (DXR), thus far the most used drug for nanocarrier-based delivery, with idarubicin (IDA), a hydrophobic anthracycline used solely for treatment hematologic cancers, and observed significantly higher activity compared to DXR, when formulated in thermosensitive SDDS. IDA is taken up over 10 times more rapidly by cancer cells than DXR *in vitro*, resulting in 4-times higher whole tumor drug uptake *in vivo* of IDA vs. DXR at the same dose. This fast triggered release and rapid uptake of IDA yielded an improved intratumoral drug distribution, translating into superior tumor response compared to DXR-SDDS treatment at same dose. Thus, IDA – a drug that is not used for treatment of solid cancers, showed superior local delivery kinetics and therefore improved therapeutic index when administered in externally triggered SDDS. Taken together, we show that a shift in selection of chemotherapeutics is needed away from the classic drugs choice towards selection based on properties of a chemotherapeutic in context of the nanoparticle and delivery mode.

Keywords: Smart drug delivery system, thermosensitive liposomes, Idarubicin, Doxorubicin, efficacy, intratumoral distribution

Introduction

Tumor response is largely determined by the ability to deliver sufficient drug levels at the target site [1, 2]. Conventional chemotherapy relies on systemic administration of cytotoxic agents which are transported by the bloodstream to a tumor site. This non-selective delivery of drugs leads to marginal accumulation in the tumor and dose-limiting side-effects, which causes the therapy to be inefficient and therapy-related morbidity [3]. Encapsulation of chemotherapeutics in nano-carriers provides a possibility to increase drug levels in tumor and improve pharmacokinetics while diminishing side-effects, but has so far limited impact on efficacy [4-9]. The disappointing efficacy of classic drug delivery carriers can be attributed to two main reasons - limited accumulation of these nano-carriers in tumor and slow drug release from these carriers. Currently approved nano-carriers depend largely on the enhanced permeability and retention (EPR) effect of solid tumors, allowing the nanoparticles to passively accumulate in tumor interstitial [10]. Importantly, the existence of an EPR effect, in particular in human tumors, is under debate [11-14]. Moreover, we and other show that nano-carriers used for chemotherapy are often relatively stable even when taken up by tumor cells, resulting in inadequate levels of bioavailable drug impairing therapeutic efficacy [6, 9, 14-16].

Smart drug delivery systems (SDDS), therefore, have been developed where content release can be activated by an external trigger, enabling drug delivery of a high concentration to a relatively small tissue volume and in short time-frame, thus improving bioavailable drug level in the tumor. Thermosensitive liposomes are the most advanced type of such triggered SDDS [17-20]. When thermosensitive SDDS enter an externally induced hyperthermic tumor (e.g. 42°C), the encapsulated drug is rapidly and massively released within the tumor vasculature, resulting in high local drug concentrations and promoting the subsequent drug uptake by tumor cells [21]. While at body temperature these SDDS are relative stable and encapsulated drug is retained during circulation.

Doxorubicin (DXR), due to its wide antitumor activity and profitable characteristics for encapsulation, has been the preferred drug for encapsulation in thermosensitive nano-carriers. With these systems, impressive drug levels have been achieved in particular when used in a so-called intravascular release setting [19-24]. This success changed the playing field as now local drug concentrations that high that the tumor cells cannot absorb the drug fast enough and redistribution throughout the body occurs. To enable maximum performance of externally-triggered SDDS-mediated drug delivery, the released drug should almost instantly enter tumor cells and should be retained to prevent washout. At present, encapsulated drugs in nano-carriers are typically selected based on clinical efficacy for a particular tumor type, for which these drugs are commonly used in the free form. We propose to use chemotherapeutics which are ideal for loco-regional treatment, with favorable cellular uptake rate (e.g. more hydrophobic) for SDDS-mediated drug delivery. Based on this paradigm we selected idarubicin (IDA), a hydrophobic anthracycline similar to DXR, which is solely used for hematologic cancers, to formulate IDA-SDDS. Here, we in depth compared IDA-SDDS and DXR-SDDS drug release, cellular uptake, intratumoral distribution and antitumor activity, and show the need for better selection of therapeutics for SDDS-mediated intratumoral delivery.

Results

IDA shows faster cellular uptake and longer retention

To assess the cellular uptake and retention of IDA and DXR, cells were exposed to the free drug at the same concentration. We show that IDA accumulation reached approximately 40% of the available drug in 5 min, followed by saturation within 0.5-1 h. DXR uptake was marginal during the first half hour and reached maximum after 4 hours of exposure (Fig. 1A, Supplementary Fig. 1A). An overall 16-fold faster cellular uptake

was observed for IDA compared to DXR (Supplementary Fig. 1b). Also, a prolonged retention of IDA in tumor cells compared to DXR was observed (Fig. 1B), together suggesting that idarubicin could be a better drug for delivery with SDDS.

These results were confirmed when comparing release from and cytotoxic activity of DXR-SDDS and IDA-SDDS *in vitro*. We observed a fast release and sequential uptake by cells of IDA from SDDS after exposed to 42°C, at a level 4-fold higher compared to DXR-SDDS (Fig. 1C, D). Interestingly, IDA locates predominantly in the cytoplasm [25, 26], while DXR transfers mostly to the nucleus (Supplementary Fig. 1C). Nevertheless, IDA is 5 to 20-fold more cytotoxic to the tested cancer cells *in vitro* (Supplementary Fig. 1D and Supplementary Table 1).

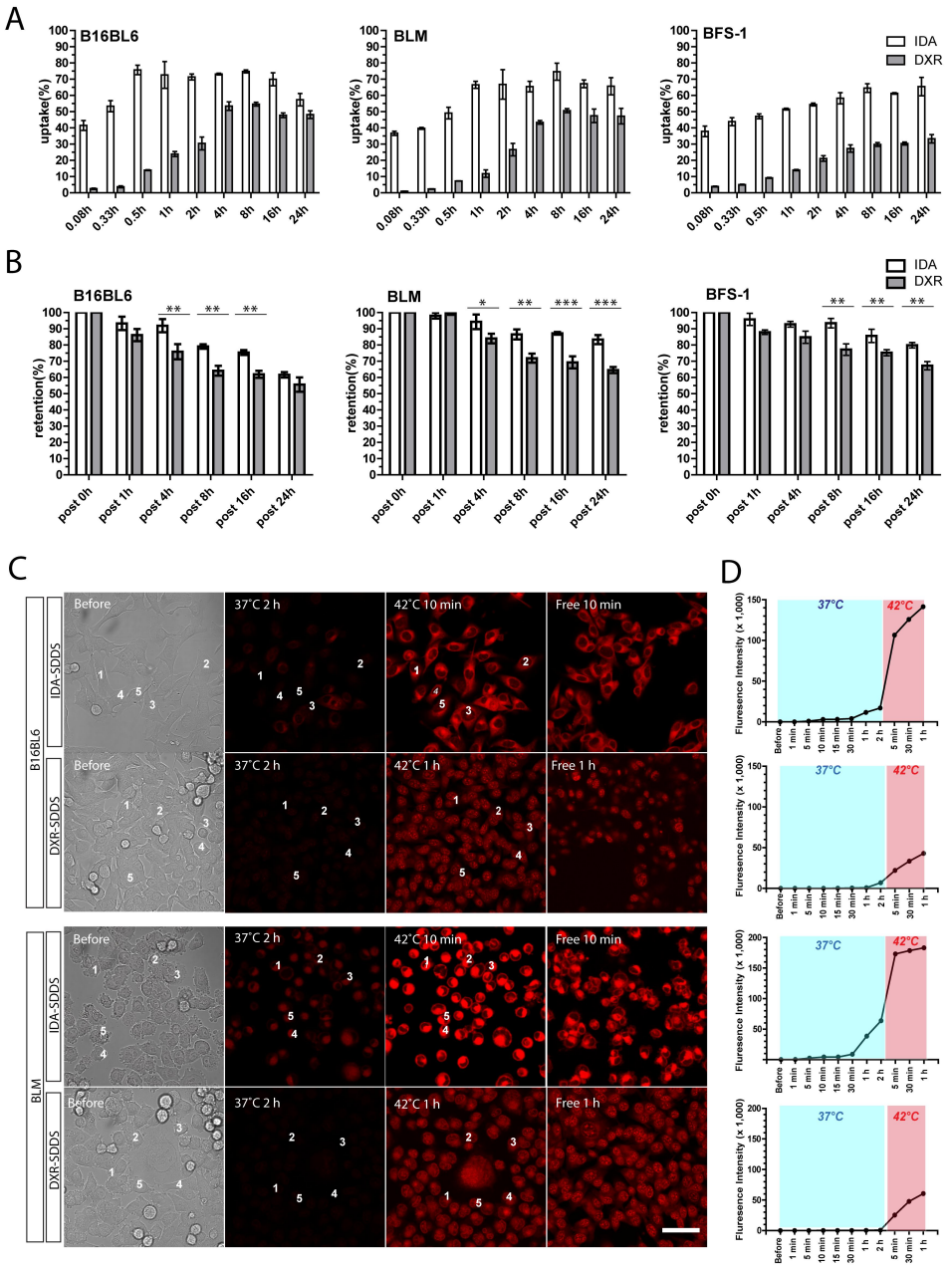

Figure 1. Faster and higher idarubicin (IDA) uptake by tumor cells in vitro compared to doxorubicin (DXR). (**A**) B16BL6 (left), BLM (middle) and BFS-1 (right) cells display faster uptake of free IDA than DXR (red,

n = 4 per cell line). (**B**) Extended cellular retention of free IDA is observed compared to DXR (n = 3 per cell line, Nonparametric Mann-Whitney test: $*p < 0.05$, $**p < 0.03$, $***p < 0.01$). Data are presented as mean ± SD. (**C**) On-line confocal microscopy images of IDA and DXR uptake by B16BL6 (upper) and BLM (lower) after release from SDDS when exposed for 2 h to 37°C followed by 1 h at 42°C. Settings: gain = 600, resolution = 512 × 512. Scale bar, 50 µm. (**D**) Five cells are randomly selected in (**c**) to track accumulation of IDA or DXR, upon release from SDDS, in tumor cells in time. Data are presented as fluorescent intensity of these 5 cells.

IDA is efficiently released from SDDS and, shows increased tumor uptake compared to DXR

Delivery of bioavailable, (i.e. free, released) drug in the intravascular release setting is dependent on the amount of SDDS-encapsulated drug passing through the heated region, as well as the time these SDDS are exposed to 42°C. Release kinetics need therefore to be fast. We observed *in vitro* that 100% of the IDA is released in response to 42°C within a matter of seconds from the SDDS used here, which is desired for intravascular release-based therapy, and is faster than DXR release that takes around 1-2 min to reach complete release (Supplementary Fig. 2A, B). To test release efficiency *in vivo*, tumor-bearing mice were exposed to HT of the tumor alone and injected systemically with IDA- or DXR-SDDS. We observed almost complete depletion of IDA from circulation 1 h after injection of 2.7 µmol/kg IDA-SDDS in HT treated mice, indicating that most SDDS must have passed the heated region with almost complete release of IDA from the SDDS (Fig 2A). In contrast, after 1 h of HT still 24% of injected DXR was present in the circulation indicating a less complete release from SDDS. On the other hand, in mice in which tumors were kept at 37°C most drug remained circulating, and thus encapsulated. Comparable results for both IDA and DXR were

obtained also at the higher dose of 9 µmol/kg (Fig. 2B). Drug accumulation in tumor 30 min after 1 h HT was 15.4±3.5 nmol per gram tumor for IDA and 4.5±0.5 nmol/g tumor for DXR (Fig. 2C). Similarly, significantly increased tumor accumulation of IDA was observed also when a high dose of 9 µmol/kg was administered (Table 1). Overall we observed a 3.8 to 4.4-fold higher accumulation of IDA compared to DXR within the first 24 h when delivered by SDDS in HT treated mice (Fig. 2D).

Table 1. Accumulation of idarubicin and doxorubicin in tumors when delivered by SDDS in combination with hyperthermia. Data are presented as mean ± SD, N = 3.

	Uptake efficiency (%ID/g tumor)		Uptake absolute quantity (nmol/g tumor)	
	#Low dosage	High dosage	Low dosage	High dosage
IDA	13.6±2.2*	13.0±3.6*	15.4±3.5*	43.8±9.7*
DXR	4.5±0.4	8.4±0.7	4.2±0.5	25.2±2.2

Low dosage: 2.7 µmol/kg; High dosage: 9 µmol/kg.
IDA: idarubicin, DXR: doxorubicin.
*Nonparametric Mann-Whitney test, $p < 0.05$.

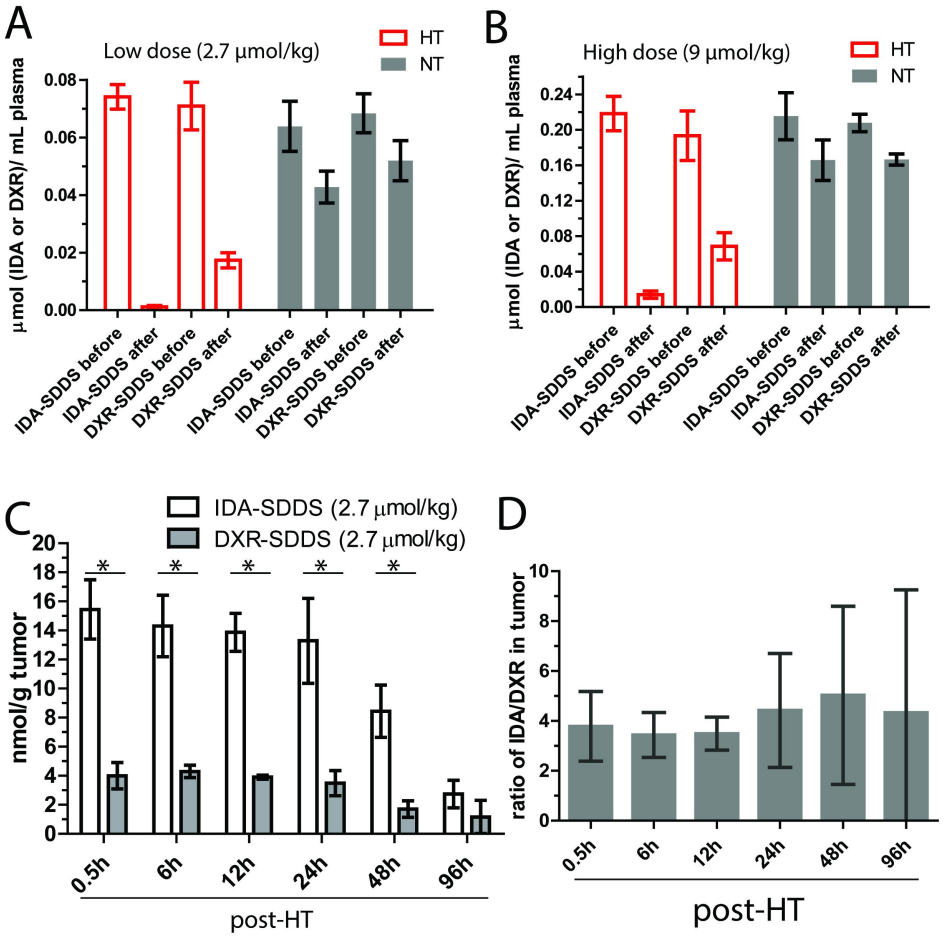

Figure 2. IDA-SDDS show a higher efficiency of content release in vivo than DXR-SDDS under HT and IDA shows higher tumor uptake. (**A, B**) Plasma drug concentration comparisons before and after 1 h local hyperthermia (HT) (42°C) or normothermia (NT) (37°C) in BFS-1 tumor bearing mice treated with low dose (**A**) or high dose (**B**) SDDS ($n \geq 3$ mice per group). Complete release is observed with IDA-SDDS plus HT. (**C**) Under HT, tumors take up released IDA more efficiently and maintained a higher drug level during 48 h post treatment compared to DXR ($n \geq 3$ mice per group, Nonparametric Mann-Whitney test: * $p < 0.03$). (**D**) The ratio of tumor drug concentration between IDA and DXR calculated from (**C**) gradually increases within 48 h after treatment,

confirming longer retention of IDA in cell after uptake. Data are represented as mean ± SD.

Intravital imaging illustrates improved IDA-SDDS release and distribution in tumor compared to DXR-SDDS

While total drug accumulation may provide some indication of possible outcome, another important aspect is intratumoral distribution [7, 14]. We applied intravital microscopy to gain insight in intratumoral drug distribution kinetics and profile in real time. We observed accelerated accumulation of IDA, preferentially around tumor-associated vessels with IDA-SDDS in HT treated mice compared to DXR-SDDS (Fig. 3A, B; Supplementary Video 1, 2). After around 35 min of treatment maximum IDA uptake of 6.0×10^{-8} nmol/pixel was reached at 60 µm from the nearest vessel (Fig. 3C). In contrast, only after 55 min maximum uptake of DXR was reached with a concentration of 0.7×10^{-8} nmol/pixel at 60 µm (Fig. 3D). Together, this results likely in a higher degree of DXR dilution and a lower drug concentration compared to IDA, and thus an insufficient cell kill. Detailed analysis of drug uptake rate and drug loss kinetics show a 10-fold faster uptake of IDA compared to DXR before reaching saturation (Fig. 3E). Redistribution of IDA seems to occur for a period of about 15 min before reaching a steady state, showing a 12.6% loss compared to 17.0% of DXR. However, likely due to difference in absolute levels a 4-fold faster loss of IDA than DXR was observed (Fig. 3F). Profile analysis of temporal intratumoral drug distribution confirms these observation indicating that maximum uptake is reached earlier with IDA as compared to DXR (Fig. 3G, H).

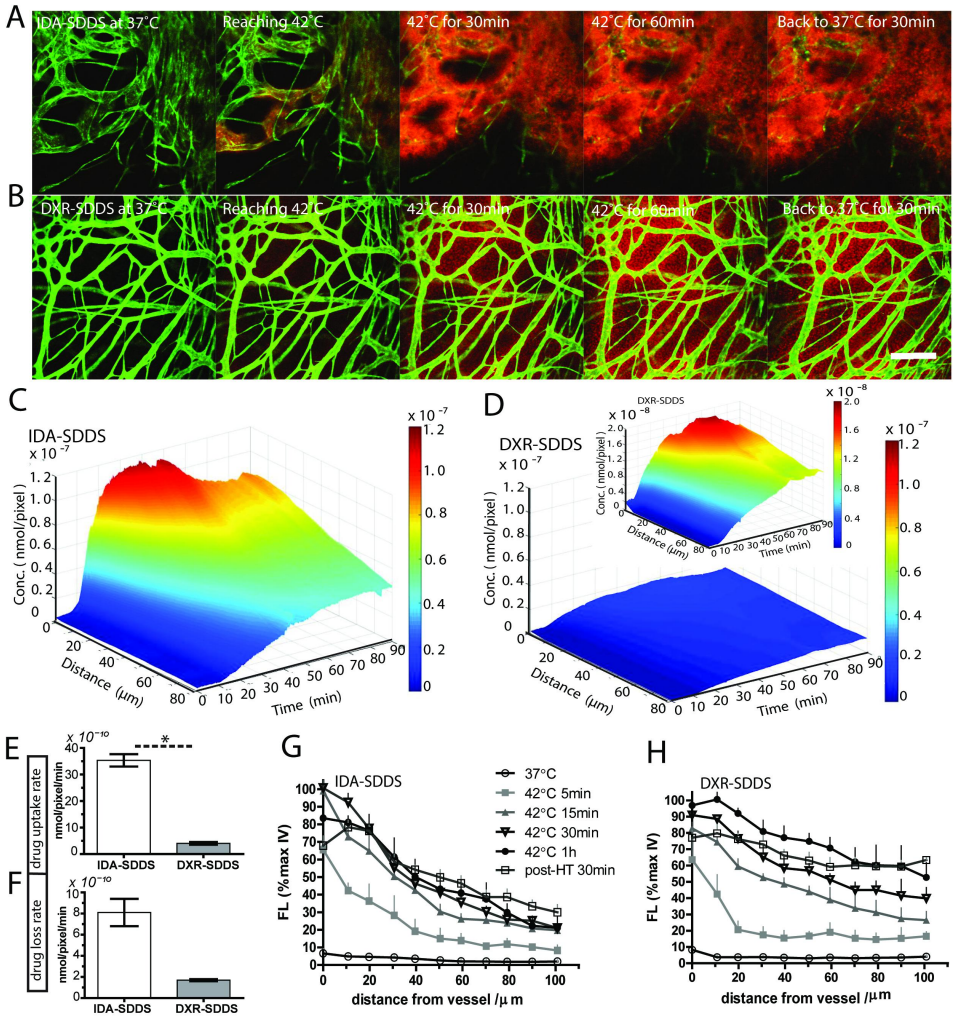

Figure 3. Rapid release from SDDS and uptake by tumor cells of idarubicin (IDA) results in high local drug levels and a steep intratumoral gradient. (**A, B**) Imaging of heat-triggered release in a window chamber fixed on eNOS-Tag-GFP mice showing green vessels. Eighteen µmol/kg of IDA-SDDS (**A**) or DXR-SDDS (B) was injected followed by 1 h local hyperthermia and 30 min normothermia, showing intravascular release of drug (red) and the subsequent drug diffusion into interstitial space of tumor. Scale bar, 200 µm. (**C, D**) 3-dimensional representation of

intratumoral drug concentration, as a factor of time and penetration distance into tumor tissue from the nearest vessel, shows higher tumor uptake of IDA (**c**) than DXR (**D**) during the treatment course (insert represents DXR concentration at a smaller scale). Maximum uptake was reached earlier for IDA showing higher drug accumulation close to tumor vessels compared to DXR (n = 3 mice per group). (**E**) Online IDA and DXR uptake rates are calculated starting from 10 to 30 min during HT, after which IDA uptake enters a saturation state (n = 3 mice per group, Nonparametric Mann-Whitney test: $*p < 0.01$). (F) Drug efflux is calculated from the peak concentration to the beginning of the steady concentration. IDA shows around 15 min of drug efflux after which a steady concentration was maintained. (**G, H**) At specified time points, release and diffusion profiles of IDA-SDDS (**G**) and DXR-SDDS are depicted (**H**). Data are presented as mean ± SD.

IDA-SDDS improves intratumoral distribution and drug concentration, enhancing therapeutic efficacy

Homogeneous distribution is preferred if levels are sufficiently high to kill all tumor cells. High accumulation around vessels may not only kill tumor cells but also tumor-associated vasculature and therefore inflict a strong tumor response [27, 28]. In agreement with the intravital data, in histological sections of tumors high levels of intracellular IDA were present around tumor associated vessels at 30 min after 1 h HT treatment with IDA-SDDS (Fig. 4A), resulting in a steep concentration gradient away from the vessel (Fig. 4C). DXR distribution was more homogeneous, but lower, with a more gradual decline into tumor tissue (Fig. 4B, C). Consequently, in efficacy studies we observed that only a single injection of IDA-SDDS at 2.7 µmol/kg inflicted a strong and durable tumor response for 21 (BLM) or 16 (BFS-1) days (Fig. 4D, E), and did so without side-effects (Supplementary Fig. 3A, B, C, D). All other treatments, including DXR-SDDS in HT treated mice, were

ineffective (Fig 4D, E). Only when DXR-SDDS was administered in HT treated mice at a higher dose of 9 µmol/kg, a comparable tumor response was observed. Importantly, the absolute tumor uptake of DXR at a dose of 9 µm/kg was 25.2±2.2 nmol/g, which is 1.6-times higher than that of IDA at dose of 2.7 µmol/kg (15.4±3.5 nmol/g, $p < 0.05$), however comparable tumor responses were observed (Table 1), indicating a more potent antitumor activity of IDA *in vivo*, which correlates with observed *in vitro* cytotoxicity (Supplemental Table 1). As expected, when mice were treated with IDA-SDDS or DXR-SDDS, while the tumor was kept at normal body temperature, tumor growth was the same as in untreated control mice, indicating that local HT is necessary to trigger drug release from SDDS and for the treatment to be effective. Histological examination of tumors after end of treatment, and 1 and 6 days thereafter confirmed necrosis of tumor and endothelial cells when IDA-SDDS or DXR-SDDS were administered at maximum tolerated dose of 2.7 µmol/kg and 9 µmol/kg, respectively. All other treatments had no detectable effect on tumor pathology (Fig. 4F).

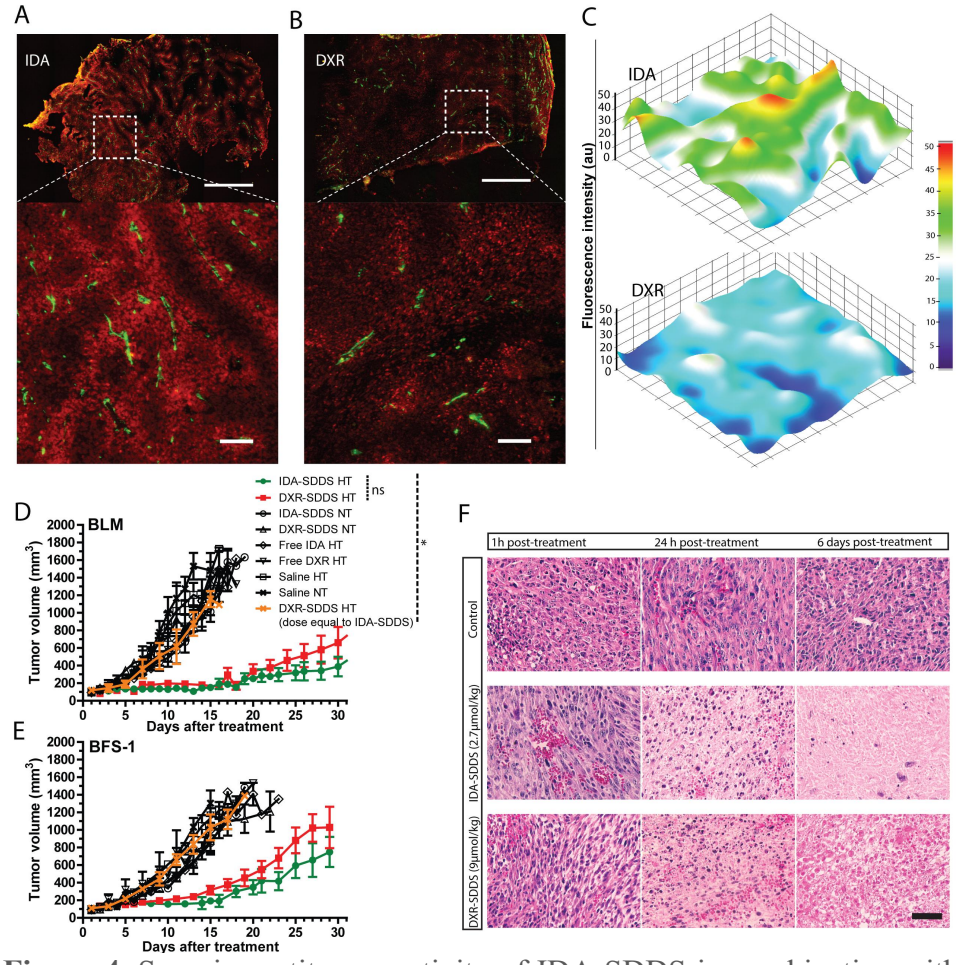

Figure 4. Superior antitumor activity of IDA-SDDS in combination with hyperthermia, compared to DXR-SDDS. (**A, B**) Histological analysis of eNOS-Tag-GFP mice bearing BFS-1 tumor treated with IDA-/DXR-SDDS combined with HT demonstrate higher perivascular accumulation of IDA (**A**), and a lower, but more uniform penetration for DXR (**B**). Top panel shows complete cross section and bottom panel a region at higher magnification (n = 2 mice per group). Settings: gain = 800, resolution = 1024 × 1024. Scale bars, 1 mm (top), 50 µm (bottom). (**C**) Fluorescence measurement of tumor sections confirms higher and steep perivascular gradient distribution of IDA compared to DXR. (**D, E**) Tumor response in

BLM (**D**) and BFS-1 (**E**) bearing mice treated with IDA-SDDS (2.7 µmol/kg, green), DXR-SDDS (2.7 µmol/kg, yellow), or DXR-SDDS (9 µmol/kg, red) combined with hyperthermia, or normothermia. Only IDA-SDDS, or DXR-SDDS at a high dose, inflicted a tumor response. When DXR-SDDS at 2.7 µmol/kg, or DOXIL at an accumulated dose of 13.8 µmol/kg (4 injections with an interval of 4 days) were administered, all mice showed progressive disease ($n \geq 5$ mice for each group, Nonparametric Mann-Whitney test. * $p < 0.01$; *ns*, not significant). Data are represented as mean ± SEM. (**F**) Fixed H&E stained tumor sections at 1 h, 24 h and 6 days post-treatment with IDA- or DXR-SDDS with HT. After 24 h post-treatment, necrosis of tumor was observed, showing destruction of tumor cells and vasculature at 6 days post treatment with IDA or DXR-SDDS plus HT, compared to normothermia controls. Scale bars, 50 µm.

Discussion

Cancer is the leading cause of death in the Western World and gaining impact fast in developing countries [29, 30]. Chemotherapy is one of the major pillars on which treatment relies [3]. However, the biggest hurdle in cancer treatment is insufficient delivery of an active compound to solid tumors, regardless that it is a chemotherapeutic, other small molecules, or an advanced pathway inhibitor [29, 31]. This results in ineffective treatment as well as dose limiting side-effects. These side-effects not only prevent use of higher dosages but are often the reason to stop treatment. Therefore nano-scale delivery devices are used to improve tumor drug concentrations and diminish side-effects. Interestingly, in spite of the specific characteristics of these nano-devices and beneficial effect on pharmacokinetics, local concentration, intratumoral distribution and possible delivery sites, nano-devices are usually loaded with the drug of choice for the specific cancer from a classic oncological point-of-view [32]. Accordingly, it is advised to focus rather on the performance of a drug in association with the SDDS of choice. For instance, one potential, and currently unrealized benefit of SDDS is the ability to deliver drugs at

therapeutic levels to tumors that are ineffective when delivered in free form due to an undesirable distribution and/or elimination profile. In this study, idarubicin, a drug that is used exclusively for the treatment of leukemia and myelodysplastic syndrome [33], was taken as an example. Due to its hydrophobicity, IDA rapidly accumulates in circulating leukemic cells, which are in direct contact with the injected drug, and this clearly benefits therapy. However, sequestration of IDA by circulating cells limits delivery of the drug to tissue-embedded tumor cells, thus making it hardly effective in most solid cancers. Encapsulation of IDA in SDDS not only prolongs circulation half-time in blood and reduces side-effect (Supplementary Fig. 4). But more importantly, by using thermosensitive SDDS in combination with local hyperthermia the intratumoral IDA concentration can be increased over 100-fold in solid tumors due to its rapid extraction by tumor cells when IDA is in free form, which thus yields a strong tumor response. Here we show that a change in thinking is needed and selection should be made for the optimal drug considering both the optimal delivery method, i.e. particular SDDS, and cytotoxicity for targeted cells. DXR has been used most widely, largely because of the wide spectrum of activity, and ease of encapsulation. However, we postulate that drug uptake by tumor cells is the rate-limiting factor when SDDS are used in combination with locally triggered delivery. Changing from DXR to a more hydrophobic anthracycline such as IDA results in improved performance of the drug-SDDS combination with respect to tumor uptake efficiency and absolute uptake quantity (Table 1), and augments drug levels in tumor cells. Hence, IDA, and similar drugs, may be promising candidates for treatment of solid tumors with thermosensitive SDDS. Moreover, use of smart drug delivery systems may open possibilities for drugs which may have been abandoned for poor performance or strong side-effects when used in the free form. As we demonstrated here, the fact that IDA is rapidly taken up by circulating cells, which would be a limiting factor when used for solid cancer treatment, becomes an advantage when encapsulated in SDDS. Understanding how to choose the best drug for SDDS-mediated delivery

is a timely question and may have a significant impact on the field by providing an answer to the hurdles currently faced.

Materials and Methods

Cytotoxicity. Murine B16BL6 melanoma, human BLM melanoma and murine BFS-1 sarcoma cells were cultured in DMEM medium with 10% FCS. Cells were seeded in 96-well-plates at a density of 5000/well for 24 h in order to adhere and enter the exponential growth phase. Medium was removed and new medium with free IDA or DXR was added followed by incubation for 1 h or 24 h, after which drug-containing medium was replaced with new medium, followed by additional incubation for 48 h or 24 h at 37°C. Cells were fixed using 10% (w:v) trichloroacetic acid (TCA), rinsed with water and stained with 0.5% sulforhodamine B (SRB) for 20 min. Thereafter, cells were washed with 1% acetic acid and left to dry. Thereafter 10 mM Tris was added to dissolve the SRB and measured at 510 nm. Cell survival as percentage of control is presented and IC_{50} values were calculated.

Cell uptake. A total of 7×10^6 cells were seeded in T75 flask and incubated overnight (12 h). Medium was removed and 5 ml of IDA or DXR containing medium (10 µM) was added followed by incubation for 5 min, 10 min, 30 min, 1 h, 2 h, 4 h, 8 h, 16 h and 24 h. Cells were collected and drug was extracted with 85% isopropanol (containing 0.75 M hydrochloride acid) for at least 24 h at 4°C.

Cellular retention. A total of 7×10^6 cells were seeded in T75 flask and incubated overnight (12 h). Medium was removed and 5 ml new medium containing IDA or DXR at a concentration of 10 µM was added for 4 h. Medium was replaced by new medium followed by incubation for 1 h, 4h, 8h, 16h and 24h, after which drugs were extracted from cells with acidic isopropanol as mentioned above.

IDA-SDDS and DXR-SDDS preparation. SDDS were composed of the phospholipids DPPC/DSPC/DSPE-PEG (60/35/5 for IDA, 70/25/5 for

DXR; molar ratio) and prepared by thin lipid film hydration method, followed by heated extrusion as described previously [19, 25]. Briefly, 100 μmol of lipids was dissolved in methanol/chloroform (1/9 v/v), followed by evaporation under vacuum and nitrogen flush. The resulting dried lipid film was hydrated in ammonium EDTA buffer (250 mM, pH 5.5 for IDA loading) or in ammonium sulfate buffer (250 mM, pH 5.5 for DXR loading). Small unilamellar liposomes were obtained by extrusion using Nuclepore® (Whatman Inc., USA) filters with pore sizes from 200 to 50 nm. Diameter and polydispersity index (pdi), as well as zeta potential were measured with a Zetasizer Nano-ZS (Malvern Instruments Ltd., UK) [25]. A PD-10 column was used to replace the external buffer to create an ion gradient between internal (ammonium buffer, pH 5.5) and external (HEPES buffer, pH 8.5) SDDS volume. According to the optimized loading methods published previously [19, 25], IDA was encapsulated at a molar drug/lipid ration of 0.3/1, at 33°C for 1 h, and DXR was encapsulated at a molar drug/lipid ratio of 0.15/1, at 39°C for 1 h. Drug loaded SDDS were collected by ultracentrifugation at 40,000 rpm for 2 h at 4°C, following by resuspension in HEPES buffer (pH 6.5) overnight at 4°C. SDDS quality was confirmed by measuring diameter and polydispersity index before and after drug loading (Supplementary Table 2), and before in vitro and in vivo application.

***In vitro* release of IDA-SDDS and DXR-SDDS.** Fifty μl of 8 mM (lipids) SDDS suspension was instantly added to 3 ml 100% fetal calf serum (FCS) at 37 or 42°C for 1 h. Real-time release of content was detected by spectrofluorometry (IDA: Ex. 485 nm/Em. 571 nm; DXR: Ex. 482 nm/Em. 594 nm) (Hitachi F-4500 Fluorescence Spectrophotometer, Japan). The average fluorescence intensity of the initial 5 seconds at 37°C was recorded as I_0, while I_t represent fluorescence recorded at time points after that. After 1 h, detergent (10% Triton X-100) was used to disrupt all SDDS to measure maximal drug fluorescence, which was designated I_{max}. Release was calculated as Release (%) = $(I_t - I_0)/(I_{max} - I_0) \times 100$ as previously described [25].

Real-time imaging of drug release from IDA-SDDS and DXR-SDDS and subsequent uptake by tumor cells. Real-time imaging of SDDS release and uptake by tumor cells was performed using confocal imaging of Attofluor® Cell Chambers (ThermoFisher) as previously described [34]. Briefly, a coverslip (25 mm in diameter) was inserted into an Attofluor chamber and subsequently sterilized. Coverslips were coated with gelatin (1 mg/ml) prior to cell seeding. B16BL6 or BLM cells (10^4 per chamber) were seeded and incubated overnight at 37°C. IDA- and DXR-SDDS were diluted to 10 μM (IDA or DXR) using cell medium and 1 ml was added into the cell chamber after which cell chambers were placed in a temperature controlled confocal microscope. Cells were incubated at 37°C for 2 h, followed by 10 min or 1 h at 42°C. A Zeiss LSM 510 META confocal microscope (543 nm helium-neon laser) equipped with a cell culture system was used to capture images. Images for both IDA- and DXR-SDDS were captured with a 40 × (NA 1.3) oil immersion lens under the same settings and analyzed using Fiji Image J.

Plasma pharmacokinetics and biodistribution of IDA- and DXR-SDDS. All animal experiments were carried out in accordance with protocols approved by the committee on Animal Research of the Erasmus Medical Center (Rotterdam, the Netherlands) and in accordance with the European directive 2010/63/eu on the protection of animals used for scientific purposes. IDA-SDDS and DXR-SDDS were injected in nude mice (NMRI nu/nu) at either efficacy dosage (2.7 μmol/kg for IDA and 9 μmol/kg for DXR) or doses as indicated. For the first timeline blood samples were drawn at 5 min, 30 min, 1 h, 2 h, 3 h, 6 h, 12 h and 24 h, in which efficacy dose injection was applied. For the second timeline, tumor-bearing mice were kept under anesthesia and applied with local HT (42°C) or NT (37°C) of the tumor, injected with IDA- or DXR-SDDS and kept for 60 min at the set temperatures, followed by 30 min at 37°C. Blood samples were collected at 5 min and 90 min post injection. Blood samples were mixed with phosphate buffered saline and Triton at a volume ratio of 30: 70: 100, followed by IDA and DXR measurement at

485 nm excitation and 590 nm emission (Wallac 1420 Victor microplate reader). Half-life ($t_{1/2}$) was calculated through WinNonlin analysis.

Organs and tumors were isolated from mice at times indicated in the text, snap frozen in liquid nitrogen and stored at -80°C until further analysis. Extraction of drugs from tissues was performed according to Laginha et al [35]. Briefly, all tissues were weighed and homogenized (Bio-Gen PRO200 Homogenizer) in 85% isopropanol (containing 0.75 M hydrochloride acid), then placed at 4°C for at least 24 h for drug extraction. IDA and DXR levels were determined as described above.

Intravital imaging of IDA and DXR release and intratumoral distribution. Instalment of the dorsal skinfold window chamber and intravital imaging was performed as described previously [25, 36]. C56BL/6 mice constitutively expressing an eNOS-Tag-GFP fusion protein in endothelial cells were installed with a skinfold window chamber, a B16BL6 melanoma was implanted in the chamber and imaged using intravital microscopy (Zeiss LSM 510 META). Equal doses of IDA- or DXR-SDDS (18 µmol/kg) were injected intravenously into mice. Window chamber tumors were exposed to local hyperthermia of 42°C, which took around 10 min to reach target temperature and were kept at 42°C for 1 h, followed by cooling down to 37°C for 30 min. Images was captured every 10 seconds at 10 × (NA 0.3) using a Helium-Neon laser (543 nm for IDA/DXR monitoring with long pass 585 nm filter) and an argon laser (488 nm for GFP endothelial cells monitoring with band pass 505-550 nm filter). Drug fluorescence intensity was quantified by Fiji Image J and Matlab.

Therapeutic efficacy of IDA- or DXR-SDDS. A tumor piece (~3 mm^3) of BLM melanoma or BFS-1 sarcoma were subcutaneously transplanted within the right hind leg of NMRI nu/nu mice. When tumors reached around 100 mm^3 in size, tumors were heated by local hyperthermia of 42°C (HT) or normothemia (37°C, NT), directly after a single injection of IDA- (2.7 µmol/kg) or DXR- (9 µmol/kg) SDDS, for 1 h as previously

reported [25, 36]. Weight and tumor growth was recorded daily and tumor volume was calculated using the formula Length x Width x Depth x 0.4. Mice were euthanized when tumor reached ~15 × 15 × 15 mm^3 in size or based on human endpoints.

Histology. After treatment, tumors were excised, fixed in 25% (v/v) paraformaldehyde for 24 h, followed by paraffin embedding, and 5 µm slices were cut and stained with hematoxylin and eosin (H&E). A second set of tumors were excised from eNOS-Tag-GFP mice, snap frozen, cut into 5 µm frozen slices and imaged by confocal microscopy to study intratumor distribution.

Statistics. Results are analyzed using Mann-Whitney U test and presented as mean ± SD or SEM. *p* values below 0.05 were considered significant.

Acknowledgements: We thank colleagues of the Erasmus Medical Instrumentation Service for assistance with the development of the window model components. We also thank Dr. Gert-Jan Kremer for kindly offering the cell transfection agents. **Authors contributions:** T.L.M.t.H. and T.L. conceived the project. T.L. performed experiments and data analysis and prepared figures. D.H., H.L., A.L.B.S. and T.L.M.t.H. participated in data analysis and figure preparation. T.L. and T.L.M.t.H. wrote the manuscript. D.H., G.C.v.R, A.B.H and T.L.M.t.H. critically revised it. **Competing interests:** No potential conflicts of interests are disclosed by the authors. **Data and materials availability:** All data associated with this study are present in the paper or the Supplementary Materials, and data deposition location is indicated in each of the relevant sections of the Materials and Methods.

Supporting data

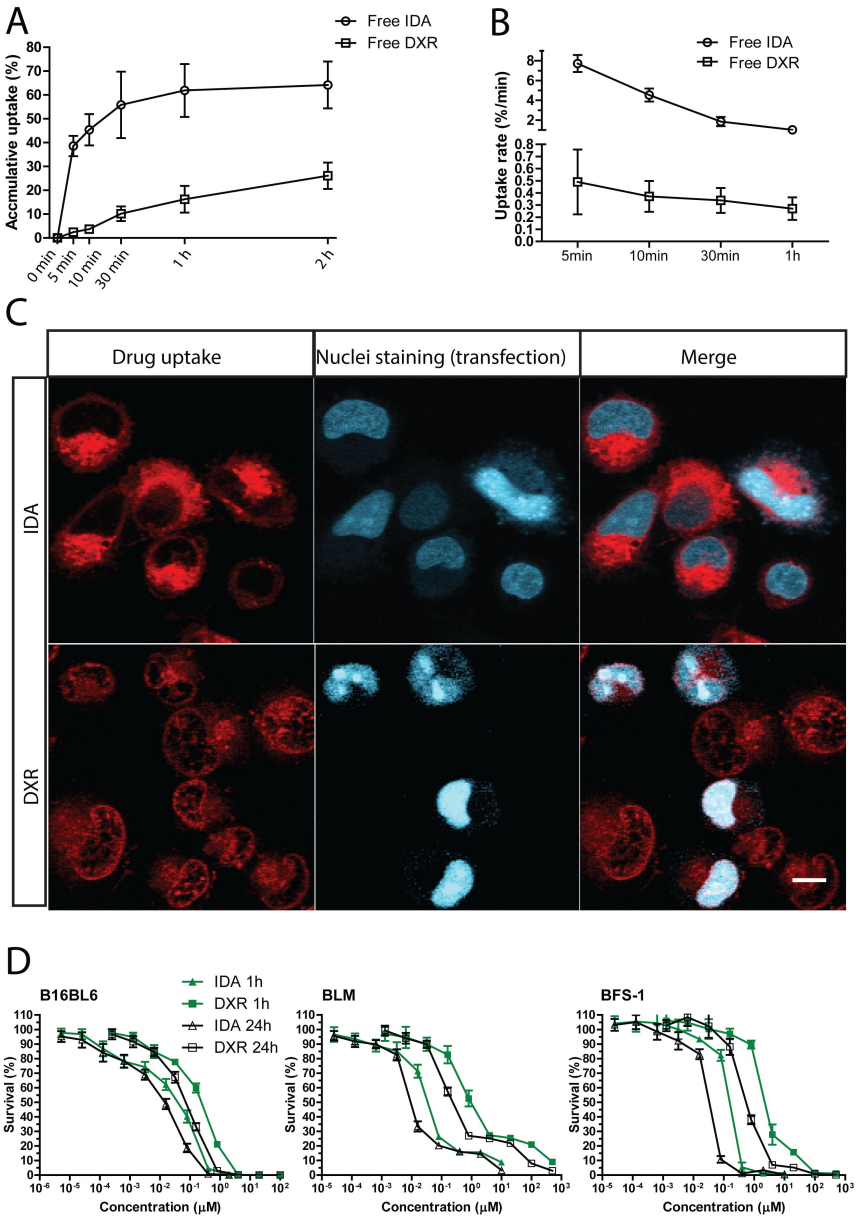

Supplementary Figure 1. Faster cellular uptake and higher cytotoxicity of idarubicin (IDA) versus doxorubicin (DXR) *in vitro*. (**A, B**) Based on

the average uptake percentage by the 3 cell lines shown in Figure 1A, calculations show a significantly higher cellular uptake rate for free IDA compared to free DXR (n = 4 per group). (**C**) IDA (red) tends to accumulate in cytoplasm and hardly goes to the nucleus (blue) while DXR (red) accumulates predominantly in cell nucleus. Settings: IDA gain = 500, DXR gain = 630, resolution = 512 × 512. Scale bar = 10 µm. (Note, nuclei were stained through transient transfection resulting in not all cells to be positive). (**D**) B16BL6, BLM and BFS-1 cells were treated with either IDA or DXR for 1 or 24 h, showing a higher toxicity for IDA as compared to DXR (n = 3 per group). Data are represented as mean ± SD.

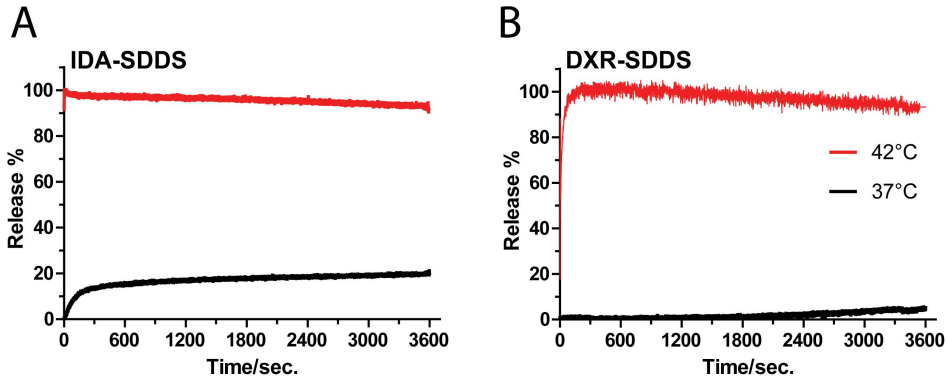

Supplementary Figure 2. IDA-SDDS exhibit faster release kinetics when exposed to 42°C hyperthermia (HT) compared to DXR-SDDS. IDA-SDDS (**A**) and DXR-SDDS (**B**) in vitro release in full calf serum at 37 or 42°C (n = 3).

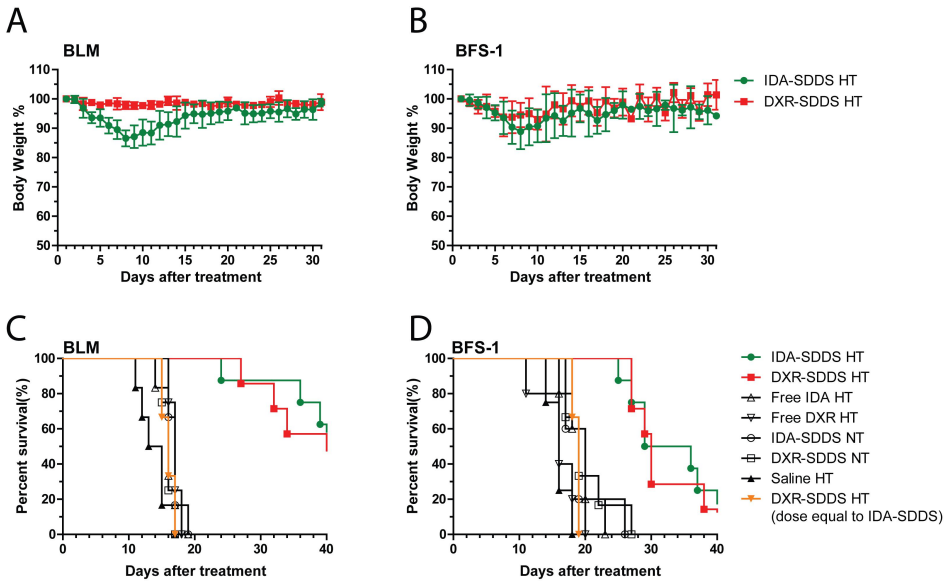

Supplementary Figure 3. Administration of idarubicin (IDA)-SDDS (2.7 μmol/kg, green line) or doxorubicin (DXR)-SDDS (9 μmol/kg, red line) in combination with local hyperthermia (HT) inhibits tumor growth in both BLM and BFS-1 bearing mice, is accompanied by acceptable side-effects resulting in improved survival rates. (**A, B**) Body weight profiles of BLM (**A**) or BFS-1 (**B**) tumor-bearing mice after treatment with IDA- or DXR-SDDS plus HT. A reduction in body weight in the first week post treatment was observed in IDA-SDDS treated mice, followed by recovery. Mice treated with free drug with or without HT, or drug-containing SDDS combined with normothermia (NT) did not show significant weight loss (data not shown). Data are presented as mean ± SD ($n \geq 5$ mice per group). (**C, D**) Survival rates of BLM (**C**) or BFS-1 (**D**) tumor-bearing mice reveal longer survival period when treated with IDA- or high dose DXR-SDDS combined with HT as compared to the other groups. However, at the maximum tolerated dose no significant difference in survival rates was observed between mice treated with IDA- or high dose DXR-SDDS plus HT ($n \geq 5$ mice per group).

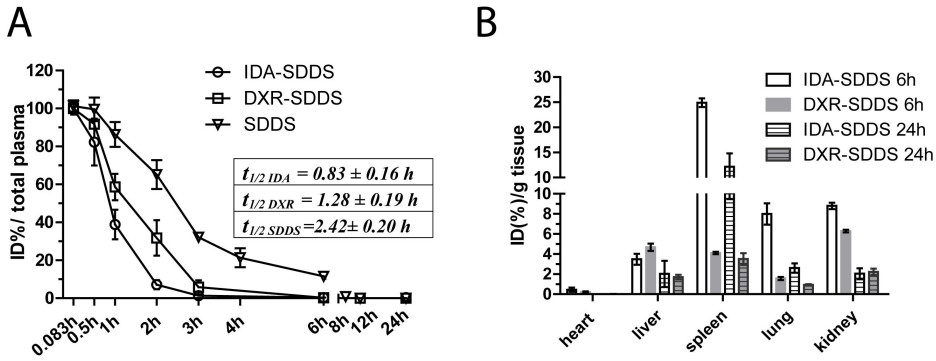

Supplementary Figure 4. Pharmacokinetics and biodistribution of IDA- or DXR-SDDS comparison in healthy mice. (A) Both IDA (2.7 μmol/kg) and DXR (9 μmol/kg) show prolonged circulation after encapsulation in SDDS, and (B) comparable biodistribution profiles ($n \geq 3$ mice per group). Data are represented as mean ± SD.

Supplementary Table 1. In vitro cytotoxicity of idarubicin and doxorubicin.

	Co-incubation for 1 h			Co-incubation for 24 h		
	B16BL6	BLM	BFS-1	B16BL6	BLM	BFS-1
IDA#	0.048 *	0.036*	0.146 *	0.017*	0.010*	0.025*
DXR#	0.273	0.904	2.437	0.086	0.217	0.597

#IC_{50} (μM) of free idarubicin or doxorubicin.

*Nonparametric Mann-Whitney test, $p < 0.01$.

Supplementary Table 2. Characterization parameters of IDA- and DXR-SDDS used in this study. Data are presented as mean ± SD, N ≥ 3.

Liposome composition (mole)	Diameter (nm)		Polydispersity index (PDI)	
	Before	After	Before	After
IDA-SDDS (DPPC/DSPC/DSPE-PEG 6/3.5/0.5)	84±2	81±2	0.05±0.02	0.04±0.03
DXR-SDDS (DPPC/DSPC/DSPE-PEG 7/2.5/0.5)	86±2	84±3	0.03±0.03	0.05±0.02

References

[1] M. J. Mitchell, R. K. Jain, R. Langer, Engineering and physical sciences in oncology: challenges and opportunities. *Nature Reviews Cancer* **17**, 659 (2017).

[2] R. K. Jain, Normalization of tumor vasculature: an emerging concept in antiangiogenic therapy. *Science* **307**, 58 (2005).

[3] S. Senapati, A. K. Mahanta, S. Kumar, P. Maiti, Controlled drug delivery vehicles for cancer treatment and their performance. *Signal transduction and targeted therapy* **3**, 7 (2018).

[4] J. Shi, P. W. Kantoff, R. Wooster, O. C. Farokhzad, Cancer nanomedicine: progress, challenges and opportunities. *Nature Reviews Cancer* **17**, 20 (2017).

[5] D. Rosenblum, N. Joshi, W. Tao, J. M. Karp, D. Peer, Progress and challenges towards targeted delivery of cancer therapeutics. *Nature communications* **9**, 1410 (2018).

[6] V. P. Torchilin, Recent advances with liposomes as pharmaceutical carriers. *Nature reviews Drug discovery* **4**, 145 (2005).

[7] T. M. Allen, P. R. Cullis, Liposomal drug delivery systems: from concept to clinical applications. *Advanced drug delivery reviews* **65**, 36 (2013).

[8] A. I. Minchinton, I. F. Tannock, Drug penetration in solid tumours. *Nature Reviews Cancer* **6**, 583 (2006).

[9] M. E. R. O'Brien *et al.*, Reduced cardiotoxicity and comparable efficacy in a phase III trial of pegylated liposomal doxorubicin HCl (CAELYX™/Doxil®) versus conventional doxorubicin for first-line treatment of metastatic breast cancer. *Annals of oncology* **15**, 440 (2004).

[10] Y. Matsumura, H. Maeda, A new concept for macromolecular therapeutics in cancer chemotherapy: mechanism of tumoritropic accumulation of proteins and the antitumor agent smancs. *Cancer research* **46**, 6387 (1986).

[11] S. Wilhelm *et al.*, Analysis of nanoparticle delivery to tumours. *Nature reviews materials* **1**, 16014 (2016).

[12] V. P. Chauhan, R. K. Jain, Strategies for advancing cancer nanomedicine. *Nature materials* **12**, 958 (2013).

[13] P. A. Netti, D. A. Berk, M. A. Swartz, A. J. Grodzinsky, R. K. Jain, Role of extracellular matrix assembly in interstitial transport in solid tumors. *Cancer research* **60**, 2497 (2000).

[14] M. W. Dewhirst, T. W. Secomb, Transport of drugs from blood vessels to tumour tissue. *Nature Reviews Cancer* **17**, 738 (2017).

[15] A. L. B. Seynhaeve, B. M. Dicheva, S. Hoving, G. A. Koning, T. L. M. ten Hagen, Intact Doxil is taken up intracellularly and released doxorubicin sequesters in the lysosome: evaluated by in vitro/in vivo live cell imaging. *Journal of controlled release* **172**, 330 (2013).

[16] Y. C. Barenholz, Doxil®—the first FDA-approved nano-drug: lessons learned. *Journal of controlled release* **160**, 117 (2012).

[17] L. H. Lindner *et al.*, Novel temperature-sensitive liposomes with prolonged circulation time. *Clinical Cancer Research* **10**, 2168 (2004).

[18] M. B. Yatvin, J. N. Weinstein, W. H. Dennis, R. Blumenthal, Design of liposomes for enhanced local release of drugs by hyperthermia. *Science* **202**, 1290 (1978).

[19] L. Li *et al.*, Mild hyperthermia triggered doxorubicin release from optimized stealth thermosensitive liposomes improves intratumoral drug delivery and efficacy. *Journal of Controlled Release* **168**, 142 (2013).

[20] D. Needham, G. Anyarambhatla, G. Kong, M. W. Dewhirst, A new temperature-sensitive liposome for use with mild hyperthermia: characterization and testing in a human tumor xenograft model. *Cancer research* **60**, 1197 (2000).

[21] A. A. Manzoor *et al.*, Overcoming limitations in nanoparticle drug delivery: triggered, intravascular release to improve drug penetration into tumors. *Cancer research*, (2012).

[22] L. Willerding *et al.*, Method of hyperthermia and tumor size influence effectiveness of doxorubicin release from thermosensitive liposomes in experimental tumors. *Journal of Controlled Release* **222**, 47 (2016).

[23] T. Tagami, M. J. Ernsting, S.-D. Li, Efficient tumor regression by a single and low dose treatment with a novel and enhanced formulation of thermosensitive liposomal doxorubicin. *Journal of controlled release* **152**, 303 (2011).

[24] P. S. Yarmolenko *et al.*, Comparative effects of thermosensitive doxorubicin-containing liposomes and hyperthermia in human and murine tumours. *International Journal of Hyperthermia* **26**, 485 (2010).

[25] T. Lu, W. J. M. Lokerse, A. L. B. Seynhaeve, G. A. Koning, T. L. M. ten Hagen, Formulation and optimization of idarubicin thermosensitive liposomes provides ultrafast triggered release at mild hyperthermia and improves tumor response. *Journal of Controlled Release* **220**, 425 (2015).

[26] P. Ma *et al.*, Development of idarubicin and doxorubicin solid lipid nanoparticles to overcome Pgp-mediated multiple drug resistance in leukemia. *Journal of biomedical nanotechnology* **5**, 151 (2009).

[27] F. Pastorino *et al.*, Vascular damage and anti-angiogenic effects of tumor vessel-targeted liposomal chemotherapy. *Cancer research* **63**, 7400 (2003).

[28] E. Ruoslahti, Specialization of tumour vasculature. *Nature Reviews Cancer* **2**, 83 (2002).

[29] S. Chakraborty, T. Rahman, The difficulties in cancer treatment. *ecancermedicalscience* **6**, (2012).

[30] P. Boyle, B. Levin, *World cancer report 2008*. (IARC Press, International Agency for Research on Cancer, 2008).

[31] M. O. Palumbo *et al.*, Systemic cancer therapy: achievements and challenges that lie ahead. *Frontiers in pharmacology* **4**, 57 (2013).

[32] M. Dobbelstein, U. Moll, Targeting tumour-supportive cellular machineries in anticancer drug development. *Nature reviews Drug discovery* **13**, 179 (2014).

[33] A. M. Carella, E. Berman, M. P. Maraone, F. Ganzina, Idarubicin in the treatment of acute leukemias. An overview of preclinical and clinical studies. *Haematologica* **75**, 159 (1990).

[34] A. L. B. Seynhaeve, T. L. M. ten Hagen, Using In Vitro Live-cell Imaging to Explore Chemotherapeutics Delivered by Lipid-based Nanoparticles. *Journal of visualized experiments: JoVE*, (2017).

[35] K. M. Laginha, S. Verwoert, G. J. R. Charrois, T. M. Allen, Determination of doxorubicin levels in whole tumor and tumor nuclei in murine breast cancer tumors. *Clinical cancer research* **11**, 6944 (2005).

[36] A. L. B. Seynhaeve, T. L. M. ten Hagen, Intravital Microscopy of Tumor-associated Vasculature Using Advanced Dorsal Skinfold Window Chambers on Transgenic Fluorescent Mice. *Journal of visualized experiments: JoVE*, (2018).

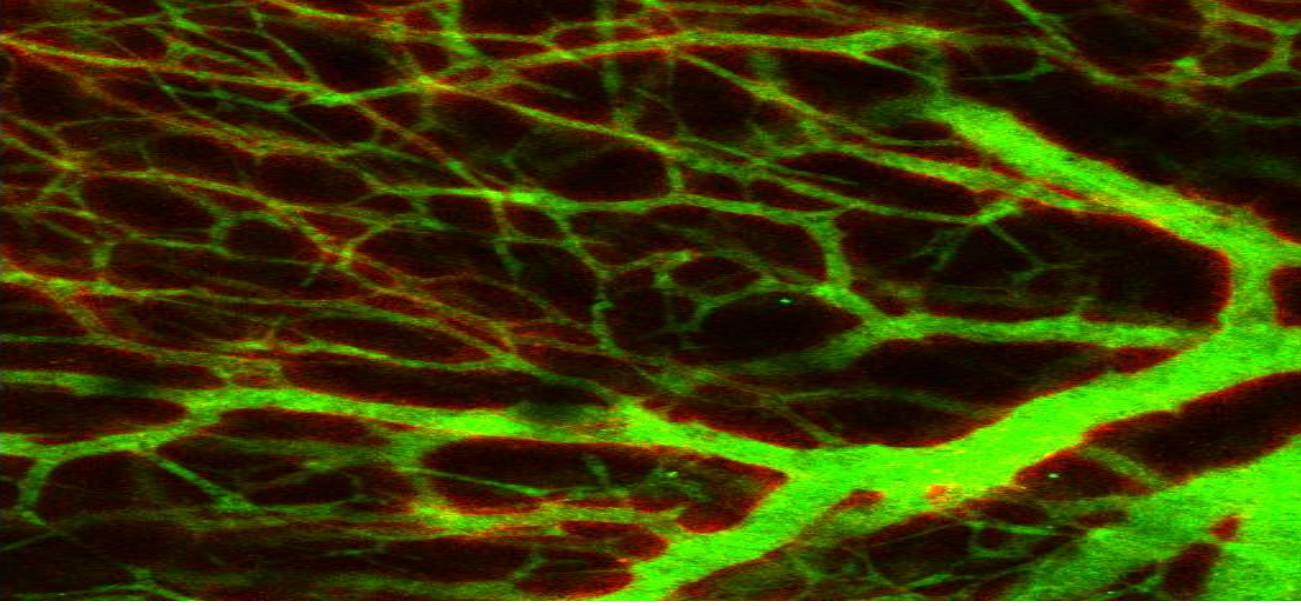

Chapter 4

Inhomogeneous crystal grain formation in DPPC-DSPC based thermosensitive liposomes determines content release kinetics

Tao Lu*, Timo L.M. ten Hagen**

Journal of Controlled Release, 2017, 247, 64-72

Abstract

Thermosensitive liposomes (TSL) receive attention due to their rapid externally controlled drug release at transition temperature in combination with hyperthermia. This rapid release feature of TSL occurs when the liposome membrane is going through a phase change which results in numerous interfaces, at so-called crystal grain boundaries. Based on experience with TSLs, our group found that thermosensitive liposomes formulated by binary compositions of DPPC and DSPC at proper ratios are able to exhibit rapid release without incorporation of release-promoting components. The aim of this study was to understand the mechanism of rapid release from bi-component DPPC-DSPC based TSL. Based on the investigation of a series of TSLs formulated by different DPPC-DSPC ratios, and through the analysis of binary-phase diagrams of DPPC-DSPC TSLs, we conclude that inhomogeneous crystal grains are formed in bi-component TSL membranes rather than mono-component, thereby facilitating content release. The resulting inhomogeneous membrane pattern is affected by DPPC/DSPC ratio, i.e. this determines the number of interfaces between solid and liquid phases at transition temperature, which can be diminished by addition of cholesterol. At appropriate DPPC/DSPC ratio, substantive solid/liquid interfaces can be generated not only between membrane domains but also between crystal grains in each domain of the liposome membranes, therefore improving content release from the TSL at transition temperatures.

Keywords:

Thermosensitive liposome, DPPC, DSPC, inhomogeneous crystal grain, phase transition, release kinetics

1. Introduction

Nanoparticle-mediated chemotherapy offers several advantages in tumor treatment, including reduced side-effects, prolonged circulation time and possibly improved intratumoral drug accumulation due to the enhanced permeability and retention (EPR) effect [1]. Especially lipid-based particles, liposomes, are successfully developed of which Doxil®/Caelyx® is one of most well-known and widely used. However, application of nanoparticles also introduces drawbacks, such as failure to adequately penetrate tumors [2]. The EPR effect is influenced by tumor microenvironment, tumor type and profile of nanoparticle, which all may hinder an optimal therapeutic effect of most conventional, passively-delivered liposomal formulations [3 , 4]. Important, and the key explanation for failure of Doxil® to surpass doxorubicin, is the slow drug release from the liposome, which limits therapeutic efficacy in spite of strikingly increased circulation time [5]. Hence, to obtain high local levels of free and bioavailable drug actively triggered release of encapsulated drug at the diseased site is a pursued possibility. One approach for local delivery is to use thermosensitive liposomes (TSL) and local hyperthermia (HT), in which the drug is rapid intravascularly released in the heated area, subsequently followed by massive uptake by tumor cells due to high concentration gradients.

The concept of thermosensitive liposomes was first introduced by Yatvin et al.[6], reporting a TSL formed by 1,2-dipalmitoyl-sn-glycero-3-phosphocholine (DPPC) alone or with 1,2-distearoyl-sn-glycero-3-phosphocholine (DSPC), which generates content release at a phase transition temperature around 42°C. Nevertheless, these TSL relatively slowly release their content limiting further application [7]. To enhance release from TSL, Needham et al. improved TSL composition by incorporating lysolipid (LPC) and 1,2-distearoyl-sn-glycero-3-phosphoethanolamine-N-methoxy(PEG)-2000 (DSPE-PEG2000) in DPPC-based formulations. These LPC-containing TSLs show over 80% release in a matter of seconds at around 41°C, achieving a rapid release profile necessary for intravascular delivery [8,9]. Currently, several different thermosensitive liposomal formulations have been reported [10].

The principle of TSL release is generally thought to result from phase separation at Tm causing interfaces or gaps in the bilayer enabling content release [10]. Ickenstein et al. proposed that lipids solidify into gel-phase domains in the membrane during cooling, and boundaries appear at adjacent domains due to spherical bending force [11]. Because of a high degree of disordered lipid-arrangement in domain boundaries, these regions possess lower melting points. This causes prior phase transition at domain boundaries, thus generating interfaces between gel/liquid-crystalline phases, which are in turn responsible for release of content [11,12]. Surfactant lysolipids tend to migrate to phase interfaces and form micelle-structures at phase transition, thus inducing nano-pores in membranes, which can be stabilized by PEG-linked lipids. Together they increase and enlarge the interfaces inflicting more rapid release [9,13]. Based on the same principle, Tagami et al. added Brij surfactants into DPPC-based TSL, which exerts comparable fast release in response to hyperthermia [14].

Most thermosensitive liposomes are formulated on the initially proposed matrix composed of DPPC and DSPC phospholipids [15-18]. Especially, in our group we have been working on DPPC-DSPC based thermosensitive liposomes for years and developed several PEG-DSPE-modified DPPC-DSPC based TSLs loaded with different drugs, showing desired temperature response [19-22]. In the follow-up study, we observed that TSLs formulated at proper DPPC/DSPC ratios exhibit rapid release at transition temperatures. However, this fast release is likely not explained by the defect mechanism of Ickenstein [11], and does not result from the nano-pore effect seen with lysolipid-based TSL as proposed by Needham et al [9]. We speculate that apart from boundaries between individual domains as defective regions in membranes, other release regions and factors exist that influence content release from DPPC-DSPC based TSLs at transition temperatures. Therefore, in this study we designed DPPC-DSPC based TSLs, investigated rapid release at certain DPPC/DSPC ratios during phase transition, and elucidated the principle to achieve an optimal heat-triggered release DPPC-DSPC based liposome system.

2. Materials and methods

2.1 Chemicals and agents

1,2-dipalmitoyl-sn-glycero-3-phosphcholine (DPPC), 1,2-distearoyl-sn-glycero-3-phosphocholine (DSPC) and 1,2-distearoyl-sn-glycero-3-phosphoethanolamine-N-PEG_{2000} (DSPE-PEG) were provided by Lipoid (Ludwigshafen, Germany). Purified carboxyfluorescein (CF) was kindly provided by Dr. Lars Lindner and colleagues. PD-10 columns were obtained from GE Healthcare (UK). Cholesterol and other chemicals were purchased from Sigma Aldrich unless otherwise specified.

2.2 Preparation of liposomes

TSLs were composed of DPPC/DSPC/DSPE-PEG in a molar ratio of x/(100-x)/5 (x=100, 80, 60, 40, 20, 0) by using the thin lipid film hydration method, followed by heated extrusion [19]. Briefly, 100 µmol of lipids was dissolved in methanol/chloroform (1/9 v/v) mixed solvent which was then evaporated at 40°C, followed by nitrogen flush for 30 min to remove residual solvent. The resulting dried lipid film was hydrated with CF (100 mM, pH 7.4) solutions at 60°C. Small unilamellar vesicles were obtained by extrusion through Nuclepore® (Whatman Inc., USA) filters with pore size of 100 nm on a Thermobarrel extruder at 65°C (Northern Lipids, Canada). Unencapsulated CF was removed with a PD-10 column. Diameter (Z-average) and polydispersity index (PDI) were measured by using Zetasizer Nano-ZS (Malvern Instruments Ltd., UK).

2.3 Differential scanning calorimetry

Determination of TSL phase transition temperatures was done through differential scanning calorimetry (DSC) (NETZSCH Scientific Instruments Ltd DSC200F). Six DPPC-DSPC based formulations were prepared as mentioned in 2.1 with or without CF loading. 30 mg of liposome with/without encapsulated CF in fetal calf serum (FCS) or in HEPES solution (pH 7.4), and the appropriate reference solution (HEPES solution), were added to the sealed aluminum container. The phase transition temperature range was measured over a temperature range of 30 to 70°C at an interval of 5 °C/min increase. High purity nitrogen was used as carrier gas at rate of 10 ml/min.

2.4 CF-loaded TSL time- and temperature-dependent release

20 μl of 1 mM [lipid] CF-TSL suspension was added to 2 ml 100% FCS in a quartz cuvette at a series of determined temperature for 10 min. Real-time release of CF was detected with a water bath combined spectrofluorimetry (Ex. 493 nm/Em. 517 nm, Ex. slit 5 nm/Em. slit 5 nm) (Hitachi F-4500 Fluorescence Spectrophotometer, Japan). The average fluorescence intensity of the initial 5 seconds was recorded as I_0 of CF-TSL release, while fluorescence was measured as I_t at 10 min. After 10 min, detergent (10% Triton X-100) was used to disrupt all liposomes to measure maximal CF fluorescence, which was recorded as I_{max}. Release (%) = $(I_t - I_0)/(I_{max} - I_0) \times 100$.

2.5 Thermokinetic release of CF-loaded TSL

Time-dependent CF release curves obtained from 2.4, were fitted using three most common kinetic models (which are zero order, first order and Higuchi equations, respectively, see below), to determine the best-fitting profile of release kinetics and corresponding release rate [23].

Zero order: $M_t = M_0 + k_0 t$
First order: $\ln(1 - M_t) = M_0 - k_1 t$
Higuchi: $M_t = M_0 + k_h t^{1/2}$

where M_t is the amount of content released at time t. M_0 is the initial amount of release at time =0. k_0, k_1 and k_h represent the release rate constant of zero-order, first-order and Higuchi, respectively. Here, M_t represents the percentage CF released at time t, which was recorded based on CF fluorescence intensity.

2.6 Activation energy of CF release

Activation energy (Ea) of CF release from TSLs composed of different DPPC and DSPC ratios can be calculated by using Arrhenius indefinite integral equation:

$$\ln k = -(Ea/R)*(1/T) + B$$

where k is CF release rate constant which can be obtained based on methods mentioned in 2.5, B is a constant, R is the universal gas constant, and T is expressed as thermodynamic temperature in kelvin.

2.7 Statistical analysis

Data were analyzed using Mann-Whitney U test or Kruskal-Wallis test followed by Dunn test when appropriate. P-values below 0.05 were considered significant.

3. Results

3.1 Differential scanning calorimetry

DPPC-DSPC based liposome formulations with or without encapsulated CF were prepared with diameters between 110 and 120 nm and PDI below 0.1 (Table 1). Liposomes were measured in FCS and HEPES buffer solution by DSC, respectively. As seen in Fig. 1, Tm increased with increasing DSPC content in the liposomal composition. Only one phase transition peak was observed with each formulation and the Tm was between those for pure DPPC and pure DSPC liposomes. These data suggest that a molecular dispersion system (solid solution) was achieved in DPPC-DSPC mixed lipid membranes. By comparison, when CF was encapsulated, liposomal Tm did not show significant changes in HEPES or FCS solution (Table 2).

Table 1 Characterization parameters of DPPC-DSPC based CF TSLs. Mean±SD, N≥3.

TSL composition (mole)	Particle size (nm) (Z-average) #	Polydispersity index
DPPC/ DSPE-PEG 100/5 (TSL 100)	117±5	0.07±0.01
DPPC/DSPC/DSPE-PEG 80/20/5 (TSL 80)	119±3	0.05±0.03
DPPC/DSPC/DSPE-PEG 60/40/5 (TSL 60)	113±2	0.07±0.02
DPPC/DSPC/DSPE-PEG 40/60/5 (TSL 40)	120±4	0.04±0.01
DPPC/DSPC/DSPE-PEG 20/80/5 (TSL 20)	115±3	0.05±0.02
DSPC/DSPE-PEG 100/5 (TSL 0)	119±6	0.06±0.02

The Z-average of particle was reported by Zetasizer, which was measured based on Comulant model.

Table 2.DPPC-DSPC liposome phase transition temperature.

Lipid composition	Internal solution	External solution	Phase transition temperature	Initial temperature of phase transition	Terminal temperature of phase transition
100% DPPC (TSL 100)	HEPES	HEPES	41.7	38.7	45.4
	CF	HEPES	41.0	40.4	43.2
		FCS	41.1	40.4	43.4
80% DPPC (TSL 80)	HEPES	HEPES	43.9	41.1	47.0
	CF	HEPES	43.7	42.5	45.9
		FCS	43.6	42.4	45.5
60% DPPC (TSL 60)	HEPES	HEPES	46.8	43.3	49.7
	CF	HEPES	46.4	44.5	48.6
		FCS	46.4	44.5	48.7
40%DPPC (TSL 40)	HEPES	HEPES	49.4	46.5	52.3
	CF	HEPES	49.5	47.1	51.4
		FCS	49.5	47.2	51.5
20% DPPC (TSL 20)	HEPES	HEPES	52.1	50.0	54.3
	CF	HEPES	52.0	50.2	54.4
		FCS	51.9	50.3	53.9
0% DPPC (TSL 0)	HEPES	HEPES	54.6	52.8	57.1
	CF	HEPES	54.2	53.6	55.9
		FCS	54.3	53.6	56.3

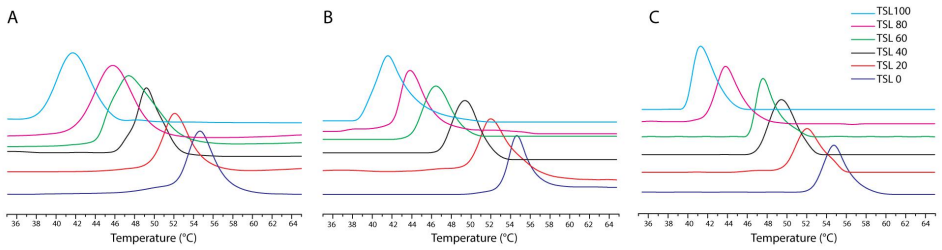

Figure 1. DSC scans of empty liposome in HEPES (A), CF-loaded liposomes in HEPES (B) or in FCS (C). TSL100-0 represent liposomes formulated at (100/5:DPPC/PEG), (80/20/5:DPPC/DSPC/PEG), (60/40/5:DPPC/DSPC/PEG), (40/60/5:DPPC/DSPC/PEG), (20/80/5:DPPC/DSPC/PEG) and (100/5:DSPC/PEG), respectively.

3.2 Pseudo-binary phase diagram of DPPC-DSPC liposomes

Based on initial and terminal temperatures of phase transition measured by DSC in Table 2, a pseudo-binary phase diagram of DPPC-DSPC liposome is plotted (Fig. 2.). Lines in green are the liquidus and solidus curves of CF-TSL measured in FCS, and lines in red are for samples measured in HEPES. Almost overlapping curves were observed in both media.

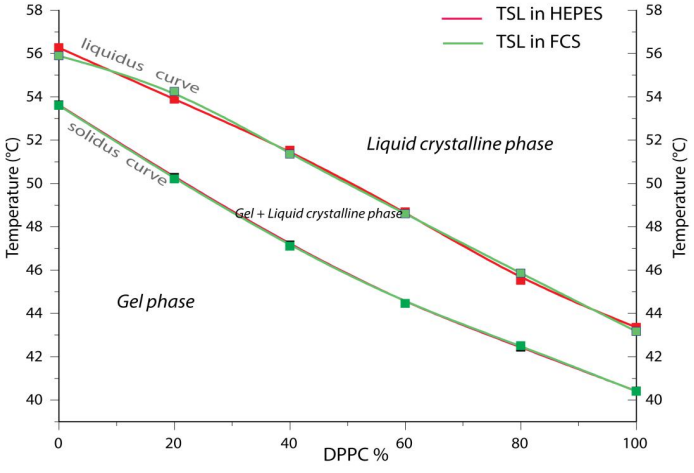

Figure 2. Pseudo-binary phase diagram of CF TSL plotted from the initiation and completion temperatures deducted from DCS measurements

in HEPES buffer (red line) and FCS (green line). Samples were formulated as DPPC-DSPC liposomes with CF loading for measurement.

3.3 Time-dependent release of CF from DPPC-DSPC formulations in FCS

DPPC-DSPC based liposome formulations with encapsulated CF were tested for triggered release in FCS at different temperatures for 600 seconds, respectively. Each CF release curve (Fig. 3) was fitted by the three release kinetic equations described in 2.5 separately to obtain the best release equation match for each formulation based on the determination coefficient R^2 (Table 3). A better coefficient of determination was obtained with the Higuchi release model when 40% or more DPPC was present in the liposomal composition. While with DPPC content equal to or lower than 20%, First order kinetics is more approprate to describe CF release profiles. However, the differences between these these three fitting models are minor.

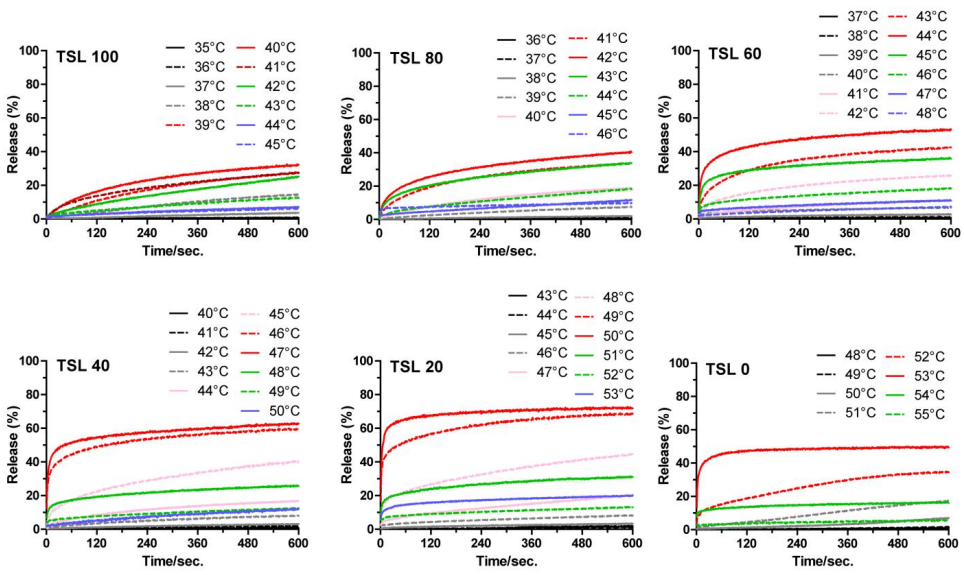

Figure 3. CF time/temperature-dependent release in FCS from TSL100, TSL80, TSL60, TSL40, TSL20 and TSL0. 100 – 0 indicates the

percentage of DPPC. Mean of at least three independent measurements is depicted.

Table 3. Kinetic profile of CF release from DPPC-DSPC based liposomal formulations.

	Determination coefficient R^2					
	TSL100	TSL80	TSL60	TSL40	TSL20	TSL0
Zero order	0.92797	0.91903	0.85759	0.88797	0.92630	0.94131
First order	0.91137	0.92038	0.89323	0.91025	**0.93410**	**0.94322**
Higuchi	**0.93806**	**0.95473**	**0.91194**	**0.95473**	0.92467	0.89401

Determination coefficient was determined by curve fitting of at least 3 independent experiments per formulation. Mean is depicted.

Table 4 CF release rate constants at Tm of DPPC-DSPC based liposomal formulations. Mean±SD.

	TSL100	TSL80	TSL60	TSL40	TSL20	TSL0
$^{\#}k_{Tm}$ (10^{-4})	130±1 $s^{-1/2}$	290±104 $s^{-1/2}$	580±139 $s^{-1/2}$	640±193 $s^{-1/2}$	270±48 s^{-1}	140±75 s^{-1}

Based on determination coefficient shown in Table 3, the release rate constants k were calculated by the most fit release equation at transition temperatures of each formulation (Higuchi: TSL100-40; First order: TSL20-0) and presented as 10^{-4} $s^{-1/2}$ or 10^{-4} s^{-1}. The first 20 seconds of measurement at Tm were used for calculation of k [16].

3.4 Temperature-dependent release of CF from DPPC-DSPC formulations in FCS

Temperature-dependent release of the six DPPC-DSPC based liposome formulations were compared at appropriate temperature ranges (Fig. 4A). It was observed that with increasing temperature, regardless of DPPC-DSPC composition, CF release from TSLs gradually increased until reaching the maximum release temperature (Tm), and was then followed by a rapid decrease as the temperature increased further. Additionally, the maximum CF release at Tm from TSLs showed a significant improvement with lower DPPC content; the highest release reached 73±4% from TSL20, while only 42±6% release was observed from TSL80 at their Tm, respectively. Liposomes composed of pure DSPC or DPPC showed however a reduced release of CF compared with other binary-component liposomes during phase transition (Fig. 4A). Based on calculations with the proper fitting release equations, CF release rate constants of each formulation were computed at Tm, respectively (Table 4). As seen, k_{Tm} shows similar trend with the change of the amount of DSPC in TSL.

A CF-release pseudo-binary phase diagram of DPPC-DSPC based TSLs was plotted based on measured temperature release ranges shown in Fig 4B, which demonstrates similar profiles with DSC based phase diagram.

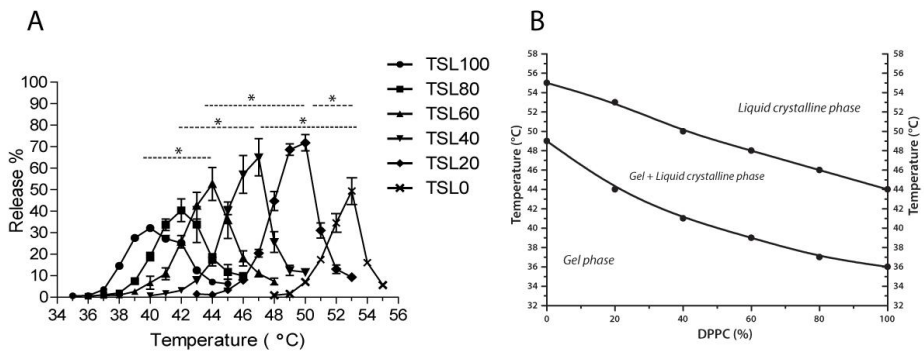

Figure 4. A: Temperature-dependent CF release from DPPC-DSPC based liposomes in FCS. Mean±SEM are shown of at least 3 independent experiments. B: Pseudo-binary phase diagram of CF TSL plotted on the basis of CF release, in which release-starting temperature was recorded as

onset of Tm and release cease-decrease temperature as the end of Tm. *Kruskal-Wallis test followed by Dunn test, *p* value<0.05.

3.5 Activation energy of CF release from DPPC-DSPC formulated TSLs

Based on CF release data in Fig 4 and the Arrhenius equation, the activation energy of CF release from these different liposomal formulations was calculated (Table 4, Fig. 5). Both TSL 60 and 40 showed significantly lower activation energy for CF release, while the other formulations exhibited higher activation energy, especially in liposomes formulated by pure DPPC or DSPC lipids, suggesting that the obstruction for CF release was minimal when these binary component liposomes have a DPPC content between 40% and 60%.

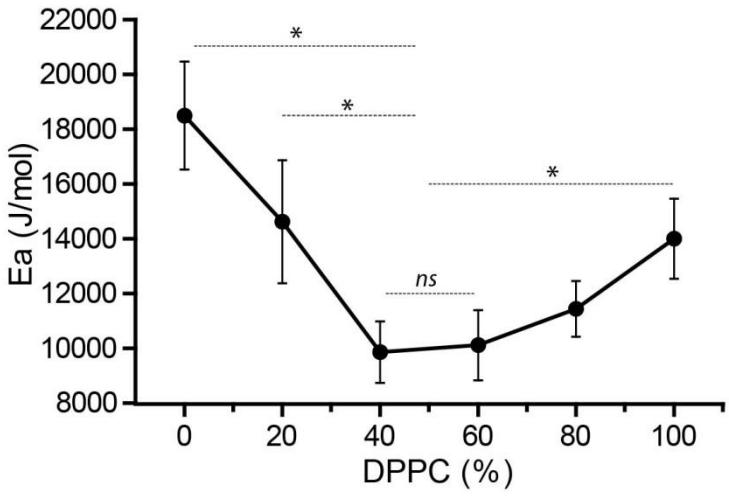

Figure 5. Activation energy of CF release from liposomes composed of various amount of DPPC-DSPC. *Kruskal-Wallis test followed by Dunn test, *p* value<0.05; *ns*, not significant at the 0.05 probability level.

3.6 The influences of PEG incorporation and PEG content on CF-TSL release

Previously we demonstrated that incorporation of more PEG-DSPE causes a higher CF leakage at phase transition [19]. We observed that 5 mol% PEG lipid in a standard formulation with DPPC-DSPC is enough to generate content release from TSLs. In order to investigate the effect of pure DPPC-DSPC TSLs composition on CF release we formulated liposomes with a minimal amount of PEG. To avoid aggregation of the nanoparticles 0.5 mol% PEG-DSPE is needed, which was added to all formulations. An obvious decreased of CF release was observed from all TSLs after reducing PEG lipid to 0.5 mol% compared to the original formulations containing 5 mol% PEG (Fig. 6). A comparable trend was observed concerning CF release at Tm which gradually increased from TSL100 (7±3% vs 42±6% at high PEG formulation; nonparametric Mann-Whitney test p=0.029) to TSL20 (46±6% vs 73±4%; p=0.016) when minimal PEG was applied. Interestingly, unlike other TSL formulations CF release from TSL0 seemed not to be influenced by PEG content, showing 40±4% and 49±10% (p=0.114) release at high and low PEG formulations, respectively.

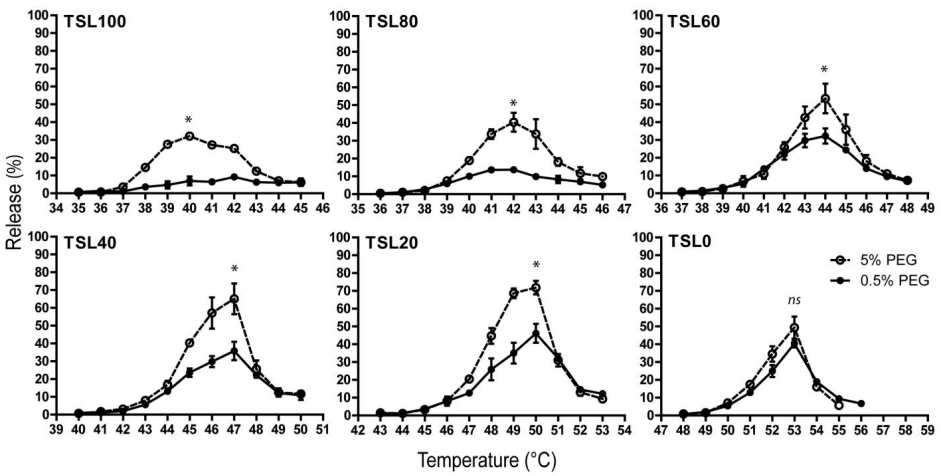

Figure 6. Effect of PEG amount (5 mol% (open symbol) and 0.5 mol% (closed symbol)) on temperature-dependent CF release from DPPC-DSPC based liposomes in FCS. Mean±SEM are shown of 3 or more independent

experiments. *Nonparametric Mann-Whitney test, *p* value<0.05; *ns*, not significant at the 0.05 probability level.

3.7 The influences of cholesterol amount on CF-TSL release

Cholesterol is commonly used in many liposomal formulations, which may however affect release kinetics profile of thermosensitive liposomes. Based on the Doxil-like formulation, we investigated CF release from TSLs composed of DSPC and 40, 20 and 10 mol% cholesterol. DSC measurements (Fig 7A) of these TSLs displayed a gradually widened and slightly declined phase transition temperature when increasing cholesterol from 10 mol% to 20 mol% in comparison with no cholesterol contained TSL. However, no phase transition can be detected when 40 mol% cholesterol was applied. Temperature-dependent release assays confirmed these observations with absent CF release at 40 mol% cholesterol, while approximate 20% CF release was observed in formulations containing 10 and 20 mol% cholesterol formulations, both of which showed dramatic release decrease compared to the original formulation.

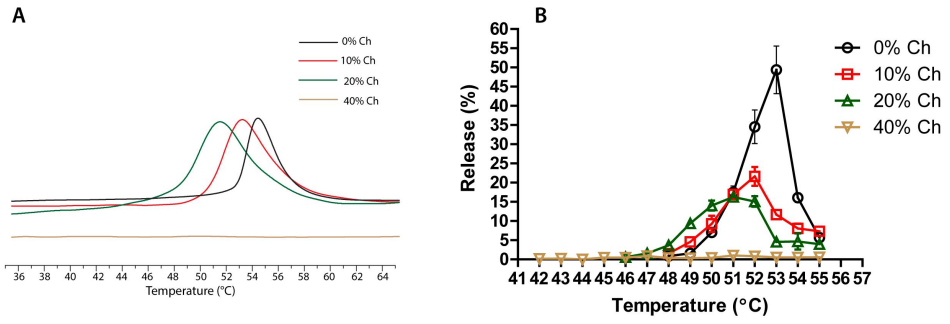

Figure 7. DSC scans (A) and temperature-dependent release (B) of liposomes composed of 40, 20, 10 and 0 mol% cholesterol and DSPC. Results of 3 independent experiments are shown Mean±SEM.

4. Discussion

Here we demonstrate that bi-component DPPC-DSPC based TSLs have an optimal lipid ratio at which release rate at transition temperature is

maximal. We observe that with the increase of the amount of DSPC, release rates increase as well (r_{Tm} in Table 5), and at an appropriate DPPC and DSPC ratio bi-component TSLs release significantly faster than mono-component liposomes at transition temperatures.

It is generally believed that thermosensitive liposomes exhibit the highest permeability when reaching their Tm, which causes maximum interfaces between solid and liquid phases in membranes, therefore leading to massive release of content [10]. Besides, temperature may be positively correlated to release rate [24] as the maximum release rates of these 6 formulations were measured at different and also increasingly higher transition temperatures. In order to elucidate DPPC-DSPC based TSL release kinetics, based on the general rules of diffusion release, namely Fick's first law, CF release rate can be given by:

$$r = -D*A* dC/dx =-K * T * A* dC/dx$$

where D represents diffusion coefficient and is proportional to temperature, which can be presented as the product of temperature T and constant K in this case. A is the diffusion area of release, and dC/dx is CF concentration gradient inside and outside of the liposomal membrane, which is the same in all TSL formulations. Herein both temperature and the release area in membrane affect CF release rates. The interfaces between solid and liquid phases in membrane of each formulation, namely release areas, reach maximum at their respective Tm. When we compare the TSL release rates using the experimental data measured at the same temperature most of these TSL are not in the maximum solid-liquid interface density. In order to compare their maximum release rates and eliminate the temperature factor we used the definite integral form of the Arrhenius equation (see below) to calculate the theoretical release rates. To do so we chose a given and same temperature for all TSL formulations but maintained the maximum release areas for each TSL formulation. Thus their solid-liquid interfaces are remained as maximum as are at their respective Tm, but the temperature is unified at in this case at 42°C to calculate the theoretical release rates of each formulation (Table 5).

$$\mathrm{In}(k_{Tm}/k_{42}) = \mathrm{In}(r_{Tm}/r_{42}) = Ea*(T_{max} - T_{42})/(R*T_{max}*T_{42})$$

where r_{Tm} is the CF release rate measured at Tm of each TSL formulation, which was obtained from the results in 3.3. Ea is the activation energy of CF release, R is the universal gas constant, and T is expressed as thermodynamic temperature in kelvin.

Table 5 CF release from different DPPC-DSPC based liposomes.

	TSL 100	TSL 80	TSL 60	TSL 40	TSL 20	TSL 0
r_{Tm} (%/min)	9.9±1.3	20.4±3.2	38.6±14.4	51.3±16.9	65.3±6.9	45.1±12.2
T_{max} (°C)	40	42	44	47	50	53
Ea (J/mol)	14029	11447	10118	9866	14621	18503
r_{42} (%/min)	10.3±1.3	20.4±3.2	37.7±14.1	48.4±16.1	56.9±6.0	35.5±9.6

r_{Tm} (%/min): the experimentally measured CF release percentage in 1 min at maximum release temperature.
T_{max}: temperature of maximum CF release.
Ea: CF release activation energy in average.
r_{42} (%/min): the theoretically calculated CF release percentage for 1 min at 42°C based on Arrhenius equation.
Mean±SD, N≥3

Release rates (r_{42}) in Table 5 show the same trend of faster CF release rates with increasing amount of DSPC in liposomes from TSL 100 to 20 but with a drop in TSL 0, implying temperature is not the main driving force that varies CF maximum-release-rates among these TSLs. We postulate that other factors intrinsic to the TSL formulation and used components determine release kinetics.

As seen in Fick diffusion equation, the increase of DSPC in TSL may increase the release area, thus leading to higher release. Hence, we hypothesize that the amount of interfaces in the liposomal membrane varies as a consequence of DPPC/DSPC ratios. The underlying mechanism we propose is that optimizing the amount of DSPC generates

more solid-liquid interfaces in the membrane, increasing the release areas, thus improving CF release rate at phase transition.

Binary phase diagrams can be used to illustrate the explanation of increased release areas in DPPC-DSPC based TSLs (Fig 2 and 4B). Unlike theoretical prediction, the experimental phase diagram did not exhibit "closed" curves in TSL 100 and 0 liposomes, which is because this is not pure bi-component system in literally. Presence of PEG lipid and interaction with serum factors as well can influence phase transition temperature of TSL 100 and 0, resulting in the deviation from the theory [25]. Figure 2, was drawn on the basis of data measured by DSC, which reflects the macro thermodynamic behavior of lipid membrane at milligram scale. While Figure 4B was plotted based on the amount of CF molecules released through the lipid membrane during phase transition, reflecting the detection of mesoscopic behavior at nanogram scale. Apparently, the latter is more sensitive as well as closer to reality when tracking lipid membrane phase transition, which is able to indicate the phase changes in lipid membrane earlier. Therefore, it is reasonable and reliable to illustrate liposomal thermostability on the basis of the extent of content release.

According to Figure 4B, the molar ratios of gel and liquid phase in liposomal membranes at respective transition temperatures can be calculated by Lever Rule (Fig. 8 and Table 6).

Lever Rule: $n_{s(\text{quantity of solids})} * L_{s(\text{distance to solidus or to Y axis})} = n_{l(\text{quantity of liquid})} * L_{l(\text{distance to liquidus or to Y axis})}$

It was found that in TSL 60, 40 and 20 at Tm, which showed massive release, the lipid membranes were composed of nearly equal amount of gel phase and liquid crystalline phase, which may generate the maximum solid/liquid interfaces in the membranes for content release. However, around two third of the lipid membrane was in liquid crystalline state in TSL 80 at Tm, thus inducing less interfaces between solid and liquid phases, and hence diminishing CF release.

Table 6 The ratios of solid and liquid phase in liposomal membranes at maximum CF release temperature of different DPPC-DSPC based liposomes.

	TSL 100	TSL 80	TSL 60	TSL 40	TSL 20	TSL 0
T_{max} (°C)	40	42	44	47	50	53
n(s):n(l) (mol/mol)	-	0.44	1.00	0.94	1.00	-

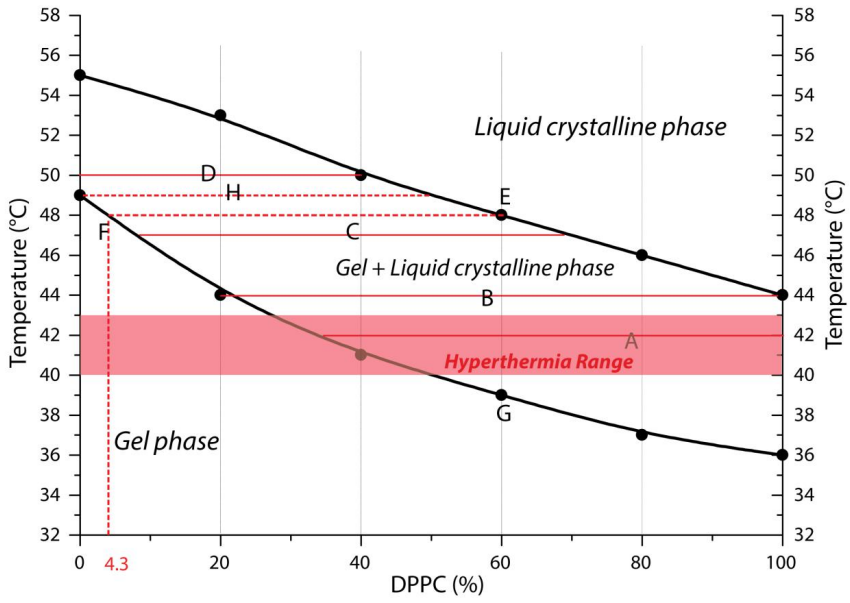

Figure 8. Pseudo-binary phase diagram modified from Fig 4B. A, B, C and D represent the maximum release temperatures of respective CF-TSLs and their distances to solidus and liquidus (along the drawn solid red line) were used to calculate solid/liquid phase ratios at Tm. For TSL 20, L_s is distance from D to left Y axis; from A to right Y axis is L_l for TSL 80.

Binary-component systems are inhomogeneous during crystal nuclei formation and growth. Based on the above depicted DPPC-DSPC pseudo-

binary phase diagram (Fig. 8), the composition of crystal grains is constantly changing when cooling down from liquid crystalline phase to gel phase. Crystal nuclei are initially formed by pure DSPC or with a little DPPC during cooling, and DPPC increasingly accumulates at the growing grains due to its lower melt point. Meanwhile solidified DSPC gradually decreases with temperature decline. For example TSL 60 in Fig. 8, when temperature declines to point E (48°C), numerous crystal nuclei are formed as solid solution which is composed of 4.3% DPPC and 95.7% DSPC. Growing crystal grains are subsequently formed by continuous accumulation of solidified lipids to the crystal nuclei with further cooling down, of which the percentage of DPPC is gradually increased with the line F (48°C, 4.3% DPPC) to G (39°C, 60% DPPC). These crystal grains stop growing when touching their adjacent grains. Therefore, the content of DSPC in a crystal grain is decreases from crystal nucleus to outward region, while the content of DPPC keeps increasing. Inhomogeneous, multilayer structured crystal grains are largely formed in bi-component membranes in this way, with gradually lowered melting points from the core to the outer layers of each crystal grain.

Hence, according to analysis of the binary phase diagram we propose that a DPPC-DSPC based bi-components liposomal membrane is composed of a large amount of these inhomogeneous, nano-sized crystal grains (Fig. 9). The contact regions of these crystal grains, namely the outmost layers of crystal grains, form the crystal grain boundaries (green stripe in Fig. 9) and, are rich in DPPC, thus leading to a lower melting point in these regions compared with inner layers of crystal grains which are rich in DSPC. Consequently, a priori phase transition occurs at these boundary regions at transition temperature when heating up, which generates these crystal grains outmost layers to melt but inner layers stay solid, thus forming solid-liquid interfaces which allow content release in bi-component TSLs. However, in mono-component liposomes homogeneous crystal grains are formed in membranes, with a homogeneous melting point from nucleus to outer region (Fig. 9). Thus, no solid-liquid interfaces are formed between crystal grains of mono-component membrane at transition temperature.

Next to the crystal grain formation, membrane defects (black stripes in Fig. 9) are formed between membrane domains due to the curved

spherical liposome surface [12]. Highly disordered arrangement of lipid molecules occurs because of different lattice orientation [11], resulting in a lower melting point in these defect regions. Hence priori phase transition takes place in these regions in both bi- and mono-component TSLs at transition temperature, forming interfaces between solid and liquid phases for content release (Fig. 9). We argue that melting not only happens at defect regions but also at numerous crystal grain boundaries during phase transition. Thus bi-component membranes generate significantly increased solid-liquid interfaces than mono-component membranes, which only melt at defect regions at Tm (Fig. 9 middle row), this results in faster and more content release in bi-component TSLs. When heating above Tm, the whole liposome membrane is in a liquid phase which takes away the solid-liquid interfaces, thus evidently decreasing release as we observed in both bi- and mono-component TSLs (Fig. 9 top row).

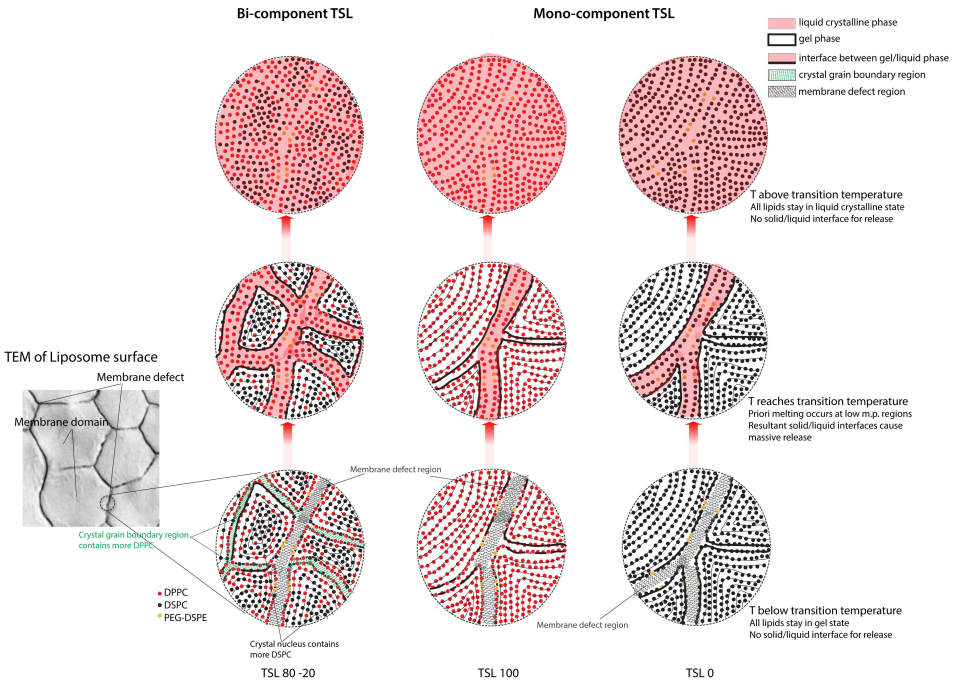

Figure 9. Crystal grains in bi-component liposomal membranes are formed as inhomogeneous microstructures with lower melting point in the outer layer, while mono-component crystal grains in a homogenous (i.e.

mono-component) structure have the same melting point across the grains. In membrane defect regions the melting point is also lower. At transition temperatures, both grain boundary (green stripe) and defect (black stripe) regions melt (pink) in bi-component TSLs, whereas only membrane defect regions melt in mono-component TSLs at transition temperatures, thus creating less gel/liquid interfaces for content release in TSL 100 and 0. When above transition temperatures, all TSLs are in pure liquid phase, thus no interfaces for release are present. The transmission electron microscopy graph of lipid membrane is cited from paper of Landon et al [26] and authorized by the publisher.

In bi-component liposomes, however, maximum release varies significantly between TSL 60, 40 and 20. Table 5 shows almost the same solid-liquid phase ratios between these TSL 60, 40 and 20 at their maximum release temperatures, but that does not imply that the amount of interfaces between gel and liquid crystalline phases are the same. One possible explanation could be that more crystal grains are formed when liposomal membranes containing more DSPC, which hence generates more solid-liquid boundaries at transition temperatures. Another possibility is that due to the longer chain length and higher rigidity of DSPC compared to DPPC molecules, more membrane defects are generated in liposomal membranes containing more DSPC as a consequence of higher curvature stress (Fig. 9 TSL 0). We indeed observed that when the size is increased (Supplementary Fig.1, Supplementary Tab. 1), lack of curvature stress in the lipid membrane caused dramatically reduced release, especially in mono-component TSLs which showed comparable extend of CF leakage (Supplementary Fig. 1 TSL 100 vs TSL 0); while bi-component TSL still demonstrated, but reduced, heat-triggered release (Supplementary Fig. 1 TSL 60).

According to the phase diagram in Figure 8, the gel phase occupies 60% of the membrane in TSL 20 when cooling down to point H (calculated by Lever Rule). In addition, more than half of the membrane in TSL 20 is solidified and formed by pure DSPC lipids at point H, thus creating a pure DSPC-based continuous phase in membrane. While during cooling of TSL 40 and 60, the continuous phases are solid solution composed of DSPC and DPPC rather than pure DSPC. Continuous phases formed by pure DSPC structurally differ from those formed by DPPC/DSPC solid

solution. This may be another reason why TSL 20 and 0, with pure DSPC as continuous phase in membranes, showed higher release than TSL 60, 40 and 100.

The activation energy of CF release (Fig. 5) gradually decreased from TSL 100 to 40, which is due to the increased number of interfaces in membranes that facilitate CF release. It requires high activation energy to release CF from TSL 20 and 0, which can be attributed to the enhanced hydrophobicity and thickness of the membrane as a consequence of continuous phases composed of pure DSPC lipid in TSL 20 and 0, thus needing high activation energy for CF release. However, it seems that release from areas with enhanced leakiness, as results of bending defects in membranes, supersedes the release obstruction resulting from high activation energy. Therefore TSL 20 and 0 still showed fast CF release.

Komatsu et al. demonstrated that content release from a liposomal aqueous core follows first order kinetics [27]. However, based on the determination coefficient R^2 (Table 3) resulted from fitting by three kinetic equations in 2.5, we found that CF release better correlates with the Higuchi model when liposome contained DPPC more than or equal to 40%. While it is proper described by the first-order release model when more than 80% of the liposomal membrane is made up by DSPC. The Higuchi model describes pore-based release models [28], which suggests that especially TSL 80-40 are likely to present a pore-like release profile during phase transition. These nano-scale pores result from the large amount of solid-liquid interfaces in bi-component membranes. While for TSL 20 and 0, due to the increase of long chain DSPC lipids in TSL the membranes become thicker, leading to increased diffusion path length fro CF in membrane, thus displaying first-order release pattern [28]. Importantly, in this study the fitting differences of these TSL release profiles are not significant.

Taken together we conclude that interfaces between gel and liquid crystalline phases are crucial for massive release of content at Tm. Moreover, while typically liposomes are coated with PEG to prolong circulation time, PEG facilitates rapid release kinetics as well. PEG lipids tend to accumulate at interface areas due to their surface activity, consequently stabilizing these interfaces to release CF [9]. Therefore, when liposomes contain a low content of PEG lipids dramatically

diminished CF release was observed (Fig. 6). The lack of such an effect in TSL 0 may be because the resulting interfaces in TSL 0 are more rigid due to pure DSPC composition, thereby more stable interfaces are generated in TSL 0 membranes enabling CF release even without help of PEG. Additionally, PEG lipid (DSPE-PEG) has the same lipid moiety as DSPC rather than DPPC, which could also explain the significant decreased release in TSL 100 containing lower PEG lipids. Cholesterol is applied to improve the stability of liposomal membranes, but it also maintains a certain degree of fluidity of the membrane above as well as below Tm [29]. Through this action cholesterol passivates the response of TSL membrane to transition temperature by inserting between lipid molecules which affects inter-molecular ordered arrangement of phospholipids in the membrane [23,29]. As a result, we think, cholesterol molecules obscure membrane defects and boundaries, leading to less or no interfaces during phase transition. In addition, incorporation of cholesterol increases the membrane lipophilicity and therefore barrier function to hydrophilic compounds which likely explains the remarkable decrease of CF release and declined thermosensitivity as observed in cholesterol containing liposomes (Fig. 7).

Considering the applicable hyperthermia range in the clinic (40-43°C), a DPPC content has to be selected which balances instability with rapid release. TSLs with a DPPC content above 80% are prone to leak at around physiological temperature because the membrane already goes through phase transition at 37°C (Fig 8). The onset of phase transition of liposomes with a DPPC content of 40% or lower on the other hand, starts at 41°C, with only a minor fraction of the lipids convert to a liquid state. Based on Level Rule, the percentage of liquid crystalline phase in the membrane at this state is still low (~17%) even at 43°C, thus generating lesser interfaces for release. Therefore, in DPPC-DSPC based thermosensitive liposomes the amount of DPPC should be above 40% and not beyond 80% for a fast triggered drug release at a preferred hyperthermia temperature.

Conclusion

Thermosensitive liposomes are promising delivery systems for solid tumor treatment combined with local hyperthermia. It is crucial that TSLs display rapid content release when exposed to the right temperature,

generating a steep drug gradient which benefits subsequent tumor uptake. The present work, based on the analysis of phase equilibrium, illustrates that inhomogeneous crystal grains consisting membranes form in DPPC-DSPC bi-component TSLs. These inhomogeneous microstructurally organized membranes offer numerous solid-liquid phase interfaces, namely nano-scale gaps, at transition temperature at crystal grain boundaries and defect regions, enabling rapid release. These induced nano-scale gaps in liposome membranes are adjustable in quantity by changing DPPC and DSPC ratios, thus presenting different release kinetics, which can be used to further develop TSLs for wider application in the clinic.

Acknowledgements

We thank Dr. Lars Lindner at Ludwig-Maximilians-University of Munich, for kindly providing purified carboxyfluoresce in powder.

Supporting data

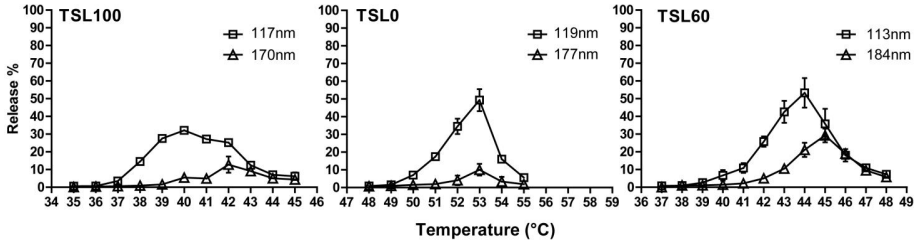

Supplementary Figure 1. Effect of liposomal diameter on CF release from mono-component or bi-component TSLs in FCS. Mean±SEM are shown of 3 independent experiments.

Supplementary Table 1 Charaterization of CF TSLs of large diameter. Mean±SD, N=3.

Liposome	Z-average (nm)	Polydispersity
TSL 100	170±7	0.05±0.02
TSL 0	177±4	0.06±0.02
TSL 60	184±7	0.05±0.03

References:

[1] Y. Matsumura, H. Maeda, A new concept for macromolecular therapeutics in cancer chemotherapy; mechanism of tumoritropic accumulation of proteins and the antitumor agent SMANCS, Cancer Res. 46 (1986) 6387-6392.
[2] X.L. Cun, J.T. Chen, S.B. Ruan, L. Zhang, J. Wan, Q. He, H.L. Gao, A novel strategy through combining iRGD peptide with tumor-microenvironment-responsive and multistage nanoparticles for deep tumor penetration, ACS Appl. Mater. Interfaces 7 (2015) 27458-27466.
[3] H. Cabral, Y. Matsumoto, K. Mizuno, Q. Chen, M. Murakami,M. Kimura, Y. Terada, M.R. Kano, K. Miyazono, M. Uesaka, N. Nishiyama, K. Kataoka, Accumulation of sub-100 nm polymeric micelles in poorly permeable tumours depends on size, Nature nanotechnology 6 (2001) 815-823.
[4] S.K. Hobbs, W.L. Monsky, F.Yuan, W.G. Roberts, L. Griffith, V.P. Torchilin, R.K. Jain, Regulation of transport pathways in tumor vessels: role of tumor type and microenvironment, Proc. Natl. Acad. Sci. 95 (1998) 4607-4612.
[5] A.L.B. Seynhaeve, S. Hoving, D. Schipper, C.E. Vermeulen, G. aan de Wiel-Ambagtsheer, S.T. van Tiel, A.M.M. Eggermont, T.L.M. ten Hagen, Tumor necrosis factor α mediates homogeneous distribution of liposomes in murine melanoma that contributes to better tumor response, Cancer Res. 67 (2007) 9455-9462.
[6] M.B. Yatvin, J. N. Weinstein, W. H. Dennis, R. Blumenthal, Design of liposomes for enhanced local release of drugs by hyperthermia, Science 202 (1978) 1290-1293.
[7] G. Kong, M.W. Dewhirst, Hyperthermia and liposomes, Int. J. Hyperth. 15 (1999) 345-370.
[8] D. Needham, G. Anyarambhatla, G. Kong, M.W. Dewhirst, A new temperature sensitive liposome for use with mild hyperthermia: characterization and testing in a human tumor xenograft model, Cancer Res. 60 (2000) 1197-1201.
[9] D. Needham, J.Y. Park, A.M. Wright J.H. Tong, Materials characterization of the low temperature sensitive liposome (LTSL): effects of the lipid composition (lysolipid and DSPE PEG2000) on the thermal transition and release of doxorubicin, Faraday Discuss. 161 (2013) 515-534.

[10] B. Kneidl, M. Peller, G. Winter, L.H. Lindner, M. Hossann, Thermosensitive liposomal drug delivery systems: state of the art review, Int. J. Nanomed. 9 (2014) 4387-4398.
[11] L.M. Ickenstein, M.C. Arfvidssonc, D. Needhamd, L.D. Mayera, K. Edwards, Disc formation in cholesterol-free liposomes during phase transition, Biochim. Biophys. Acta. 1614 (2003) 135-138.
[12] A.G. Lee, Functional properties of biological membranes: a physical–chemical approach, Prog. Biophys. Mol. Biol. 29 (1975) 3-56.
[13] J.K. Mills, D. Needham, Lysolipid incorporation in dipalmitoylphosphatidylcholine bilayer membranes enhances the ion permeability and drug release rates at the membrane phase transition, Biochim. Biophys. Acta. 1716 (2005) 77-96.
[14] T. Tagami, M.J. Ernsting, S.D. Li, Optimization of a novel and improved thermosensitive liposome formulated with DPPC and a Brij surfactant using a robust in vitro system, J. Control. Release 154 (2011) 290-297.
[15] M.H. Gaber, K. Hong, S.K. Huang, D. Papahadjopoulos, Thermosensitive sterically stabilized liposomes: formulation and in vitro studies on mechanism of doxorubicin release by bovine serum and human plasma, Pharm Res. 12 (1995) 1407-1416.
[16] M. Hossann, M. Wiggenhorn, A. Schwerdt, K. Wachholz, N. Teichert, H. Eibl, R.D. Issels, L.H. Lindner, In vitro stability and content release properties of phosphatidylglyceroglycerol containing thermosensitive liposomes, Biochim. Biophys. Acta. 1768 (2007) 2491-2499.
[17] L.H. Lindner, M.E. Eichhorn, H. Eibl, N. Teichert, M. Schmitt-Sody, M. Dellian, Novel temperature-sensitive liposomes with prolonged circulation time, Clin. Cancer Res. 10 (2004) 2168-2178.
[18] F. Guo, M. Yu, J.P. Wang, F.P. Tan, N. Li, Smart IR780 theranostic nanocarrier for tumor-specific therapy: hyperthermia-mediated bubble-generating and folate-targeted liposomes, ACS Appl. Mater. Interfaces 7 (2015) 20556-20567.
[19] L. Li, T.L.M. ten Hagen, D. Schipper, T.M. Wijnberg, G.C. van Rhoon, A.M. Eggermont, L.H. Lindner, G.A. Koning, Triggered content release from optimized stealth thermosensitive liposomes using mild hyperthermia, J. Control. Release 143 (2010) 274-279.
[20] L. Li, T.L.M. ten Hagen, M. Hossann, R. Suss, G.C. van Rhoon, A.M. Eggermont, D. Haemmerich, G.A. Koning, Mild hyperthermia

triggered doxorubicin release from optimized stealth thermosensitive liposomes improves intratumoral drug delivery and efficacy, J. Control. Release 168 (2013) 142-150.
[21] T. Lu, W.J.M. Lokerse, A.L.B. Seynhaeve, G.A. Koning, T.L.M. ten Hagen, Formulation and optimization of idarubicin thermosensitive liposomes provides ultrafast triggered release at mild hyperthermia and improves tumor response, J. Control. Release 220 (2015) 425-437.
[22] W.J.M. Lokerse, E.C.M. Kneepkens, T.L.M. ten Hagen, A.M.M. Eggermont, H. Grull, G.A. Koning, In depth study on thermosensitive liposomes: Optimizing formulations for tumor specific therapy and in vitro to in vivo relations, Biomaterials 82 (2016) 138-150.
[23] G.A. Hughes, Nanostructure-mediated drug delivery, Nanomedicine: Nanotechnology, Biology, and Medicine 1 (2005) 22-30.
[24] R.A. Demel, S.C. Kinsky, C.B. Kinsky, L.L.M. van Deenen, Biochim. Biophys. Acta. 150 (1968) 655-665.
[25] S. Mabrey, J.M. Sturtevant, Investigation of phase transitions of lipids and lipid mixtures by sensitivity differential scanning calorimetry, Proc. Natl. Acad. Sci. 73 (1976) 3862-3866.
[26] C.D. Landon, J.Y. Park, D. Needham, M.W. Dewhirst, Nanoscale drug delivery and hyperthermia: The materials design and preclinical and clinical testing of low temperature-sensitive liposomes used in combination with mild hyperthermia in the treatment of local cancer, Open Nanomed. J. 1 (2011) 38-64.
[27] H. Komatsu, S. Okada, Increase permeability of phase-separated liposomal membranes with mixtures of ethanol-induced interdigitated and non-interdigitated structures, Biochim. Biophys. Acta. 1237 (1995) 169-175.
[28] G. Singhvi, M. Singh, Review: in-vitro drug release characterization models, Int. J. Pharm. Studies Res. 2 (2011) 77-84.
[29] L. Coderch, J. Fonollosa, M. De Pera, J. Estelrich, A. De La Maza, J.L. Parra, Influence of cholesterol on liposome fluidity by EPR relationship with percutaneous absorption, J. Control. Release 68 (2000) 85-95.

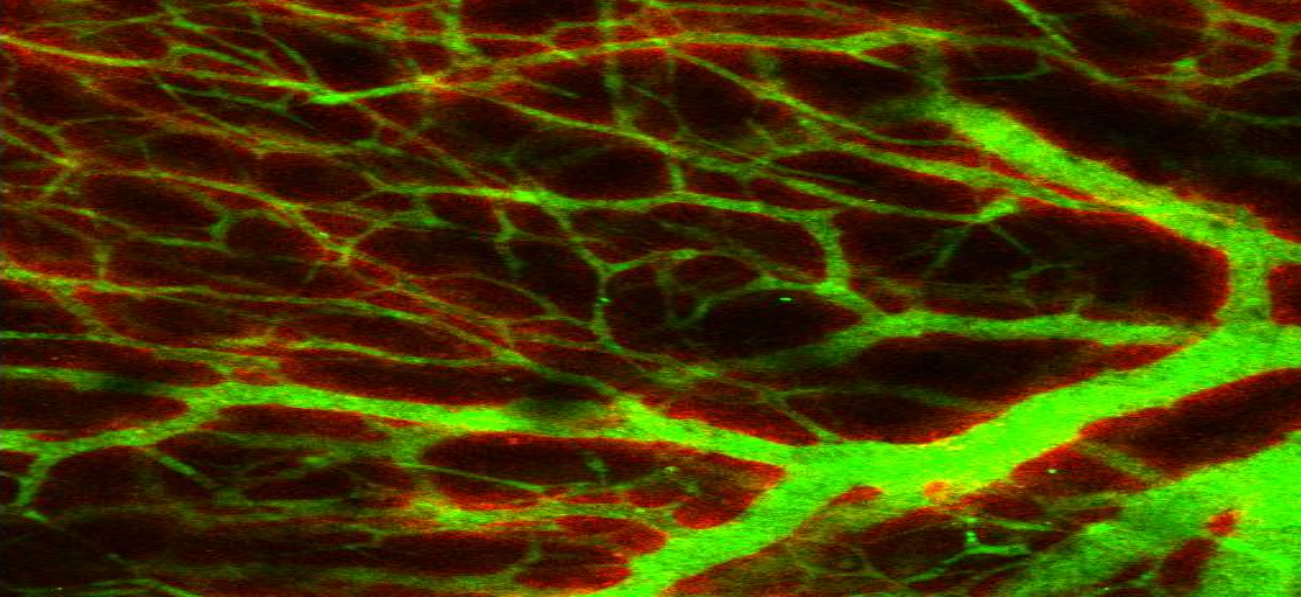

Chapter 5

A novel kinetic model to describe the release of trigger-responsive drug delivery systems

Tao Lu*, Timo L.M. ten Hagen*

Submitted

Abstract

Stimuli-responsive release is a hot topic in pharmaceutical sciences. Thermosensitive liposome as one of the stimuli-responsive drug delivery systems receives more attentions, due to its abilities that generate rapid and massive drug release at heated area by local hyperthermia at proper temperature (e.g. T_{max}) and do not release contents in non-heated locations. This special triggered release behavior at T_{max} is hard to described by mathematical kinetic models that are used commonly. The aim of this study was to find out the proper kinetic equation to describe this kind of rapid and massive release of triggered release systems. We summarized all commonly used kinetic models based on reported literatures and fitted the release data with these models, finding that only Korsmeyer-Peppas model showed better fitting results among these existing equations. However, the poor fitting effect was observed in liposomes with size below 100 nm by using Korsmeyer-Peppas model. Therefore, we proposed a new empirical equation that demonstrated improved fitting effects not only in liposomes with large size but also in size at 70 nm. Besides, the new proposed kinetic model also showed good fitting results on all releases within the whole release temperature range.

Keywords:

Triggered-responsive release, release kinetic models, thermosensitive drug delivery liposome, phase transition temperature, fitting effect,

1. Introduction

During the history of pharmaceutical science, medicine preparations have developed from traditional tablets, pills, capsules and injections to the current sustained-release preparations. Increasing novel pharmaceutical preparations are under investigating in the recent decades, especially the so-called nano-scale smart drug delivery systems. These delivery systems are responsive to the changes in local environment thus producing a controllable release of drug at the target sites. Several types of smart drug delivery systems were reported to trigger release of their contents upon environmental stimuli, such as glucose-sensitive [1], pH-sensitive [2], light-sensitive [3] and thermo-sensitive [4] formulations. Especially nano-scaled smart drug delivery systems receive increasing attention due to several advantages they offered, such as prolonged circulation time of drug in blood [5] and improved drug uptake by tumor [6], thus these smart drug delivery systems will be the direction of development in pharmaceutical science.

Thermosensitive liposomes (TSL) are one of the most promising smart delivery systems, which has demonstrated minimal leakage at normal temperature, but rapid controlled drug release in any location when combined with a local hyperthermia [4, 7-10]. This rapid release feature of the TSL occurs at a temperature range that these liposomal membrane going through a phase transition, which causes openings in the membrane to release contents [7]. During the phase transition, manipulating the temperatures can alter the openings density on liposomal membrane, thus controlling the release to reach a maximum rate, at which the temperature is called T_{max} (Figure 1).

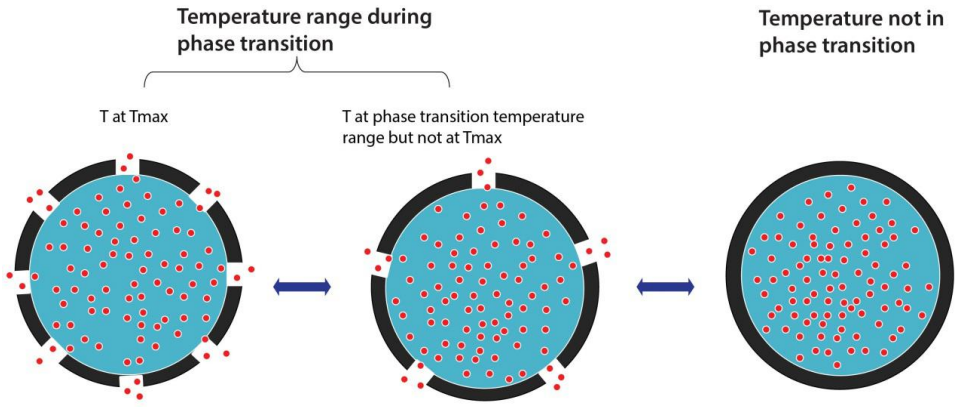

Figure 1. An example graph illustrates the release of thermosensitive liposomes (TSL). When temperature does not reach phase transition, TSL do not show release; while temperature reaches phase transition range, TSL generate some release to massive and rapid release when at maximum release temperature.

Generally at phase transition TSLs exhibit a release pattern consisted of an initial ultra-fast component and a follow-up slow sustained release component, of which the initial part commonly shows massive release of payload within a matter of dozens of seconds or minutes after triggered by hyperthermia, presenting a "Γ" shape-like release curve. This special "Γ" shape release pattern is completely different from sustained release preparations (Figure 2).

To better understand drug release profiles and predict in vivo performance, mathematical models are used to describe drug release profiles. There have been a number of mathematical models to depict drug release kinetics of different formulations (Table 1) [11-13]. Among these kinetic equations, zero-order, first-order and Higuchi models are the most commonly used to describe sustained-controlled release formulations [14]. It is generally believed that drug release from conventional liposome follows first-order kinetics [15, 16]. We studied the release behaviors of different thermosensitive liposomal formulations, finding that within the phase transition temperature range, the fastest release was obtained when temperature reached the T_{max}. Before and after the T_{max}, first-order or Higuchi equation is feasible to fit the release patterns of payload [7]. However, these equations showed very poor

fitting results for drug release curves at T_{max}. The fast release of drug at the targeted sites from thermosensitive liposomes in vivo can reduce the drug loss as a consequence of wash-away by blood. Therefore, studying the release at T_{max} of TSLs and its mathematical equation is of important clinical significance. To describe the entire drug release profile of thermosensitive liposomes at T_{max}, in this study we investigated the maximum release curves of thermosensitive liposomes with different compositions and sizes, and aimed to search and establish a suitable kinetic equation that fits the heat-triggered release drug delivery system at T_{max}.

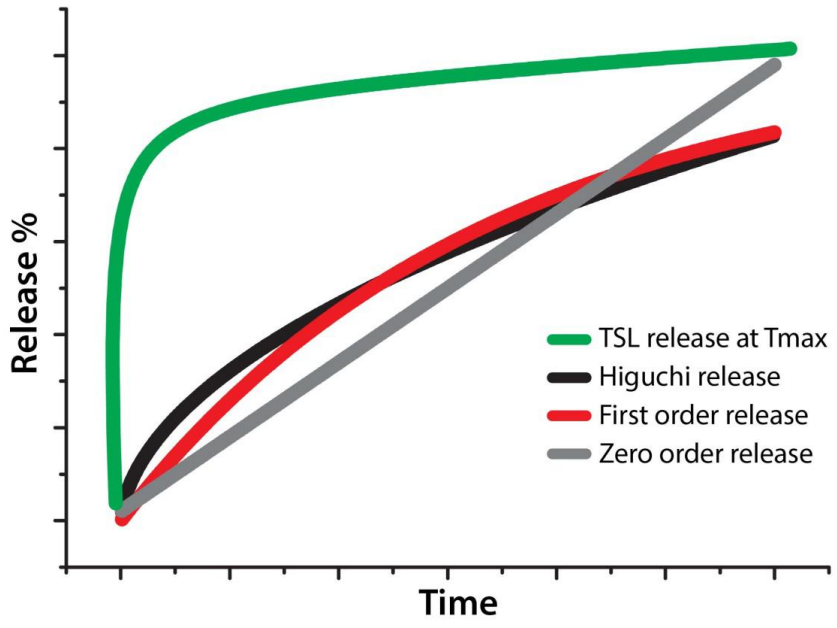

Figure 2. An example graph shows the shape of release curves of Zero-order, First-order, Higuchi, compared to the "Γ" shape-like release curve of thermosensitive liposomes at T_{max}.

Table 1. Commonly used kinetic models in pharmaceutical science research.

Release kinetic model	Mathematical equation
Zero order	$Q = Q_0 + k*t$
First order	$Q/ Q_0=1-e^{(-k*t)}$
Higuchi	$Q =k * t^{1/2}$
Hixson-Crowell	$Q^{1/3}- Q_0^{1/3} = k*t$
Korsmeyer-Peppas	$Q/ Q_\infty=k*t^n$
Weibull	$Q/ Q_0 = 1-e^{(-k(t-T))}$
Baker-Lonsdale	$(1-(1- Q/ Q_\infty)^{2/3})* Q/ Q_\infty=2/3*k*t$
Hopfenberg	$Q/ Q_\infty=1-(1-k*t)^3$
Gompertz	$Q/ Q_\infty=e^{(-\alpha*\exp(\beta*\log t))}$

Q represents the amount of drug released at time t; Q_0 is the initial amount of drug; Q_∞ represents the amount of drug released at an infinite time; k is the release constant.

2. Methods and materials

2.1 Chemicals and agents

1,2-dipalmitoyl-sn-glycero-3-phosphcholine (DPPC), 1,2-distearoyl-sn-glycero-3-phosphocholine (DSPC) and 1,2-distearoyl-sn-glycero-3-phosphoethanolamine-N-PEG_{2000} (DSPE-PEG) were provided by Lipoid (Ludwigshafen, Germany). Fetal calf serum (FCS) was purchased from Sigma Aldrich. Purified carboxyfluorescein (CF) was kindly provided by Dr. Lars Lindner and colleagues. PD-10 columns were obtained from GE Healthcare (UK). Other chemicals were purchased from Sigma Aldrich unless otherwise specified.

2 .2 Preparation of liposomes

Thermosensitive liposomes were composed of DPPC/DSPC/DSPE-PEG in a molar ratio of x/(100-x)/5 (x=100, 80, 60, 40, 20, 0, namely TSL 100, TSL 80, TSL 60, TSL 40, TSL 20 and TSL 0) by using the thin lipid film hydration method, followed by heated extrusion [7]. Briefly, 100 μmol of lipids was dissolved in methanol/chloroform (1/9 v/v) mixed solvent

which was then evaporated at 40°C, followed by nitrogen flush for 30 min to remove residual solvent. The resulting dried lipid film was hydrated with CF (100 mM, pH 7.4) solutions at 60°C. Unilamellar vesicles with different diameter were obtained by extrusion through Nuclepore® (Whatman Inc., USA) filters with pore size of 200 nm, 100 nm or 50 nm on a Thermobarrel extruder at 65°C (Northern Lipids, Canada). Unencapsulated CF was removed with a PD-10 column. Diameter (Z-average) and polydispersity index (PDI) were measured by using Zetasizer Nano-ZS (Malvern Instruments Ltd., UK).

2.3 CF-loaded TSL time- and temperature-dependent release

20 µl of 1 mM [lipid] CF-TSL suspension was added to 2 ml 100% FCS in a quartz cuvette at a series of determined temperature for 10 min. Real-time release of CF was detected with a water bath combined spectrofluorimetry (Ex. 493 nm/Em. 517 nm, Ex. slit 5 nm/Em. slit 5 nm) (Hitachi F-4500 Fluorescence Spectrophotometer, Japan). The average fluorescence intensity of the initial 5 seconds was recorded as I_0 of CF-TSL release, while fluorescence was measured as I_t at 10 min. After 10 min, detergent (10% Triton X-100) was used to disrupt all liposomes to measure maximal CF fluorescence, which was recorded as I_{max}. Release (%) = $(I_t - I_0)/(I_{max} - I_0) \times 100$ [7].

2.4 Fitting by kinetic equations

The maximum release percentages at phase transition were fitted with the kinetic equations shown in Table 1 by using Origin 7.5. The optimal release equation was selected based on determination coefficient (R^2) and goodness of fitting (Chi^2/DOF) which represents the deviation between experimental data and fitted curves.

3. Results

3.1 Determination of T_{max} for each TSL formulation through temperature-dependent release

Thermosensitive liposomes with different compositions prepared in qualified sizes (70, 120 and 170 nm) and desired PDI (below 0.1) were

applied in this study (Supplementary Table 1). Temperature-dependent release assay was applied to reveal the maximum CF release temperature for each TSL formulation. Results show the maximum release temperatures at 40 and 41°C for TSL 100, 42 and 43°C for TSL 80, 44°C for TSL 60, 47°C for TSL 40, 49 and 50°C for TSL 20 and 53°C for TSL 0 (Figure 3). Dramatically decreased release was observed in TSL with larger diameter, which is consistent with our previous results [7] and others [17, 18].

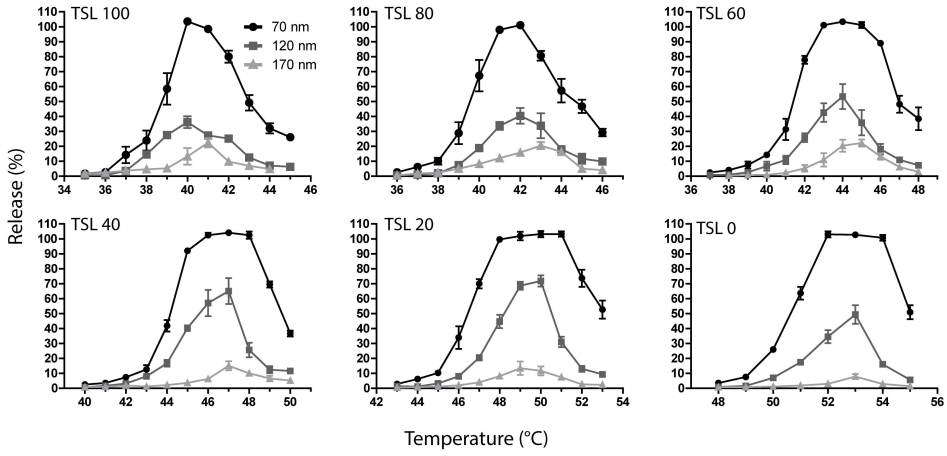

Figure 3. The maximum release temperature of each TSL formulation is determined by applying temperature-dependent release study in FCS. Mean ± SD are shown of 3 independent experiments.

3.2 Evaluation of release through fitting by various kinetic models

The release data at T_{max} of each TSL were fitted through these commonly used release kinetic equations (Table 1). We found most equations either showed poor determination coefficients or hardly fit. By comparison, Korsmeyer-Peppas equation can describe the release profiles at T_{max} with a better fitting effect than other release models. Especially, Korsmeyer-Peppas release model showed a good fitting effect in liposomes with size 170 nm and 120 nm (Figure 4A). However, the fitting curves were not very consistent with experimental data when we applied thermosensitive liposomes at 70 nm (Figure 4A). Determination coefficients R^2 of fitting by Korsmeyer-Peppas equations also showed a decline when 70 nm was

tested (Figure 4B). Chi^2/DOF which represents the goodness of fitting indicates an average value over 30 in liposomes at 70 nm, demonstrating a poor goodness of fit using Korsmeyer-Peppas model on smaller sized liposomes (Figure 4C), although in sizes of 120 and 170 nm minimal deviations were seen (average Chi^2/DOF below 3) (Figure 4C).

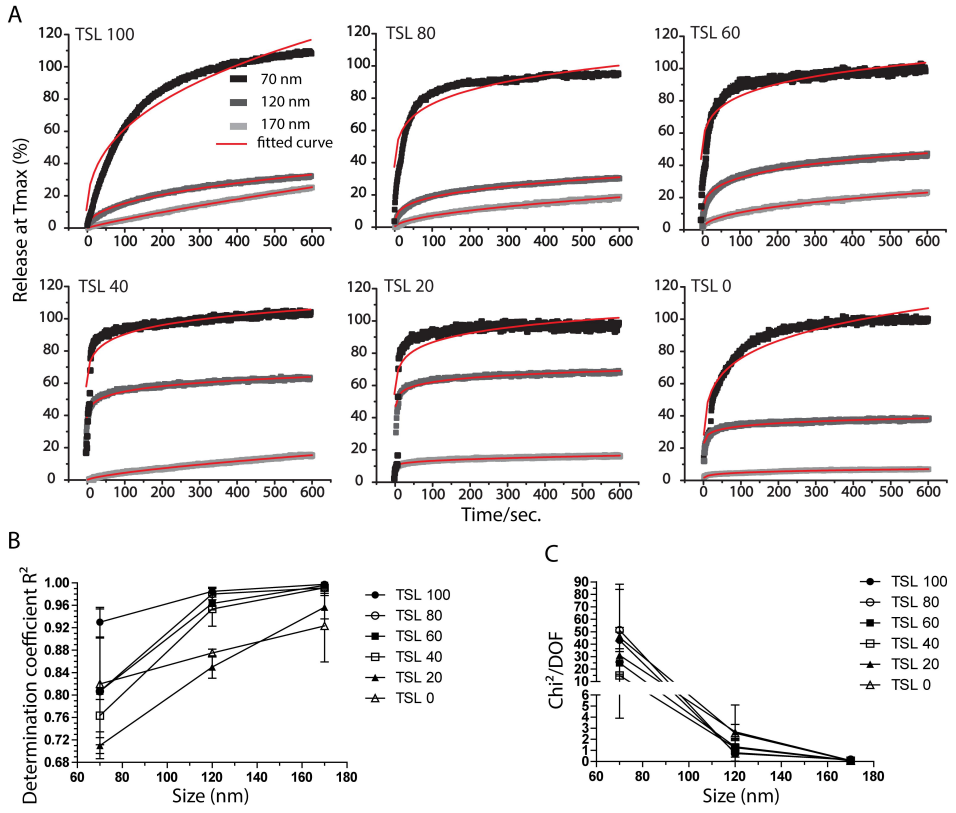

Figure 4. Korsmeyer-Peppas model fitted curves shows poor fitting effect in liposome with size of 70 nm compared to 120 and 170 nm (A). The determination coefficient R^2 (B) and Chi2/DOF (C) indicate the low goodness of fitting when using Korsmeyer-Peppas on TSL at 70 nm. Mean ± SD are shown of 3 independent experiments.

3.3 Establishment of a new release model

To fit release data of 70 nm at T_{max} with a better model, we inverted the release curve (Figure 5). It is obvious to observe that the reciprocal of

release decreases dramatically with time increasing at the initial phase of heating, followed by a slow decrease, suggesting a inversely proportional change against time. Namely:

$$\frac{1}{y} \propto \frac{1}{t}$$

Based on the shape of this curve, we proposed the following empirical equation to describe the release at T_{max}:

$$1/y = 1/k * (1/t + a)$$

where *a* is an empirical constant and k is proportional constant.

Change it to

$$y = \frac{k*t}{1+a*t} \quad (1)$$

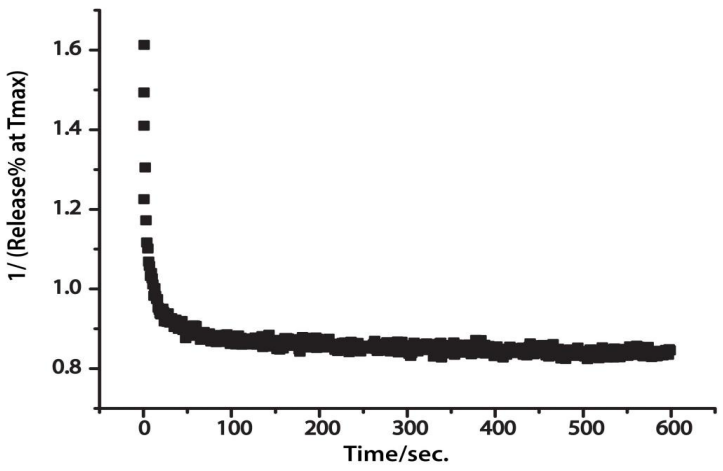

Figure 5. A release curve of TSL at 70 nm is inverted, showing the reciprocal of release at T_{max} is inversely proportional to time.

3.4 Non-linear fitting the release through the new kinetic model

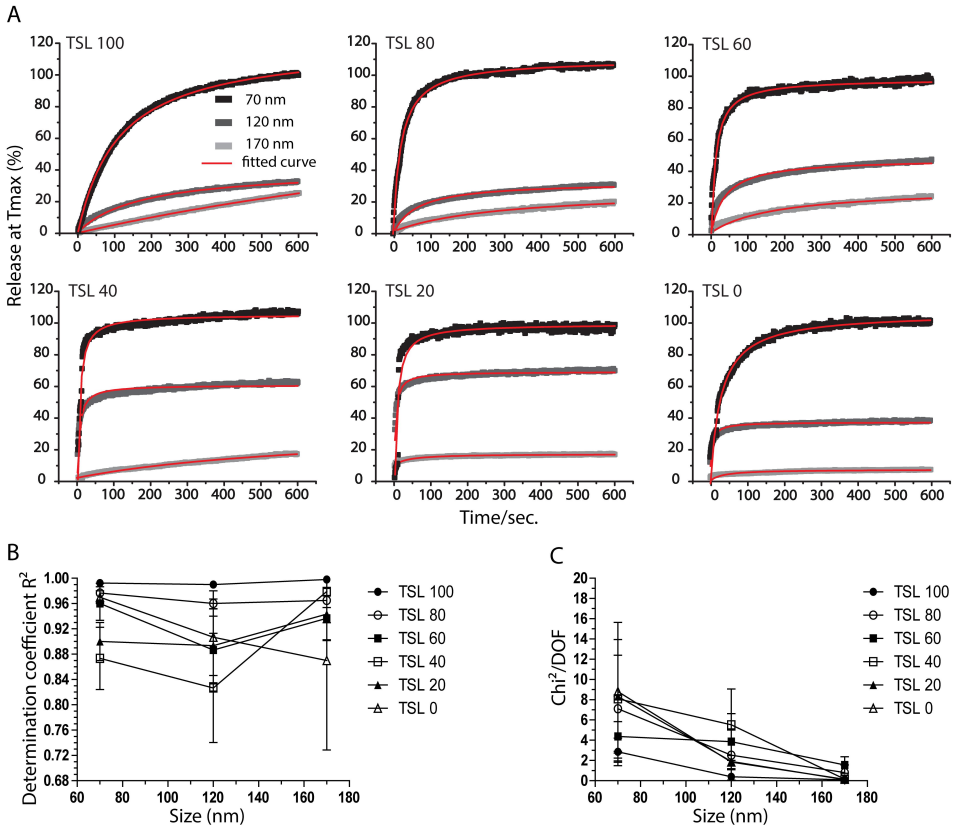

Figure 6. Our new model demonstrates improved fitting effect in liposome with size of 70 nm (A). The determination coefficient R^2 (B) and Chi2/DOF (C) indicate that fitting through our proposed model shows higher goodness of fitting in TSL at 70 nm and comparable fitting effect in TSL at 120 and 170 nm compared to Korsmeyer-Peppas. Mean ± SD are shown of 3 independent experiments.

Applying our proposed equation (2) to fit these 6 TSL formulations with 3 different sizes, the results were shown in Figure 6A. Comparable fitting effects were observed in liposomes with diameters at 120 and 200 nm as Korsmeyer-Peppas kinetic model. Additionally, the new model especially showed improved fitting effect in liposome with diameter at 70 nm.

Similar R^2 values were observed in these 3 different sized liposomes, showing the better stability of fitting effect through this new kinetic model (Figure 6B). Similarly, Chi^2/DOF indicated not only comparably low values at 120 and 170 nm, but also significant declined values at 70 nm by showing an average below 6, which manifests an improved goodness of fitting when using our proposed release model (Figure 6C).

3.5 Fitting through the linear forms of Korsmeyer-Peppas and the new kinetic models

To confirm the applicability of this new kinetic model, these release data were also fitted by the linear equations of Korsmeyer-Peppas (equation 2) and our proposed new model (equation 3), respectively.

Korsmeyer-Peppas model:

$$\ln y = n * \ln t + \ln k1 \quad (2)$$

New model:

$$1/y = (1/k1) * (1/t) + a/k1 \quad (3)$$

where k1 represents proportional constant.

The R^2 values of linear fitting of Tmax release were indicated in Table 2. Both models at linear equation are able to fit the release data at Tmax. Like the results of non-linear fitting, the new model still shows better fitting effects than Korsmeyer-Peppas model in small sized liposomes, showing average R^2 of 0.82±0.11 and 0.86±0.09 at 70 nm and 120 nm, respectively. While at size of 170 nm, the linear form of Korsmeyer-Peppas model exhibits a higher average R^2 value at 0.93±0.10 compared to the new model.

Table 2. The determination coefficient R^2 values of fitting through linear form of Korsmeyer-Pappas model and our new model of release at T_{max}. Mean ± SD, N = 3.

Size	Kinetic model	TSL 100	TSL 80	TSL 60	TSL 40	TSL 20	TSL 0	Average
70 nm	Korsmeyer-Peppas	0.77±0.17	0.73±0.09	0.76±0.01	0.68±0.07	0.55±0.10	0.83±0.07	0.72±0.04
	New	0.89±0.07	0.95±0.05	0.76±0.13	0.79±0.10	0.81±0.1	0.70±0.08	0.82±0.10
120 nm	Korsmeyer-Peppas	0.96±0.04	0.96±0.03	0.86±0.03	0.92±0.05	0.76±0.07	0.69±0.24	0.86±0.19
	New	0.82±0.13	0.87±0.14	0.91±0.01	0.75±0.09	0.89±0.07	0.89±0.06	0.86±0.09
170 nm	Korsmeyer-Peppas	0.96±0.04	0.89±0.01	0.99±0.01	0.95±0.03	0.87±0.13	0.92±0.05	0.93±0.10
	New	0.86±0.15	0.96±0.02	0.76±0.09	0.92±0.03	0.84±0.09	0.65±0.25	0.83±0.14

4. Discussion

Unlike conventional liposomal formulations which generally produce slow and passive release of content, thermosensitive liposomes demonstrate an active and maximum (or complete) release within minutes once reaching the transition temperature (T_{max}). This specific release behavior at T_{max} of thermosensitive liposomes has not been described by any proper kinetic models. In our previous work of DPPC-DSPC based thermosensitive liposomes, we reported that formulation TSL 100-40 more follow Higuchi release model and TSL 20 and 0 follow First-order better based on release at non-maximum release temperature [7]. Yet the releases at maximum release temperature did not fit to Zero-order, First-order or Higuchi model. Here we tested all commonly used release models and demonstrate that only Korsmeyer-Peppas model and our proposed new model showed good fitting results for release at T_{max}.

Generally the release kinetics of most conventional liposomes are supposed to follow First-order model [15, 16]. There are also reports that First-order equation was used to describe the release behavior of triggered release liposome [15]. However, we find that the release of thermosensitive liposomes, especially at Tmax presenting a "Γ" shape-like curve, does not fit well by First-order equation. First-order model hardly shows desired fitting results, neither determination coefficient values nor Chi^2/DOF (Table 3). In contrast, fitting through Korsmeyer-Peppas model and our new model exhibit higher R^2 values in these TSL formulations, suggesting the better fitting effect than first-order model. However, higher R^2 values may not always indicate the higher goodness of fitting (TSL 100 at 70 nm in Figure 2 and Table 3). The significantly high Chi^2/DOF results observed in TSL 100 to 0 at 70 nm reveals that Korsmeyer-Peppas model is less desired to fit release behavior of triggered-release liposomes with diameter of 70 nm (Table 3). By comparison, our new model demonstrates higher goodness of fitting by showing an average Chi^2/DOF value of 6.6±2.4 (Table 3), suggesting that this kinetic equation can better describe release behavior at smaller sized liposomes (e.g. below 100 nm) which actually are more commonly used in the research and in clinic. In addition, the same outcome was observed when using linear form of these kinetic models, which confirms the applicability of our new kinetic model for fitting of triggered release at T_{max}.

Massive and rapid release at Tmax, this special release profile is of importance and also the typical attribute of thermosensitive liposomes. This new kinetic model demonstrates significantly better fitting results at T_{max} than other established kinetic models. For temperatures not at Tmax, a relatively slow release is observed. In most cases reported previously, the releases at non-Tmax commonly are described by First-order or Higuchi models [7, 15]. However, our new kinetic equation also indicates comparable fitting results at non-maximum release temperatures. TSL with 70 nm diameter are illustrated as an example. During the whole release temperature ranges of TSL 100 to 0, this new kinetic model presents desirable fitting effects at each temperature point, showing average R^2 value above 0.9 and Chi^2/DOF with an average below 15 (Figure 7). Similar results were observed in TSL with sizes of 120 nm and 170 nm (data not shown), indicating the wide applicability of our new

release kinetic model which can be used to fit the release during the whole temperature range.

Table 3. Non-linear fitting of release at T_{max} through Korsmeyer-Peppas, our proposed and First-order kinetic models. Mean ± SD, N = 3

Size	Kinetic model		TSL 100	TSL 80	TSL 60	TSL 40	TSL 20	TSL 0	Average
70 nm	Korsmeyer-Peppas	R^2	0.93±0.03	0.81±0.10	0.81±0.00	0.76±0.03	0.61±0.10	0.89±0.01	0.81±0.07
		Chi^2/DOF	43.0±6.7	51.3±36.8	25.0±0.1	14.8±10.9	31.0±22.4	45.4±38.5	35.1±13.9
	New	R^2	0.99±0	0.98±0.02	0.96±0.02	0.86±0.02	0.90±0.03	0.97±0.01	0.95±0.05
		Chi^2/DOF	2.9±1.4	7.1±5.3	4.4±1.5	8.1±5.8	8.3±5.6	8.8±6.8	6.6±2.4
	First-order	R^2	0.38±0.38	0.68±0.12	-	-	-	0.77±0.18	-
		Chi^2/DOF	63.1±49.3	86.7±56.3	-	-	-	28.7±7.5	-
120 nm	Korsmeyer-Peppas	R^2	0.98±0	0.98±0.01	0.96±0.01	0.95±0.03	0.84±0.11	0.76±0.2	0.92±0.06
		Chi^2/DOF	0.8±0.3	0.7±0.7	1.3±0.6	1.2±0.8	2.7±0.7	2.6±2.5	1.6±0.9
	New	R^2	0.99±0	0.96±0.02	0.89±0.07	0.8±0.05	0.89±0.04	0.91±0.05	0.91±0.06
		Chi^2/DOF	0.4±0.1	2.5±2.5	3.8±2.8	5.5±3.5	1.9±0.3	1.8±0.7	2.7±1.8
	First-order	R^2	0.63±0.03	-	-	-	-	-	-
		Chi^2/DOF	22.0±1.2	-	-	-	-	-	-
170 nm	Korsmeyer-Peppas	R^2	0.99±0	0.99±0	0.99±0	0.99±0.01	0.97±0.02	0.92±0.07	0.97±0.03
		Chi^2/DOF	0.1±0.1	0.2±0.0	0.1±0.0	0.1±0.0	0.1±0.1	0.1±0.1	0.1±0.1
	New	R^2	0.99±0	0.96±0.02	0.94±0.04	0.98±0.02	0.92±0.06	0.79±0.18	0.95±0.04
		Chi^2/DOF	0.1±0.0	0.8±0.8	1.6±0.8	0.2±0.1	0.1±0.1	0.1±0.1	0.4±0.6
	First-order	R^2	0.99±0.01	-	-	0.80±0.28	-	-	-
		Chi^2/DOF	0.7±0.8	-	-	1.2±1.5	-	-	-

- represents that data cannot be fitted.

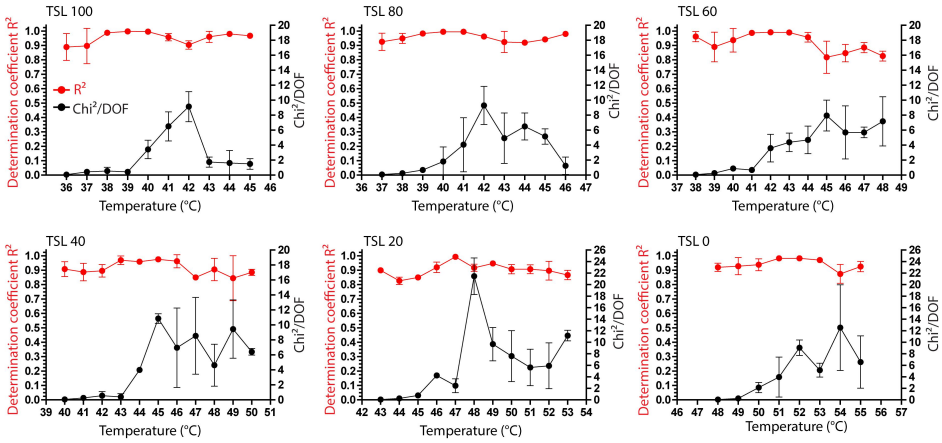

Figure7. TSL with 70 nm size selected as examples, illustrate that our proposed kinetic equation can fit not only the release at T_{max} but also the release at non-T_{max}, showing all determination coefficient R^2 above 0.9 and Chi^2/DOF values below 15. Mean ± SD are shown of 3 independent experiments.

5. Conclusion

The rapid and substantial release occurs when thermosensitive liposomes are exposing to desirable hyperthermia, presenting a "Γ" shape of release curve, which is the feature of not only thermosensitive liposomes and also other smart triggered release drug delivery systems. It is necessary to find a proper mathematical model to describe this special release behavior at maximum release temperature as this can be used to predict the release kinetics and mechanism of triggered release drug carriers. This study shows that in currently used kinetic models only Korsmeyer-Peppas equation can describe this release profile relatively better when thermosensitive liposomes with size above 100 nm. We proposed a new kinetic model illustrates the significant improvement in both determination coefficient and goodness of fitting, thus showing better fitting effect than Korsmeyer-Peppas model regardless of the size of TSL. Furthermore, our kinetic model also exhibits good fitting results at non-T_{max}. These results implies the potential universal applicability of our kinetic model used in release fitting for trigger-responsive release drug

delivery systems. Due to the fact that our new release model is an empirical equation concluded based on quantitative experimental data, the theoretical derivation of this release kinetic equation still needs follow-up investigation.

Supporting data

Supplementary Table 1 Characterization of CF TSL with different compositions and sizes. Mean ± SD, N = 3.

Liposome	Z-average (nm)[a]			Polydispersity		
TSL 100	72±2	117±5	169±5	0.04±0.02	0.07±0.01	0.04±0.02
TSL 80	71±1	119±3	166±4	0.05±0.01	0.05±0.03	0.04±0.01
TSL 60	73±1	113±2	162±5	0.05±0.02	0.07±0.02	0.07±0.01
TSL 40	72±1	120±4	169±4	0.05±0.02	0.04±0.01	0.06±0.02
TSL 20	74±1	115±3	172±3	0.06±0.03	0.05±0.02	0.05±0.03
TSL 0	74±2	119±6	172±2	0.06±0.02	0.06±0.02	0.07±0.02

[a] The Z-average of particle was reported by Zetasizer, which was measured based on Comulant model.

References

[1] D. Shi, M. Ran, L. Zhang, H. Huang, X. Li, M. Chen, M. Akashi, Fabrication of biobased polyelectrolyte capsules and their application for glucose-triggered insulin delivery, ACS applied materials & interfaces, 8 (2016) 13688-13697.
[2] D. Samanta, J.L. Meiser, R.N. Zare, Polypyrrole nanoparticles for tunable, pH-sensitive and sustained drug release, Nanoscale, 7 (2015) 9497-9504.
[3] H. Kim, H. Lee, K.Y. Seong, E. Lee, S.Y. Yang, J. Yoon, Visible Light-Triggered On-Demand Drug Release from Hybrid Hydrogels and its Application in Transdermal Patches, Advanced healthcare materials, 4 (2015) 2071-2077.
[4] T. Lu, W.J.M. Lokerse, A.L.B. Seynhaeve, G.A. Koning, T.L.M. ten Hagen, Formulation and optimization of idarubicin thermosensitive liposomes provides ultrafast triggered release at mild hyperthermia and improves tumor response, Journal of Controlled Release, 220 (2015) 425-437.
[5] X. Han, Z. Li, J. Sun, C. Luo, L. Li, Y. Liu, Y. Du, S. Qiu, X. Ai, C. Wu, Stealth CD44-targeted hyaluronic acid supramolecular nanoassemblies for doxorubicin delivery: probing the effect of uncovalent pegylation degree on cellular uptake and blood long circulation, Journal of Controlled Release, 197 (2015) 29-40.
[6] H. Maeda, J. Wu, T. Sawa, Y. Matsumura, K. Hori, Tumor vascular permeability and the EPR effect in macromolecular therapeutics: a review, Journal of controlled release, 65 (2000) 271-284.
[7] T. Lu, T.L.M. ten Hagen, Inhomogeneous crystal grain formation in DPPC-DSPC based thermosensitive liposomes determines content release kinetics, Journal of Controlled Release, 247 (2017) 64-72.
[8] L.H. Lindner, M.E. Eichhorn, H. Eibl, N. Teichert, M. Schmitt-Sody, R.D. Issels, M. Dellian, Novel temperature-sensitive liposomes with prolonged circulation time, Clinical Cancer Research, 10 (2004) 2168-2178.
[9] D. Needham, G. Anyarambhatla, G. Kong, M.W. Dewhirst, A new temperature-sensitive liposome for use with mild hyperthermia: characterization and testing in a human tumor xenograft model, Cancer research, 60 (2000) 1197-1201.

[10] L. Li, T.L.M. ten Hagen, M. Hossann, R. Süss, G.C. van Rhoon, A.M.M. Eggermont, D. Haemmerich, G.A. Koning, Mild hyperthermia triggered doxorubicin release from optimized stealth thermosensitive liposomes improves intratumoral drug delivery and efficacy, Journal of Controlled Release, 168 (2013) 142-150.
[11] P. Costa, J.M. Sousa Lobo, Evaluation of mathematical models describing drug release from estradiol transdermal systems, Drug development and industrial pharmacy, 29 (2003) 89-97.
[12] J. Dredán, I. Antal, I. Rácz, Evaluation of mathematical models describing drug release from lipophilic matrices, International journal of pharmaceutics, 145 (1996) 61-64.
[13] S. Dash, P.N. Murthy, L. Nath, P. Chowdhury, Kinetic modeling on drug release from controlled drug delivery systems, Acta Pol Pharm, 67 (2010) 217-223.
[14] G.A. Hughes, Nanostructure-mediated drug delivery, in: Nanomedicine in Cancer, Pan Stanford, 2017, pp. 47-72.
[15] M. Hossann, M. Wiggenhorn, A. Schwerdt, K. Wachholz, N. Teichert, H. Eibl, R.D. Issels, L.H. Lindner, In vitro stability and content release properties of phosphatidylglyceroglycerol containing thermosensitive liposomes, Biochimica et Biophysica Acta (BBA)-Biomembranes, 1768 (2007) 2491-2499.
[16] T.M. Allen, L.G. Cleland, Serum-induced leakage of liposome contents, Biochimica et Biophysica Acta (BBA)-Biomembranes, 597 (1980) 418-426.
[17] A. Nagayasu, T. Shimooka, H. Kiwada, Effect of vesicle size on in vivo release of daunorubicin from hydrogenated egg phosphatidylcholine-based liposomes into blood circulation, Biological and Pharmaceutical Bulletin, 18 (1995) 1020-1023.
[18] M. Hossann, T. Wang, M. Wiggenhorn, R. Schmidt, A. Zengerle, G. Winter, H. Eibl, M. Peller, M. Reiser, R.D. Issels, Size of thermosensitive liposomes influences content release, Journal of controlled release, 147 (2010) 436-443.

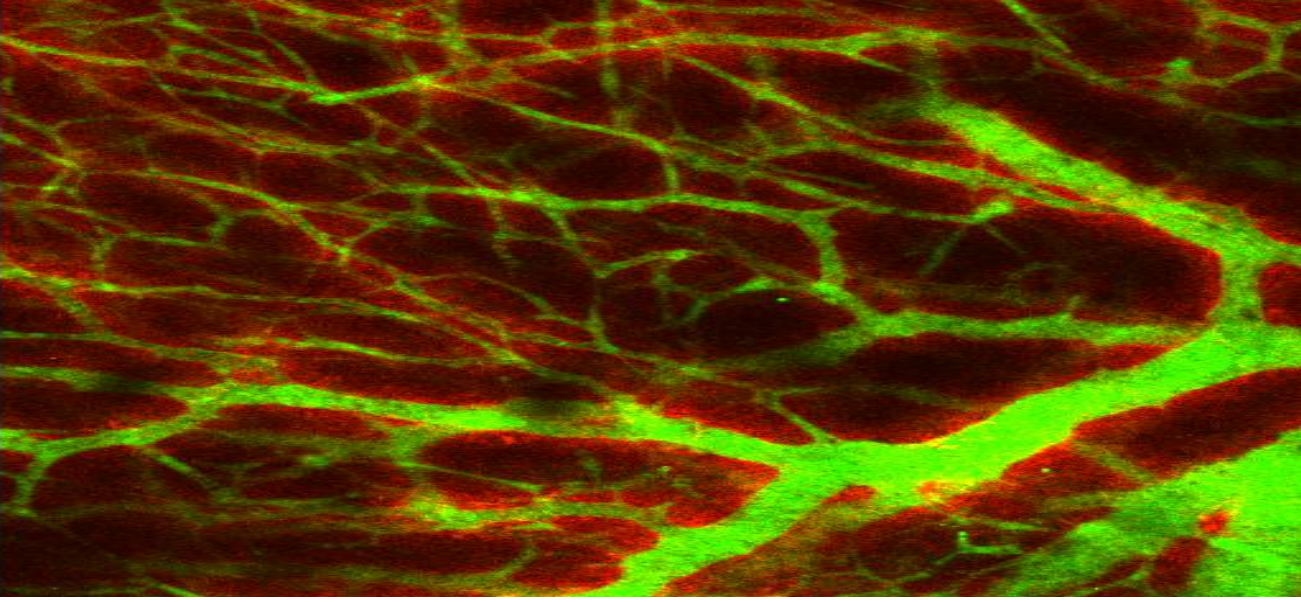

Chapter 6

Discussion

Conventional nanocarriers for solid tumors chemotherapy

Traditional chemotherapy for solid tumor treatment applies systemic administration of cytotoxic compounds in free from and bloodstream brings these cytotoxic drugs to the tumor tissues. This requires the cytotoxic compounds to possess proper size and oil/water solubility, desirable pharmacokinetics, and high dosing administration feasibility, which limits the options of drug candidates in chemotherapeutic treatment. Besides, these non-selective cytotoxic compounds also attack the healthy tissues and organs in the body and thus lead to a variety of adverse side effects, which in fact is a major reason behind the high mortality rate of cancer patients [1]. The appearance of nanoscale drug carriers brings the possibilities that 1) reduce systemic toxicity by encapsulating chemotherapeutics inside these nanocarriers, avoiding the direct contact of cytotoxic compounds to healthy tissues during delivery [2]; 2) and improve pharmacokinetic properties and drug stability in bloodstream, e.g. increased delivery of poorly water-soluble compounds, which augments the options for chemotherapeutic drugs [3]. For treatment, these nanocarriers with chemotherapeutic compounds encapsulation can extravasate into tumor tissues through the leaky vascular network in tumors termed as enhanced permeability and retention (EPR) effect (Figure 1) [4]. Demonstrating EPR effect is believed to be the general feature of solid tumors, including leaky blood vessels and poor lymphatic drainage, and is resulted from rapid and defective angiogenesis which induces gaps in endothelial cell lining, thus allowing those nanocarriers running with the blood to passively accumulate in solid tumor tissues [5, 6].

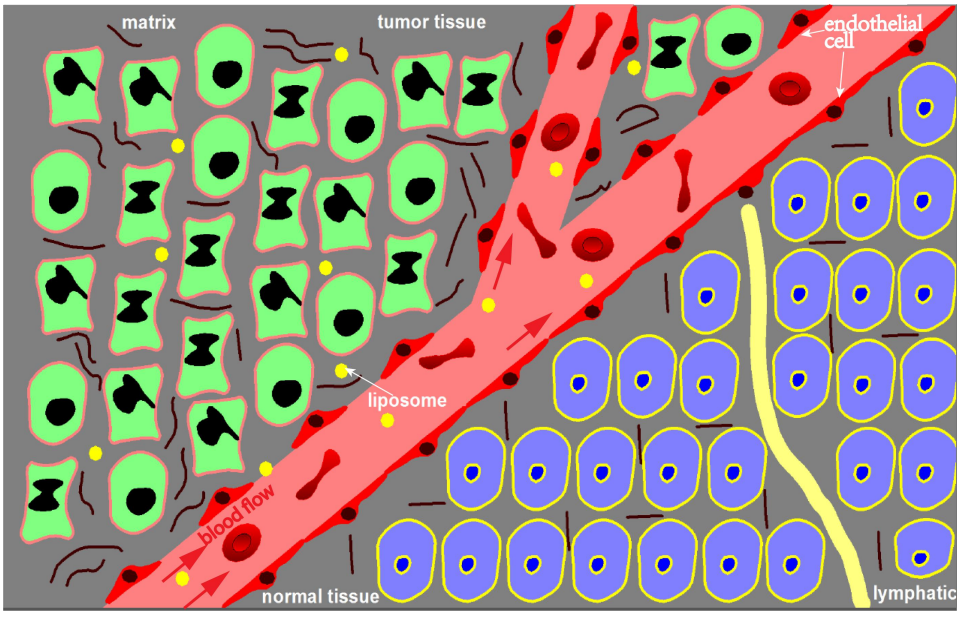

Figure 1. The schematic representation of the enhanced permeability and retention phenomenon in tumor vessel. Tumor vessels exhibit loose arrangement of endothelial cells leading to gaps in between facilitating nanocarriers extravasation under the flow of blood, while endothelial cells stand orderly in normal vessels and nanoparticles are not easy to extravasate.

Although there have been several nanocarrier-based drugs approved for cancer therapy in the market (Table 1) and showed either increased effectiveness in some solid tumors or improved patient's compliance [7-15], for most tumors treatment therapeutic efficacy improvement is under expectation when using these conventional nanocarriers with chemotherapeutics. Several reasons can be attributed to this outcome: 1) the circulation time. Nanocarriers lacks enough circulation time in blood, which seriously influences these nanoparticles accumulation in tumor via EPR effect. 2) the heterogeneity of EPR effect. The leakiness level of tumor vessels can be various due to the diversity of tumor growth, tumor types and host species. Hence, EPR varies in effectiveness and hardly produces significant outcome in most tumor patients, affecting the extent

of nanocarriers extravasation from tumor vessel [16, 17]. 3) the extracellular matrix in tumor tissue forming a barrier to the nanocarriers. Even these nanocarriers cross leaky vessels, unlike free chemotherapeutic molecules which are easy to diffuse further simply based on concentration gradient, the disorganized and complex interstitial tumor matrix has a greater impact on these “big” nanoparticles compared to those small drug molecules, hindering nanocarriers for a deeper penetration even though benefiting from EPR-based accumulation, thus limiting the amount of accumulation as well [18, 19]. 4) the slow drug release from nanocarriers. Most conventional nanocarrier-based delivery systems have a quite slow drug release profile due to the high intrinsic stability, which leads to an insufficient drug concentration and limited bioavailable drug molecules in the tumor interstitium or tumor cells [20-22]. Altogether these factors influence the effectiveness of EPR differently, thus limiting the therapeutic benefit when applying those nanocarriers. In fact, a recent meta-analysis of pre-clinical data published over the past ten years indicates that only around 0.7% of administered nanocarriers can accumulate [23]. Although approaches were applied to improve nanocarriers performance, such as active targeting nanocarrier, which are designed to incorporate tumor cell-specific ligands on the surface and thus to increase tumor uptake of nanocarriers [24], however, several studies indicate that incorporation of ligands on nanocarriers improves the cellular internalization by the target cells but does not significantly increase the amount of nanocarriers that extravasate into tumor compared to non-targeted nanocarriers [25-29] due to complexity of tumor microenvironment [30-34]. Therefore, these nanocarries solely replying on the EPR effect, may be inadequate to achieve an improved efficacy in tumor treatment.

Table 1. Approved nanocarriers-based drug for cancer therapy in the market.

Product	**Nanocarrier**	**Drug**	**Indication**	**Approval**
DaunoXome®	Liposome	Daunorubicin	Kaposi's sarcoma	1996
DepoCyt®	Liposome	Cytosine Arabinoside (cytarabine)	Neoplastic meningitis	1999
Doxil®/Caelyx®	Liposome	Doxorubicin	Kaposi's sarcoma Ovarian cancer Breast cancer Multiple myeloma	1995 1999 2003 2007 (Europe, Canada)
Genexol-PM® (IG-001) [Samyang Biopharm]	PEG-PLA polymeric micelle	Paclitaxel	Breast cancer Lung cancer Ovarian cancer	2007 (South Korea)
Marqibo®	Liposome	Vincristine	Acute lymphoid leukemia	2012 (USA)
Mepact®	Liposome	Mifamurtide MTP-PE	Osteosarcoma	2009 (EU)
Myocet®	Liposome	Doxorubicin	Breast cancer (cyclophosphamide)	2000 (Europe)
NanoTherm®	Iron oxide nanoparticle	No drug	Thermal ablation glioblastoma	2010 (Europe)

Smart nanocarriers for triggered release drug delivery systems

To accelerate drug release from nanocarriers and improve intratumoral bioavailable drug level, one solution is to use smart nanocarriers locally release chemotherapeutics inside tumor vessels which allows tumor cells to take up the drugs more efficiently due to the subsequent extensive diffusion of drug molecules from vessels to interstitial - this will avoid the drawbacks of EPR effect in conventional nanocarriers. For this purpose, thermosensitive liposomes (TSLs), as one of most promising smart nanocarriers at present, can be used to deliver chemotherapeutic compounds and locally release cargo at the target sites by an external heating trigger, thus increasing bioavailable drug concentration in the tumor. There have been many reports showed great improvement by applying TSLs in combination with a local hyperthermia (HT) in solid tumor treatment in comparison to using conventional nanocarriers drug delivery systems in the pre-clinical and clinical trials [35-41]. Thermosensitive liposomes offer several advantages for solid tumor treatment – 1) It is relatively easy to locally generate a steady hyperthermia in tumor compared to other triggers; 2) TSLs deliver drugs to anywhere of the tumor with the bloodstream and do not need to extravasate into tumor interstitial; 3) TSLs produce a sensitive heat-triggered release of chemotherapeutics only at the heated tumor, but do not release drug at the non-heated sites, which especially important to an ideal thermosensitive liposomal formulation. To produce an ideal performance and achieve an optimal therapeutic efficacy of using thermosensitive liposomes, the proper drug compounds for TSL encapsulation and the TSL formulation composition are crucially important to TSL effectiveness in solid tumor treatment.

Drug selection for thermosensitive liposome

To date, based on literatures calculated from PubMed several chemotherapeutic drugs have been reported in thermosensitive liposomes for solid tumor treatment including cisplatin (15 publications) [42],

methotrexate (4 publications) [43], melphalan (3 publications) [44], taxol (8 publications) [45], 5-fluorouracil (3 publications) [46], vincristine (1 publication) [47], gemcitabine (6 publications) [39] and doxorubicin (over 100 publications) [38]. These drugs are potent chemotherapeutics in the clinic, but an optimal performance in TSL-mediated system may be not always reachable by encapsulating these drugs. The physicochemical characteristics of drug influence the effectiveness of TSL in cargo loading, stability and cargo release after triggering. Most of above mentioned chemotherapeutic compounds show a low loading efficiency and loading capacity in thermosensitive liposomes, because of applying passive loading method that only benefits encapsulation of highly water-soluble drug molecules [48]. The entrapped drug compounds need to be stable after encapsulation (e.g. forming a crystal or precipitate inside TSL) to reduce leakage when TSL is exposed to serum/blood environment in vivo at body temperature [49]. Furthermore, encapsulated drug also need to release rapidly when passing through heated region in order to obtain efficient local drug concentrations in tumor.

Doxorubicin (DXR) receives most attentions and is regarded as a standard drug, due to its proper characteristics that make it meet these conditions after encapsulation in thermosensitive liposomes. DXR is an amphiphilic compound (with a pKa at 8.6 and logP at 0.5 [50]) that can be encapsulated into pre-formed TSLs based on a transmembrane pH or ion gradient, referred to as active loading method [51]. The encapsulated ionized DXR molecules form drug crystal with anions inside TSL aqueous core, thus producing a stable and high drug loading. The fluorescent property of DXR makes the handy online monitoring of release for in vitro and in vivo studies. Experimental observations have demonstrated a fast triggered release of DXR in several different DXR-TSL formulations, in generally showing a completely release of DXR within minutes [37, 38, 52, 53]. This improved loading efficiency, capacity, stability and fast release makes DXR as a promising drug candidate than most other drugs for TSL encapsulation.

Another important factor to the encapsulated drug is the cell uptake rate, which determines the level of bioavailable drug inside tumor cells. Locally triggered release from thermosensitive liposomes will not make much sense if the substantial released drug molecules cannot be taken up efficiently even though the compounds are released very fast. Redistribution back to vessels can occur to these untaken free drug molecules, resulting to a waste and reduced efficacy. We selected idarubicin (IDA) as entrapment drug for TSL, which is structurally similar to doxorubicin but slightly more hydrophobic (with pKa at 8.6 nad logP at 1.9 [50]) that is supposed to be taken up by cells quickly [54], to compare with DXR-TSL. In Chapter 2 we described the success of developing an optimized idarubicin-thermosensitive liposome formulation (IDA-TSL) [55]. Due to its amphiphilic property, IDA can be encapsulated based on the same principle as DXR. We have shown that using EDTA ions form the stable precipitate with IDA inside TSL and increase the loading capacity of IDA to 45 mol% (drug to lipid molar ratio), which is around 2-3 times higher than DXR loading, thereby suggesting an improved local delivery efficiency of IDA using thermosensitive liposomes. Because of the increased hydrophobicity, IDA demonstrates an ultrafast triggered release at 42°C by showing a 100% release in a matter of seconds in vitro (Chapter 2), and dramatically increased cell uptake (Chapter 3). An average of over 10 times higher cellular uptake rate of IDA than DXR was observed in the first 5 min exposure, which is especially significative to TSL-mediated chemotherapeutics delivery to achieve a high drug uptake efficiency in tumor cells. However, we also observed more leakage of IDA from TSL at 37°C than DXR (20% vs 4%), which is due to the entrapment of IDA in TSL membrane as a result of hydrophobicity interaction between IDA and membrane bilayer. This suggests that highly hydrophobic drug may cause increased leakage or stability issue after loading in thermosensitive liposome though it has a fast cellular uptake rate. And also the water-like environment in vessels and tumor interstitial are not beneficial to diffusion and penetration of drug molecules in tumor if they are too

hydrophobic [56]. Similarly, highly hydrophilic compounds may also not be optimal candidates for TSL application because of the difficulty in passing liposome membranes and cell membranes which can slow down drug uptake by the tumor tissue. Carboxyfluorescein (CF), a highly hydrophilic dye, used as a model drug encapsulated in TSL, indicates a relatively slower and uncompleted release at 42°C compared to DXR-TSL [57, 58]. Though CF shows very fast and homogeneous diffusion from vessels after release, which is desired to drug for efficient penetration in deep tumoral cells, a rapid back-diffusion to vessels is observed on these free CF molecules from tumor interstitial (in fact cells do not take up CF; but if they could absorb CF, it is reasonable to expect that the high hydrophilicity will definitely influence the uptake efficiency of CF). Therefore, for an optimal TSL-mediated drug delivery system the entrapped drug with appropriate physicochemical features is necessary when considering to achieve a desirable balance between loading capacity, stability, release and cellular uptake, such as choosing amphiphilic drugs.

Formulation selection for thermosensitive liposome

The formulation composition is also important to thermosensitive liposome performance. Desired compositions give an optimal TSL formulation that is able to reduce leakiness at body temperature and benefit a maximal drug release at phase transition temperature (Tm) of liposome membrane, improving site-specific drug delivery. To date, several thermosensitive liposomal formulations have been reported (summarized in Table 2.). The first thermosensitive liposome formulation, described by Yatvin in 1978, is consisted of DPPC and DSPC, loading with neomycin or methotrexate [43, 59]. Due to relative slow contents release and limited stability, the results of this TSL system are not that promising. Gaber et al described a thermosensitive liposome formulation with the addition of cholesterol and PEG lipid, also called as traditional thermosensitive liposome (TTSL) [60]. The addition of PEG lipid prolongs the stability of thermosensitive liposome and also benefits the release [61], leading to an efficient DXR release around 60% in human

plasma after 30 min after a heating trigger [60]. This TTSL incorporates cholesterol, which is deemed to enhance liposome stability as well by augmenting hydrophobic interaction between hydrophobic moieties of PC and cholesterol molecules [62]. In 2000, Needham et al, described a new thermosensitive liposomal formulation (LTSL) by adding a lysolipid - MSPC [40] to improve contents release under HT. As TSL membrane undergoes a gel state to liquid state phase transition that starts at grain boundary regions around Tm, thus generating "doors" (namely the interfaces between solid and liquid phases) for drug release [52, 63]. The incorporated MSPC is a surfactant-like lipid, which is speculated to desorb from the bilayer and leave nano pores at grain boundaries in liposome membrane at Tm, together with the stabilization from PEG-lipids, thereby enlarging these "doors" for a substantial and ultrafast drug release [52, 64]. Formulated LTSL-DXR indicates ~60% release in the first 20 sec and almost completed release of DXR in 2 min at its Tm at 41.3°C [64]. This fast-trigger release is important for TSL-mediated system providing a highly efficient local drug delivery and has brought this formulation (ThermoDox®) into clinical trials [65]. However, the adding of lyso-lipid MSPC also causes the increased leakage at body temperature, which results in ~30-40% leakage of DXR in vitro studies. Tagami et al. applied Brij 78 in a new TSL formulation. He claimed surfactant Brij 78 is supposed to function as lyso lipid and PEG, thus providing a rapid drug release upon heating [37, 66]. To avoid the overcome the drawback by using lyso-lipids, Lindner et al. developed a new TSL formulation by using DPPC, DSPC $DPPG_2$ [67]. The synthetic lipid $DPPG_2$ shows the similar effect like PEG lipids, thereby stabilizing the vesicle and increasing its circulation half-life [68]. Negligible leakage of DXR (below 5% in 20 min) is observed at 37°C in serum environment when encapsulated in this $DPPG_2$-containing TSL formulation, and around 100% release of DXR can be reached within 2-3 min at 42°C [53]. Similarly, Li et al. based on the formulation of Yatvin, developed a stabilized TSL formulation by adding an optimal 5mol% PEG-lipid, showing less DXR leakage (~20% in 1 h in serum) at body temperature

but also a slightly slower triggered release under 42°C (~75% in 1 min) when compared with LTSL formulation [38, 58]. Next to it, Lokerse et al. further optimized Li's formulation, indicating that TSL containing 70mol% DPPC, 25mol% DSPC and 5mol% PEG generates optimal stability and release for DXR at 37 and 42°C, respectively [69].

Table 2. Overview of reported thermosensitive liposome formulations

The designer of thermosensitive liposome	Thermosensitive liposome composition (mol/mol)
Yatvin et al. (1978)	DPPC/DSPC: 3/1
Gaber et al. (1995)	DPPC/HSPC/Cholesterol/DPPE-PEG: 50/25/15/3
Needham et al. (2000)	DPPC/MSPC/DSPE-PEG: 90/10/4
Tagami et al. (2011)	DPPC/Brij78: 94/4
Lindner et al. (2004)	DPPC/DSPC/$DPPG_2$: 50/20/30
Li et al. (2010)	DPPC/DSPC/DSPE-PEG: 80/15/5
Lokerse et al. (2016)	DPPC/DSPC/DSPE-PEG: 70/25/5

DPPC: 1,2-dipalmitoyl-*sn*-glycero-3-phosphocholine
DSPC: 1,2-distearoyl-*sn*-glycero-3-phosphocholine
DPPE-PEG: 1,2-dipalmitoyl-sn-glycero-3- phosphoethanolamine-N-[methoxy(polyethyleneglycol)-2000
MSPC: 1-stearoyl-2-hydroxysn-glycero-3-phosphatidyl-choline
DSPE-PEG: 1,2-distearoyl-sn-glycero-3-phosphatiylethanol-amine-N-[methoxy (polyethyleneglycol)-2000]
Brij 78: polyoxyethylene (20) stearyl ether
$DPPG_2$: 1.2-dipalmitoyl-sn-glycero-3-phosphoglyceroglycerol

The key to thermosensitive liposomes is whether the contents can be released rapidly in the site of interest, which directly affects the chemotherapeutic activity. Using different lipids or other materials (e.g. lyso-lipid, $DPPG_2$, surfactants etc.) can augment the sensitivity of liposome to heating, and improve heat-triggered release rate by in fact increasing the interfaces between solid and liquid phases during liposomal membrane phase transition which is the essence that the release of thermosensitive liposomes relies on. In Chapter 4, by using DPPC-DSPC

based TSLs as an example we explained why two compositions at least are needed in a thermosensitive liposomal formulation to produce more interfaces in membrane during phase transition and described how the interface regions can be affected by manipulating the DPPC-DSPC molar ratios to achieve an best trigger release at Tm. We found that the maximal release of each TSL formulation at respective Tm is significantly different, by showing differences from ~30% to 72% release of contents in a time scale of 10 min of heating [57]. This indicates that the amounts of interfacial region of solid-liquid phase are different at their Tm, which in other words suggests the grain boundary density of each TSL membrane is different because these boundary regions melt first, thus initiating the interfaces between solid and liquid phase [52].We plotted binary phase diagram based on the release profiles of each DPPC-DSPC formulation and illustrated that bi-components TSLs (DPPC plus DSPC) have high grain boundary density, thereby inducing more interfacial regions at corresponding transition temperatures for increased release. By contrast, mono-component TSLs, consisted of only DPPC or DSPC, can only release contents from limited melted boundary regions which are membrane defects due to the curvature stress, thus slowing down the release rate during phase transition. Among these bi-component vesicles, containing higher ratio of DSPC (higher melting point lipid in this study), generates more grains of which the lipids with lower melting point (DPPC) are rich in the edge during cooling down, inducing more boundary regions in liposomal membrane. Hence, we observed bi-component TSL 20 and 40 show significantly higher release rate than TSL 60 and 80 (Chapter 4), though the maximum release temperatures of them are much higher (47°C and 50°C) than TSL 60/80, beyond the applicable hyperthermia temperature used in the clinic. Considering the clinic feasibility of heating, a DPPC molar percentage between 40% - 80% is suggested in a DPPC-DSPC based TSL formulation for a better local drug delivery. Besides, PEG-lipids or other molecules with similar function are crucially important to TSL formulation, not only stabilizing the vesicle at body temperature for circulation but also supporting drug release by

stabilizing the "release openings" in membrane at Tm. We also proved that cholesterol is not suggestive to be used in a TSL formulation, which remarkably decrease the sensitivity of vesicle to heating [57, 70]. Additionally, decreasing the size of TSL increases its release rate because of the increased membrane defect regions resulted from increased curvature stress, but also reduces the stability and loading capacity of drug payload of these vesicles (Chapter 4 and 5) [71]. These findings indicate that, from a formulation point of view, bi-/multi-component lipids, the proper ratio of each lipid and proper vesicle size are considerable to thermosensitive liposomes yielding improved trigger drug release.

Efficacy of TSL in vivo

A thermosensitive liposome formulated with optimal drug and composition, may not always give an optimal performance in vivo as what it shows in vitro [72], due to the complexity of tumor structure. Almost all reported drug encapsulated thermosensitive liposomes have shown increased drug level in tumor under local hyperthermia and improved efficacy to different degrees compared to free drug. However, the in vivo behavior of drug delivery is not clear but vital because it determines whether an optimal treatment efficacy can be achieved, and provides indications on how to maximize the benefits of using TSL-mediated drug delivery system. Manzoor et al. demonstrated an on-line, rapid intravascular DXR release from LTSL-DXR in a heated tumor, which forms a high concentration gradient for extravascular diffusion of DXR, thus yielding a significantly deep and wide penetration in tumor than applying free DXR [73]. But a wash out of most untaken DXR which is released from LTSL from tumor vessels is observed as well, suggesting a suboptimal effectiveness of using thermosensitive liposomal DXR. In Chapter 3, we used IDA-TSL as an example in comparison with DXR-TSL regarding to their in vivo on-line drug release under hyperthermia by using intravital microscopy. IDA indicates a maximal tumor uptake after ~20 min upon heating, by showing ~8 times higher

uptake rate than DXR which takes around 1 h to reach peak uptake. Interestingly, the more hydrophobic property of IDA did not impede itself further diffusion, showing even higher IDA concentration than DXR in the distal region from vessels. Consequently, thermosensitive liposomal IDA shows a greatly higher intratumoral accumulation and a stronger therapeutic activity under the same dosage by comparison with thermosensitive liposomal DXR. Although IDA-TSL has more leakiness at 37°C and IDA is currently solely used for hematological cancers and would never be a candidate for treatment of solid cancers, the remarkably increased tumor uptake efficiency of IDA suggests that selection of appropriate drug are needed for appropriate formulation, which together improves the performance of thermosensitive liposome in vivo, thus achieving an optimal chemotherapeutic response.

Thermosensitive liposome release kinetics

To better understand drug release profiles and predict in vivo performance, mathematical models are used to describe drug release behavior. There have been a number of mathematical models to depict drug release kinetics of different formulations [74-76]. Among these kinetic equations, zero-order, first-order and Higuchi models are the most commonly used to describe sustained-controlled release formulations [77]. It is generally believed that drug release from conventional liposome follows first-order kinetics [49, 78]. Though there are reports that directly use first-order equation to calculate release rate of some thermosensitive liposomal formulations [52, 53], it has not seen a proper model that can describe the release behavior for thermosensitive liposome. In Chapter 4, we found our TSL formulations before and after the maximum release temperatures, show a better fitting effect with first-order or Higuchi equation [57]. However, the release profiles at Tm, which are the particular feature of thermosensitive liposomes, indicate very poor fitting results on both models. In Chapter 5, we studied the release behaviors of different thermosensitive liposomal formulations, demonstrating that Korsmeyer-Peppas equation can describe this release profile relatively

better when thermosensitive liposomes with size above 100 nm. Besides, we proposed a new kinetic equation that illustrates the significant improvement in both determination coefficient and goodness of fitting regardless of the size of TSLs. This new equation also shows good fitting effect of TSL release at non-Tm, implying the potential universal fitting applicability for other trigger-responsive drug delivery systems. Due to the fact that our new release model is an empirical equation concluded based on quantitative experimental data, the theoretical derivation of this release kinetic equation still needs follow-up investigation.

Conclusion

Thermosensitive liposomes in combination with local hyperthermia promote the development of nanoparticle based drug delivery, also bring promising improvement of chemotherapy for cancer treatment in the clinic. The overall goal of this thesis is, from the perspectives of drug selection as well as the formulation composition, to present the use thermosensitive liposomes to achieve a maximal in vivo drug delivery, thus yielding an optimal treatment efficacy. We selected idarubicin, a relatively hydrophobic anticancer drug for non-solid tumor, for TSL encapsulation and compared with the "standard loaded drug" – doxorubicin encapsulated TSL. An improved local drug delivery and tumor uptake is obtained, indicating that encapsulation of cytotoxic drug in TSL can remarkably increase tumor kill, even if this chemotherapeutic drug is not for solid tumor treatment in clinic. Next to it, the composition of TSL needs to be formulated with proper ratio of lipids matching up with loaded drug to provide a desirable trigger release at sites of interest under heating. Encapsulating suitable compound based on the way it will be delivered and released is of great importance, and also suitable carrier formulation is needed to enhance its cargo delivery. There is no one best drug or best formulation for TSL application. Choosing appropriate drug and appropriate TSL formulation composition will yield an optimal performance for tumor chemotherapy.

Reference

[1] S. Senapati, A.K. Mahanta, S. Kumar, P. Maiti, Controlled drug delivery vehicles for cancer treatment and their performance, Signal transduction and targeted therapy, 3 (2018) 7.
[2] Y. Malam, M. Loizidou, A.M. Seifalian, Liposomes and nanoparticles: nanosized vehicles for drug delivery in cancer, Trends in pharmacological sciences, 30 (2009) 592-599.
[3] L. Zhang, F.X. Gu, J.M. Chan, A.Z. Wang, R.S. Langer, O.C. Farokhzad, Nanoparticles in medicine: therapeutic applications and developments, Clinical pharmacology & therapeutics, 83 (2008) 761-769.
[4] Y. Matsumura, H. Maeda, A new concept for macromolecular therapeutics in cancer chemotherapy: mechanism of tumoritropic accumulation of proteins and the antitumor agent smancs, Cancer research, 46 (1986) 6387-6392.
[5] D. Peer, J.M. Karp, S. Hong, O.C. Farokhzad, R. Margalit, R. Langer, Nanocarriers as an emerging platform for cancer therapy, Nature nanotechnology, 2 (2007) 751.
[6] H. Hashizume, P. Baluk, S. Morikawa, J.W. McLean, G. Thurston, S. Roberge, R.K. Jain, D.M. McDonald, Openings between defective endothelial cells explain tumor vessel leakiness, The American journal of pathology, 156 (2000) 1363-1380.
[7] K. Venkatakrishnan, Y. Liu, D. Noe, J. Mertz, M. Bargfrede, T. Marbury, K. Farbakhsh, C. Oliva, A. Milton, Pharmacokinetics and pharmacodynamics of liposomal mifamurtide in adult volunteers with mild or moderate hepatic impairment, British journal of clinical pharmacology, 77 (2014) 998-1010.
[8] M.A. Rodriguez, R. Pytlik, T. Kozak, M. Chhanabhai, R. Gascoyne, B. Lu, S.R. Deitcher, J.N. Winter, Vincristine sulfate liposomes injection (Marqibo) in heavily pretreated patients with refractory aggressive non-Hodgkin lymphoma: report of the pivotal phase 2 study, Cancer: Interdisciplinary International Journal of the American Cancer Society, 115 (2009) 3475-3482.
[9] K.S. Lee, H.C. Chung, S.A. Im, Y.H. Park, C.S. Kim, S.-B. Kim, S.Y. Rha, M.Y. Lee, J. Ro, Multicenter phase II trial of Genexol-PM, a Cremophor-free, polymeric micelle formulation of paclitaxel, in patients with metastatic breast cancer, Breast cancer research and treatment, 108 (2008) 241-250.

[10] F.M. Muggia, J.D. Hainsworth, S. Jeffers, P. Miller, S. Groshen, M. Tan, L. Roman, B. Uziely, L. Muderspach, A. Garcia, Phase II study of liposomal doxorubicin in refractory ovarian cancer: antitumor activity and toxicity modification by liposomal encapsulation, Journal of Clinical Oncology, 15 (1997) 987-993.
[11] M.J. Glantz, K.A. Jaeckle, M.C. Chamberlain, S. Phuphanich, L. Recht, L.J. Swinnen, B. Maria, S. LaFollette, G.B. Schumann, B.F. Cole, A randomized controlled trial comparing intrathecal sustained-release cytarabine (DepoCyt) to intrathecal methotrexate in patients with neoplastic meningitis from solid tumors, Clinical cancer research, 5 (1999) 3394-3402.
[12] E. Rivera, Liposomal anthracyclines in metastatic breast cancer: clinical update, The oncologist, 8 (2003) 3-9.
[13] P.R. Gil, D. Hühn, L. Loretta, D. Sasse, W.J. Parak, Nanopharmacy: Inorganic nanoscale devices as vectors and active compounds, Pharmacological research, 62 (2010) 115-125.
[14] A. Wicki, D. Witzigmann, V. Balasubramanian, J. Huwyler, Nanomedicine in cancer therapy: challenges, opportunities, and clinical applications, Journal of controlled release, 200 (2015) 138-157.
[15] G. Batist, G. Ramakrishnan, C.S. Rao, A. Chandrasekharan, J. Gutheil, T. Guthrie, P. Shah, A. Khojasteh, M.K. Nair, K. Hoelzer, Reduced cardiotoxicity and preserved antitumor efficacy of liposome-encapsulated doxorubicin and cyclophosphamide compared with conventional doxorubicin and cyclophosphamide in a randomized, multicenter trial of metastatic breast cancer, Journal of Clinical Oncology, 19 (2001) 1444-1454.
[16] V.P. Chauhan, R.K. Jain, Strategies for advancing cancer nanomedicine, Nature materials, 12 (2013) 958.
[17] M. Bolkestein, E. de Blois, S.J. Koelewijn, A.M.M. Eggermont, F. Grosveld, M. de Jong, G.A. Koning, Investigation of factors determining the enhanced permeability and retention effect in subcutaneous xenografts, Journal of Nuclear Medicine, 57 (2016) 601-607.
[18] P.A. Netti, D.A. Berk, M.A. Swartz, A.J. Grodzinsky, R.K. Jain, Role of extracellular matrix assembly in interstitial transport in solid tumors, Cancer research, 60 (2000) 2497-2503.
[19] M.W. Dewhirst, T.W. Secomb, Transport of drugs from blood vessels to tumour tissue, Nature Reviews Cancer, 17 (2017) 738.

[20] A.L.B. Seynhaeve, B.M. Dicheva, S. Hoving, G.A. Koning, T.L.M. ten Hagen, Intact Doxil is taken up intracellularly and released doxorubicin sequesters in the lysosome: evaluated by in vitro/in vivo live cell imaging, Journal of controlled release, 172 (2013) 330-340.
[21] G.J.R. Charrois, T.M. Allen, Drug release rate influences the pharmacokinetics, biodistribution, therapeutic activity, and toxicity of pegylated liposomal doxorubicin formulations in murine breast cancer, Biochimica et Biophysica Acta (BBA)-Biomembranes, 1663 (2004) 167-177.
[22] S.C. White, P. Lorigan, G.P. Margison, J.M. Margison, F. Martin, N. Thatcher, H. Anderson, M. Ranson, Phase II study of SPI-77 (sterically stabilised liposomal cisplatin) in advanced non-small-cell lung cancer, British journal of cancer, 95 (2006) 822.
[23] S. Wilhelm, A.J. Tavares, Q. Dai, S. Ohta, J. Audet, H.F. Dvorak, W.C.W. Chan, Analysis of nanoparticle delivery to tumours, Nature reviews materials, 1 (2016) 16014.
[24] N. Bertrand, J. Wu, X. Xu, N. Kamaly, O.C. Farokhzad, Cancer nanotechnology: the impact of passive and active targeting in the era of modern cancer biology, Advanced drug delivery reviews, 66 (2014) 2-25.
[25] D.B. Kirpotin, D.C. Drummond, Y. Shao, M.R. Shalaby, K. Hong, U.B. Nielsen, J.D. Marks, C.C. Benz, J.W. Park, Antibody targeting of long-circulating lipidic nanoparticles does not increase tumor localization but does increase internalization in animal models, Cancer research, 66 (2006) 6732-6740.
[26] M.M. Schmidt, K.D. Wittrup, A modeling analysis of the effects of molecular size and binding affinity on tumor targeting, Molecular cancer therapeutics, 8 (2009) 2861-2871.
[27] K. Riviere, Z. Huang, K. Jerger, N. Macaraeg, F.C. Szoka Jr, Antitumor effect of folate-targeted liposomal doxorubicin in KB tumor-bearing mice after intravenous administration, Journal of drug targeting, 19 (2011) 14-24.
[28] D. Goren, A.T. Horowitz, S. Zalipsky, M.C. Woodle, Y. Yarden, A. Gabizon, Targeting of stealth liposomes to erbB-2 (Her/2) receptor: in vitro and in vivo studies, British journal of cancer, 74 (1996) 1749.
[29] M.H. Vingerhoeds, P.A. Steerenberg, J. Hendriks, L.C. Dekker, Q. Van Hoesel, D.J.A. Crommelin, G. Storm, Immunoliposome-mediated targeting of doxorubicin to human ovarian carcinoma in vitro and in vivo, British journal of cancer, 74 (1996) 1023.

[30] T. Lammers, F. Kiessling, W.E. Hennink, G. Storm, Drug targeting to tumors: principles, pitfalls and (pre-) clinical progress, Journal of controlled release, 161 (2012) 175-187.
[31] J.N. Weinstein, W. van Osdol, Early intervention in cancer using monoclonal antibodies and other biological ligands: micropharmacology and the "binding site barrier", Cancer research, 52 (1992) 2747s-2751s.
[32] M. Juweid, R. Neumann, C. Paik, M.J. Perez-Bacete, J. Sato, W. van Osdol, J.N. Weinstein, Micropharmacology of monoclonal antibodies in solid tumors: direct experimental evidence for a binding site barrier, Cancer research, 52 (1992) 5144-5153.
[33] K.D. Orcutt, J.J. Rhoden, B. Ruiz-Yi, J.V. Frangioni, K.D. Wittrup, Effect of small-molecule–binding affinity on tumor uptake in vivo: a systematic study using a pretargeted bispecific antibody, Molecular cancer therapeutics, (2012).
[34] R.K. Jain, T. Stylianopoulos, Delivering nanomedicine to solid tumors, Nature reviews Clinical oncology, 7 (2010) 653.
[35] R.T.P. Poon, N. Borys, Lyso-thermosensitive liposomal doxorubicin: an adjuvant to increase the cure rate of radiofrequency ablation in liver cancer, Future Oncology, 7 (2011) 937-945.
[36] T.M. Zagar, Z. Vujaskovic, S. Formenti, H. Rugo, F. Muggia, B. O'Connor, R. Myerson, P. Stauffer, I.C. Hsu, C. Diederich, Two phase I dose-escalation/pharmacokinetics studies of low temperature liposomal doxorubicin (LTLD) and mild local hyperthermia in heavily pretreated patients with local regionally recurrent breast cancer, International Journal of Hyperthermia, 30 (2014) 285-294.
[37] T. Tagami, M.J. Ernsting, S.-D. Li, Efficient tumor regression by a single and low dose treatment with a novel and enhanced formulation of thermosensitive liposomal doxorubicin, Journal of controlled release, 152 (2011) 303-309.
[38] L. Li, T.L.M. ten Hagen, M. Hossann, R. Süss, G.C. van Rhoon, A.M.M. Eggermont, D. Haemmerich, G.A. Koning, Mild hyperthermia triggered doxorubicin release from optimized stealth thermosensitive liposomes improves intratumoral drug delivery and efficacy, Journal of Controlled Release, 168 (2013) 142-150.
[39] S. Limmer, J. Hahn, R. Schmidt, K. Wachholz, A. Zengerle, K. Lechner, H. Eibl, R.D. Issels, M. Hossann, L.H. Lindner, Gemcitabine treatment of rat soft tissue sarcoma with phosphatidyldiglycerol-based

thermosensitive liposomes, Pharmaceutical research, 31 (2014) 2276-2286.
[40] D. Needham, G. Anyarambhatla, G. Kong, M.W. Dewhirst, A new temperature-sensitive liposome for use with mild hyperthermia: characterization and testing in a human tumor xenograft model, Cancer research, 60 (2000) 1197-1201.
[41] M.L. Hauck, S.M. LaRue, W.P. Petros, J.M. Poulson, D. Yu, I. Spasojevic, A.F. Pruitt, A. Klein, B. Case, D.E. Thrall, Phase I trial of doxorubicin-containing low temperature sensitive liposomes in spontaneous canine tumors, Clinical Cancer Research, 12 (2006) 4004-4010.
[42] Y.N. Dou, J. Zheng, W.D. Foltz, R. Weersink, N. Chaudary, D.A. Jaffray, C. Allen, Heat-activated thermosensitive liposomal cisplatin (HTLC) results in effective growth delay of cervical carcinoma in mice, Journal of controlled release, 178 (2014) 69-78.
[43] J.N. Weinstein, R.L. Magin, R.L. Cysyk, D.S. Zaharko, Treatment of solid L1210 murine tumors with local hyperthermia and temperature-sensitive liposomes containing methotrexate, Cancer research, 40 (1980) 1388-1395.
[44] T.P. Chelvi, S.K. Jain, R. Ralhan, Hyperthermia-mediated targeted delivery of thermosensitive liposome-encapsulated melphalan in murine tumors, Oncology research, 7 (1995) 393-398.
[45] Y. Wei, Y. Wang, D. Xia, S. Guo, F. Wang, X. Zhang, Y. Gan, Thermosensitive Liposomal Codelivery of HSA–Paclitaxel and HSA–Ellagic Acid Complexes for Enhanced Drug Perfusion and Efficacy Against Pancreatic Cancer, ACS applied materials & interfaces, 9 (2017) 25138-25151.
[46] C. Al Sabbagh, N. Tsapis, A. Novell, P. Calleja-Gonzalez, J.-M. Escoffre, A. Bouakaz, H. Chacun, S. Denis, J. Vergnaud, C. Gueutin, Formulation and pharmacokinetics of thermosensitive stealth® liposomes encapsulating 5-fluorouracil, Pharmaceutical research, 32 (2015) 1585-1603.
[47] M. Li, Z. Li, Y. Yang, Z. Wang, Z. Yang, B. Li, X. Xie, J. Song, H. Zhang, Y. Li, Thermo-sensitive liposome co-loaded of vincristine and doxorubicin based on their similar physicochemical properties had synergism on tumor treatment, Pharmaceutical research, 33 (2016) 1881-1898.

[48] Y. Barenholz, Relevancy of drug loading to liposomal formulation therapeutic efficacy, Journal of liposome research, 13 (2003) 1-8.
[49] T.M. Allen, L.G. Cleland, Serum-induced leakage of liposome contents, Biochimica et Biophysica Acta (BBA)-Biomembranes, 597 (1980) 418-426.
[50] L. Gallois, M. Fiallo, A. Laigle, W. Priebe, A. Garnier-Suillerot, The overall partitioning of anthracyclines into phosphatidyl-containing model membranes depends neither on the drug charge nor the presence of anionic phospholipids, European journal of biochemistry, 241 (1996) 879-887.
[51] Y. Barenholz, Liposome application: problems and prospects, Current opinion in colloid & interface science, 6 (2001) 66-77.
[52] J.K. Mills, D. Needham, Lysolipid incorporation in dipalmitoylphosphatidylcholine bilayer membranes enhances the ion permeability and drug release rates at the membrane phase transition, Biochimica et Biophysica Acta (BBA)-Biomembranes, 1716 (2005) 77-96.
[53] M. Hossann, M. Wiggenhorn, A. Schwerdt, K. Wachholz, N. Teichert, H. Eibl, R.D. Issels, L.H. Lindner, In vitro stability and content release properties of phosphatidylglyceroglycerol containing thermosensitive liposomes, Biochimica et Biophysica Acta (BBA)-Biomembranes, 1768 (2007) 2491-2499.
[54] G. Minotti, P. Menna, E. Salvatorelli, G. Cairo, L. Gianni, Anthracyclines: molecular advances and pharmacologic developments in antitumor activity and cardiotoxicity, Pharmacological reviews, 56 (2004) 185-229.
[55] T. Lu, W.J.M. Lokerse, A.L.B. Seynhaeve, G.A. Koning, T.L.M. ten Hagen, Formulation and optimization of idarubicin thermosensitive liposomes provides ultrafast triggered release at mild hyperthermia and improves tumor response, Journal of Controlled Release, 220 (2015) 425-437.
[56] F.B. Pruijn, J.R. Sturman, H.D.S. Liyanage, K.O. Hicks, M.P. Hay, W.R. Wilson, Extravascular transport of drugs in tumor tissue: effect of lipophilicity on diffusion of tirapazamine analogues in multicellular layer cultures, Journal of medicinal chemistry, 48 (2005) 1079-1087.
[57] T. Lu, T.L.M. ten Hagen, Inhomogeneous crystal grain formation in DPPC-DSPC based thermosensitive liposomes determines content release kinetics, Journal of Controlled Release, 247 (2017) 64-72.

[58] L. Li, T.L.M. ten Hagen, D. Schipper, T.M. Wijnberg, G.C. van Rhoon, A.M.M. Eggermont, L.H. Lindner, G.A. Koning, Triggered content release from optimized stealth thermosensitive liposomes using mild hyperthermia, Journal of Controlled Release, 143 (2010) 274-279.
[59] M.B. Yatvin, J.N. Weinstein, W.H. Dennis, R. Blumenthal, Design of liposomes for enhanced local release of drugs by hyperthermia, Science, 202 (1978) 1290-1293.
[60] M.H. Gaber, K. Hong, S.K. Huang, D. Papahadjopoulos, Thermosensitive sterically stabilized liposomes: formulation and in vitro studies on mechanism of doxorubicin release by bovine serum and human plasma, Pharmaceutical research, 12 (1995) 1407-1416.
[61] D. Needham, T.J. McIntosh, D.D. Lasic, Repulsive interactions and mechanical stability of polymer-grafted lipid membranes, Biochimica et Biophysica Acta (BBA)-Biomembranes, 1108 (1992) 40-48.
[62] X.-M. Liu, B. Yang, Y.-L. Wang, J.-Y. Wang, Photoisomerisable cholesterol derivatives as photo-trigger of liposomes: Effect of lipid polarity, temperature, incorporation ratio, and cholesterol, Biochimica et Biophysica Acta (BBA)-Biomembranes, 1720 (2005) 28-34.
[63] O.G. Mouritsen, M.J. Zuckermann, Model of interfacial melting, Physical review letters, 58 (1987) 389.
[64] D. Needham, J.-Y. Park, A.M. Wright, J. Tong, Materials characterization of the low temperature sensitive liposome (LTSL): effects of the lipid composition (lysolipid and DSPE–PEG2000) on the thermal transition and release of doxorubicin, Faraday discussions, 161 (2013) 515-534.
[65] P.C. Lyon, M.D. Gray, C. Mannaris, L.K. Folkes, M. Stratford, L. Campo, D.Y.F. Chung, S. Scott, M. Anderson, R. Goldin, Safety and feasibility of ultrasound-triggered targeted drug delivery of doxorubicin from thermosensitive liposomes in liver tumours (TARDOX): a single-centre, open-label, phase 1 trial, The Lancet Oncology, 19 (2018) 1027-1039.
[66] T. Tagami, M.J. Ernsting, S.-D. Li, Optimization of a novel and improved thermosensitive liposome formulated with DPPC and a Brij surfactant using a robust in vitro system, Journal of controlled release, 154 (2011) 290-297.
[67] L.H. Lindner, M.E. Eichhorn, H. Eibl, N. Teichert, M. Schmitt-Sody, R.D. Issels, M. Dellian, Novel temperature-sensitive liposomes with

prolonged circulation time, Clinical Cancer Research, 10 (2004) 2168-2178.
[68] B. Kneidl, M. Peller, G. Winter, L.H. Lindner, M. Hossann, Thermosensitive liposomal drug delivery systems: state of the art review, International journal of nanomedicine, 9 (2014) 4387.
[69] W.J.M. Lokerse, E.C.M. Kneepkens, T.L.M. ten Hagen, A.M.M. Eggermont, H. Grüll, G.A. Koning, In depth study on thermosensitive liposomes: optimizing formulations for tumor specific therapy and in vitro to in vivo relations, Biomaterials, 82 (2016) 138-150.
[70] L. Coderch, J. Fonollosa, M. De Pera, J. Estelrich, A. De La Maza, J.L. Parra, Influence of cholesterol on liposome fluidity by EPR: relationship with percutaneous absorption, Journal of Controlled Release, 68 (2000) 85-95.
[71] M. Hossann, T. Wang, M. Wiggenhorn, R. Schmidt, A. Zengerle, G. Winter, H. Eibl, M. Peller, M. Reiser, R.D. Issels, Size of thermosensitive liposomes influences content release, Journal of controlled release, 147 (2010) 436-443.
[72] J.P. May, M.J. Ernsting, E. Undzys, S.-D. Li, Thermosensitive liposomes for the delivery of gemcitabine and oxaliplatin to tumors, Molecular pharmaceutics, 10 (2013) 4499-4508.
[73] A.A. Manzoor, L.H. Lindner, C.D. Landon, J.-Y. Park, A.J. Simnick, M.R. Dreher, S. Das, G. Hanna, W. Park, A. Chilkoti, Overcoming limitations in nanoparticle drug delivery: triggered, intravascular release to improve drug penetration into tumors, Cancer research, (2012).
[74] P. Costa, J.M. Sousa Lobo, Evaluation of mathematical models describing drug release from estradiol transdermal systems, Drug development and industrial pharmacy, 29 (2003) 89-97.
[75] J. Dredán, I. Antal, I. Rácz, Evaluation of mathematical models describing drug release from lipophilic matrices, International journal of pharmaceutics, 145 (1996) 61-64.
[76] S. Dash, P.N. Murthy, L. Nath, P. Chowdhury, Kinetic modeling on drug release from controlled drug delivery systems, Acta Pol Pharm, 67 (2010) 217-223.
[77] G.A. Hughes, Nanostructure-mediated drug delivery, in: Nanomedicine in Cancer, Pan Stanford, 2017, pp. 47-72.
[78] H. Komatsu, S. Okada, Increased permeability of phase-separated liposomal membranes with mixtures of ethanol-induced interdigitated and

non-interdigitated structures, Biochimica et Biophysica Acta (BBA)-Biomembranes, 1237 (1995) 169-175.

Summary

Treatment of cancer has always been an important research focus. Novel promising therapies are continually proposed, but surgery, chemotherapy and radiotherapy are still the common treatment methods in the clinic. These therapies, especially chemotherapy, are often accompanied by severe side effects due to the non-selective nature of these treatment methods. The use of nano-carriers containing chemotherapeutic compounds is currently an important strategy to target drug delivery and therefore reduced side-effects in healthy tissue. However, limited tumoral accumulation of nano-carriers, insufficient drug release, and slow uptake of the drug by cancer cells all contribute to reduced efficacy of treatment. To deal with these limitations, thermosensitive liposomes (TSLs) are being developed that can be triggered to locally release cargo at the tumor site by mild local hyperthermia. The success of loading doxorubicin (DXR) in TSLs has shown improvement of tumor drug level, drawing increasing attention of research to formulate different doxorubicin-loaded TSLs for a better tumor response. However, not only the composition of the thermosensitive liposomal formulation, but also of the encapsulated drug needs to be considered together for a better cancer treatment. The aim of the work described in this thesis was to study and improve both thermosensitive liposomes and drug uptake by cancer cells.

Chapter 1 introduces the background of the study and the different topics involved in this thesis.

In **Chapter 2**, we developed a thermosensitive liposome formulation with a new drug idarubicin (IDA) encapsulated. Compared to the widely used DXR, IDA is relatively more hydrophobic and used for blood cancer in

the clinic currently. We optimized IDA-TSL formulation to obtain the lowest leakage at body temperature and optimal release at mild hyperthermia (42°C) *in vitro*. After that, *in vitro* cell tests and *in vivo* efficacy studies were conducted, showing improved tumor response compared to control groups. The results demonstrate the superior performance of IDA-loaded TSLs in treatment of cancer.

From a drug selection point of view, **Chapter 3** focuses on further investigation of IDA and DXR as encapsulated drugs in thermosensitive liposomes. Deep and quantitative comparison of IDA-TSL and DXR-TSL were performed with regard to *in vitro* release kinetics and cellular uptake and retention, *in vivo c*irculation and distribution, real time release profiles inside tumor during hyperthermia and post hyperthermia, intratumoral distribution and accumulation of released IDA and DXR, and efficacy in tumors. These results show that IDA-TSLs give more efficient delivery, release and tumor cellular uptake, we hypothesize to be a consequence of hydrophobicity, thus leading to a stronger tumor response compared to DXR-TSL.

From a TSL composition point of view, **Chapter 4** investigates the mechanism of rapid release of our thermosensitive liposomal composition. Carboxyfluorescein (CF) was used as a model drug loaded inside TSLs composd of different lipid ratios with and without cholesterol. We found that proper ratios of lipid composition produces maximal release portals in TSL membrane at phase transition temperature, which improves triggered release under mild hyperthermia. Besides, it is not suggested to add cholesterol due to the resulting reduced thermosensitivity.

Nowadays, thermosensitive liposome release profiles are described by First-order mathematical models, which is used to depict the conventional, non-thermosensitive liposome release. There is to our knowledge no proper mathematical model to describe thermosensitive liposomal release behaviors. Hence, in **Chapter 5** we searched for a proper release equation to describe the unique triggered release during phase transition of

thermosensitive liposomes. After fitting with several commonly used release models, we established an empirical equation, which shows an optimal fitting describing the effect of release at phase transition temperature and non-phase transition temperature as well.

Chapter 6 discusses the results of the studies in relation to the current status of mild hyperthermia mediated thermosensitive liposomes for drug delivery, and proposes the advice that selection of encapsulated drug and TSL formulation need to be considered based on a rationale that produces optimal tumoral delivery.

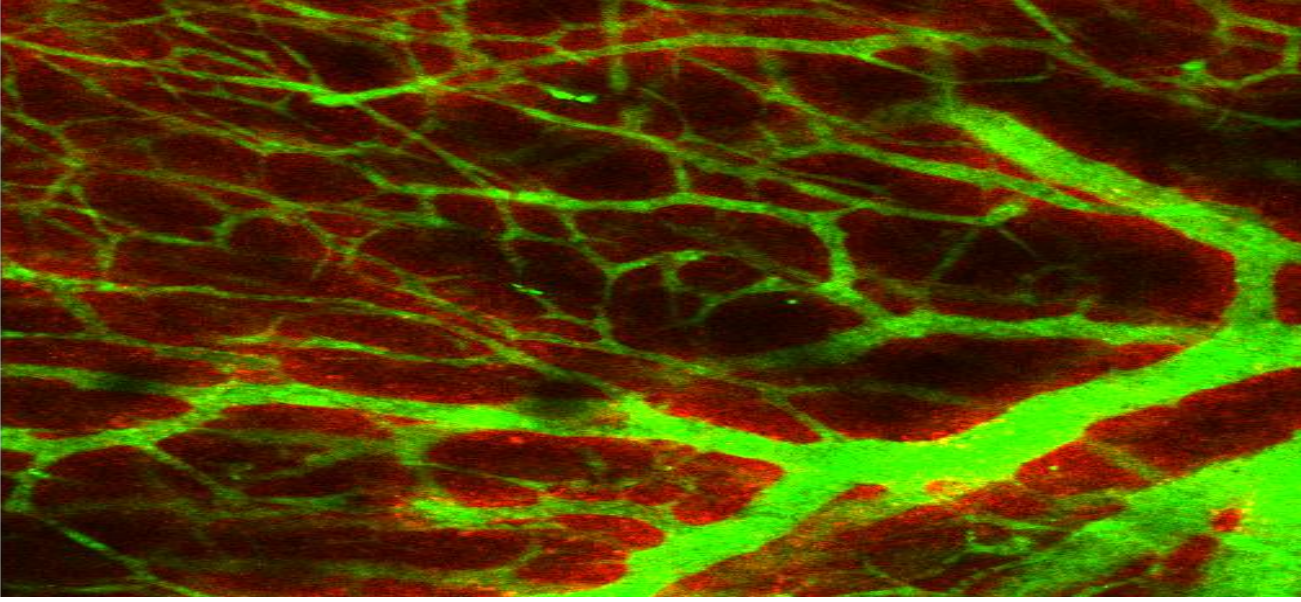

Chapter 7

Dutch summary

Samenvatting

De behandeling van kanker is altijd een belangrijke focus van onderzoek geweest. Nieuwe veelbelovende therapieën worden voortdurend voorgesteld, maar chirurgie, chemotherapie en radiotherapie zijn nog steeds de belangrijkste behandelingsmethoden in de kliniek. Deze therapieën, vooral chemotherapie, gaan vaak gepaard met ernstige bijwerkingen vanwege het niet-selectieve karakter van deze behandelmethoden. Het gebruik van nanodragers die chemotherapeutische verbindingen bevatten, is momenteel een belangrijke strategie voor gerichte medicijnafgifte en daarom verminderde bijwerkingen in gezond weefsel. Beperkte tumorale accumulatie van nanodragers, onvoldoende geneesmiddelafgifte ervan en langzame opname van het geneesmiddel door kankercellen dragen allemaal bij aan een verminderde werkzaamheid van tumorbehandeling. Om met deze beperkingen om te gaan, worden thermogevoelige liposomen (TSLs) ontwikkeld die kunnen worden geactiveerd om plaatselijk lading in de tumor af te geven door milde lokale hyperthermie. Het succes van TSLs gevuld met doxorubicine (DXR) heeft een verbetering in intratumorale accumulatie laten zien. Hierdoor is in vervogonderzoek naar nieuwe formuleringen voornamelijk doxorubicine gebruikt. Wij argumenteren dat niet alleen de keuze van de thermogevoelige liposomale formulering, maar ook van het ingekapselde medicijn moet samen worden overwogen voor een betere kankerbehandeling. Het doel van het werk onderzoek beschreven in dit proefschrift was het bestuderen en verbeteren van thermogevoelige liposomen om opname van geneesmiddelen door kankercellen te verbeteren.

Hoofdstuk 1 introduceert de achtergrond van de studie en de verschillende onderwerpen die bij dit proefschrift zijn betrokken.

In hoofdstuk 2 ontwikkelden we een thermogevoelige liposoomformulering met een nieuw medicijn idarubicine (IDA) ingekapseld. Vergeleken met de veel gebruikte DXR is IDA relatief meer hydrofoob en wordt het momenteel gebruikt voor de behandeling van bloedkanker in de kliniek. We hebben de IDA-TSL-formulering geoptimaliseerd om de laagste lekkage bij lichaamstemperatuur en optimale afgifte bij milde hyperthermie (42 °C) *in vitro* te verkrijgen. Daarna werden *in vitro* en *in vivo* studies uitgevoerd, die een verbeterde tumorrespons aantoonden voor IDA-TSL in vergelijking met DXR-TSL en controlegroepen. De resultaten demonstreren de haalbaarheid van het formuleren van de nieuwe met IDA beladen TSL's om tumor te behandelen.

Vanuit het oogpunt van drugkeuze richt hoofdstuk 3 zich op verder onderzoek van IDA en DXR als geneesmiddelen ingekapseld in thermogevoelige liposomen. Diepe en kwantitatieve vergelijking van IDA-TSL en DXR-TSL werd uitgevoerd met betrekking tot hun *in vitro* afgiftekinetiek en cellulaire opname en retentie, *in vivo* circulatie en distributie, real-time afgifteprofielen in tumor tijdens hyperthermie en post-hyperthermie, intratumorale distributie en accumulatie van afgegeven IDA en DXR en werkzaamheid in tumoren. Deze resultaten tonen aan dat IDA-TSL een efficiëntere aflevering, afgifte en tumorcellulaire opname, mogelijk als gevolg van hydrofobiciteit, verschaft, hetgeen aldus leidt tot een sterkere tumorrespons in vergelijking met DXR-TSL.

Vanuit een gezichtspunt van TSL-samenstelling, onderzoekt Hoofdstuk 4 het mechanisme van snelle afgifte van onze thermogevoelige liposomale samenstelling. Carboxyfluoresceïne (CF) werd gebruikt als een modelgeneesmiddel geladen in TSL samengesteld uit verschillende lipideverhoudingen, met en zonder cholesterol. We zagen dat de juiste verhoudingen van de lipidensamenstelling maximale afgifteportalen in het TSL-membraan bij de fase-overgangstemperatuur produceren, wat de geactiveerde afgifte onder milde hyperthermie verbetert. Bovendien

wordt toevoeging van cholesterol afgeraden aangezien hiermee de thermosensibiliteit vermindert.

Tegenwoordig worden thermogevoelige liposoomafgifteprofielen beschreven door wiskundige modellen van de eerste orde die worden gebruikt om afgifteprofielen te beschrijven van conventionele niet-thermisch gevoelige liposomen. Er is, zo ver wij weten, geen goed wiskundig model beschikbaar om afgifte van stoffen door thermogevoelige liposomen te beschrijven. Daarom hebben we in hoofdstuk 5 gezocht naar een goede vergelijking om deze unieke, getriggerde afgifte tijdens faseovergang van warmtegevoelige liposomen te beschrijven. Na veelgebruikte afgiftemodellen te hebben getoets, hebben we een empirische vergelijking opgesteld, die een optimaal passend fit laat zien voor afgifte bij faseovergangstemperatuur en niet-faseovergangstemperatuur.

Hoofdstuk 6 bespreekt de resultaten van de studies hier gepresenteerd met betrekking tot de huidige status van temperatuurgevoelige nano-carriers. Tevens wordt de conclusie bereikt dat naast het vinden van nieuwe formuleringen ook de keuze van het chemotherapeuticum moet worden bepaald met de realisatie dat optimale afgifte, verdeling in de tumor en opname door tumorcellen leidend zijn.

Appendics

Acknowledgement/Dankwoord

List of publication

Portfolio

CV

Acknowledgements/Dankwoord

It is with both joy and sentiment do I start writing this very last but not least chapter of my thesis. Looking back, this long journey for PhD over the past five years has been exceptional and filled with peaks and valleys. I would like to convey my greatest gratitude to people who walked with me during this memorable journey. The work presented in this thesis would never be possible without your support and help.

Dear **Prof. Dr. Adriaan Houtsmuller**, my promotor, thank you for all the remarks and suggestions during our paper and thesis discussion. You became my promotor when I was in third year, but I really enjoy discussion with you. Every time when I come to your office, you always take some time talking with me no matter how busy you are at that moment. Especially in the last stage of my PhD, I came to you with anxiety often, your patience and encouragement always calm me down.

Dear **Dr.Timo ten Hagen**, my supervisor, thank you so much for giving me the opportunity to join your research group. I still remembered how you interviewed me in February 2013 via Skype. That was my first time to have a Skype meeting and I was still a bit worried about my listening for English at that time. You slowed down your speed and made your voice more clear to let me understand easily. Working with you for the past five years, we are not always happy with each other all the time. Sometimes we had lots of debates, disagreements and even quarrels. I suppose that I am not the easiest PhD student to supervise. But I have learned so much about how to be a critical scientist and how to do proper research from you. I always admire your broad and deep knowledge in lots of things.Also thank you for giving me all the freedom to do any research. I fully appreciate everything you did for me, your support, your encouragement and your jokes that let me walk so far during past five years working with you.

Dear **Ann**, thank you for sharing your valuable experimental experience and suggestion to me when I just joined this group 5 years ago. Your passion and patience to scientific research impressed me and let me learned a lot. I admire you can speak three different languages, and now you are learning Chinese as well. Hope you enjoy it. 加油 (jia you)!

Dear **Joost**, thank you for your kind and patient help and teaching me on all animal experiments before you left. You are really a skilled technician and of course a very nice person. Hope you enjoy your work in new environment.

Prof. Dr. Dieter Haemmerich, I am glad to meet you in the Orlando meeting in 2015. Thank you for your kind help for the imaging analysis of our paper.

Dr. Gert van Cappellen and **Dr. Gert-Jan Kremers**, thank you so much for your help and suggestion to solve different kinds of confocal microscope related problems and issues I met during my experiments.

Mesha, we have known each other for quite long time. Thank you for giving me advices and share experiences to me when I was a green hand in this group. I really enjoy the time working with you. It seems you spent very long time on PhD, and I understand you met lots of difficulties in your life. But you are one of the most tough female I ever see and now you are a great mom and wife as well. Hope you can finish your PhD and start a new life soon.

Sara, it was very nice you joined this group for a post-doc in 4 years ago. I still remember those days that we both were busy with making liposomes day-in and day-out. You always like talking different things in your life and I also enjoy listening to your family stories on that big farm in Spain. These full of flavor of life stories are very useful to buffer some headache-time induced by the experiments. Thank you for introducing me to Spanish culture and of course, your food.

Reza Amin, right now I still cannot pronounce your religion name easily, so let me just call you Reza. It is so nice to meet you. You do have quite a lot experience in these liposome stuff. And I really like discussing and debating with you about all kinds of scientific and daily-life questions. Now, as you said, you just get your new “toy” - HPLC, so just enjoy it!

Liu Hui, we have also known each other for quite long time. It is very nice that every time you can come to restaurant with me after a hard day’s work, and I just do not want to cook myself. Thank you for the time we discussed experimental projects and shared valuable experience. Doing PhD here is not an easy thing, but you do not need to worry too much, you will make it definitely. I am done, and you, will be there soon.

Lous and **Wenqiu**, you both just started your PhD work in our group, I heard you are doing quite well so far, that is a very sign for your research and life here. Best wishes for your PhD work.

I also want to express my thanks to all Chinese friends I met in Rotterdam, thank you all for making my stay here so pleasant and thank you for the fantastic dinners and fun with you guys. 好哥们吴斌，那会一起来的荷兰，眼看着你从连米都不会淘进化到现在出神入化的厨艺，这真不科学！？谢谢这么多年来对我关心，支持和帮助。而你也即将毕业，很高兴你已经找到了理想的工作和有爱的女朋友，祝早日成婚。高雅，自嘲女汉子的你其实一直是大家心中最仗义的软妹子，很高兴你和大卫开启了人生新篇章，也非常感谢一直以来对我的帮助和分享。波哥，一口乡音的科研狂人，谢谢当年组织活动带我们这些后辈融入这边生活。若愚，很高兴能刚来荷兰就认识你，也非常感谢在我毕业的繁忙期，给了我很多建议和帮助。长斌，我让惊叹的是你的交际圈，加上你的学识，不愧于北半球一哥的称号，感谢曾经那些一起吃饭一边讨论科研吐槽实验的 MC 加班日子。平真，你也是我来 MC 早期认识的人，平时一副风轻云淡的样子，没想到做起实验也是极度疯狂，谢谢每次聚餐和你一起聊科研和未来的时光。孙伟，谢谢和你既是 MC 同事也是室友，谢谢曾经让我蹭饭的日子，也因为你我才能认识后来你们专业那么多优秀的中国同学。刘老师和温蓓，谢谢你们曾经组织很多活动邀请我们参加，让我知道了狼人杀，勾级等桌游。谢谢热心的小俊的经验分享，舟桥和潇磊学长的组织活动，谢谢和展民莹

颖夫妇，黄玲，婉露，文辉，徐磊，王文世，超平，文浩瑶瑶夫妇，国影唐寅夫妇，忆冰，余诺，马骅，李娟，世豪，这些年的交流分享和帮助建议，谢谢能认识这些优秀的前辈学长：宝月，恒哥，凯英，刘静静，梁秋实，辛闻，魁魁，李杉，艺瑾，占曙光，海燕，轶林... 也谢谢认识了很多出色的后辈同学：蔡烨，王璐，杨琴，徐笑非，孙媛媛，金銮，满芝，邹润雨，陈忠丽... 还要感谢曾经一起玩的来自不同城市的伙伴，高文，蔺博超，杜广盛，陈思，丹莉，Betty, 二姐，刘洋，张啸林... 同时也谢谢曾经一起的那些有趣又有爱的室友们：玉婷，经常帮我炖汤的小张和秦菁，琪琪，陈旖旎，吴迪，简怡宇，陈希恺，郭鸿儒... 很荣幸能在这遇到你们每一个人，感谢你们的出现让我在异国的求学生活变得珍贵而难忘，也祝愿大家未来幸福安好，我们以后再聚！

感谢国内的小伙伴对我在外的关心和支持，谢谢蕾姐，班长，李卫，王珂以及太多无法在此一一列出名字的伙伴，谢谢你们，愿我们的友谊长存！

感谢舅舅舅妈，爷爷奶奶，姑姑们对我这些年在外的关心和支持，下次回去一定和你们见面！

Finally, I have my parents to thank for their support and love they have been giving over the years. 亲爱的老爸老妈， 从我硕士开始就离家，到现在差不多有九个年头了，我们一直聚少离多， 非常感谢你们一直对我的包容，理解，支持，安慰和关心。在外的独自求学之路，并不容易，很多时候，我无需多言你们就能理解我的处境，你们的鼓励与支持总让我有信心看淡挫折，继续走下去。我知道我不论在哪，不论遇到什么事，你们，永远是我最坚强的后盾！等我毕业，等我回来！

List of publications

1. ***Lu T**, Lokerse W, Seynhaeve A, Koning G, ten Hagen T**.* Formulation and optimization of idarubicin thermosensitive liposomes provides ultrafast triggered release at mild hyperthermia and improves tumor response. *Journal of Controlled Release, 2015*

2. ***Lu T***, ten Hagen T**.* Inhomogeneous crystal grain formation in DPPC-DSPC based thermosensitive liposomes determines content release kinetics. *Journal of Controlled Release* , *2017*

3. ***Lu T**, Haemmerich D, Liu H, Seynhaeve A, van Rhoon G, Houtsmuller A, ten Hagen T**.* Thinking out nanoparticle: Externally triggered smart drug delivery systems demand chemotherapeutics with kinetics superior for local delivery. *Under revision*

4. ***Lu T***, ten Hagen T**.* A novel kinetic model to describe the release of trigger-responsive drug delivery systems. *Submitted.*

5. Liu H, ***Lu T**, Kremers G, Seynhaeve A, ten Hagen T**.* A simple reproducible and inexpensive microcarrier-based spheroid 3D invasion assay to monitor cell movement in extracellular matrix in vitro. *Submitted*

6. *Salvage J*, Smith T,* ***Lu T**, Sanghera A, Standen G, Tang Y, Lewis A.* Synthesis, characterisation, and in vitro cellular uptake kinetics of nanoprecipitated poly(2-methacryloyloxyethyl phosphorylcholine)-b-poly(2-(diisopropylamino)ethyl methacrylate) (MPC-DPA) polymeric nanoparticle micelles for nanomedicine applications. *Applied Nanoscience, 2015*

7. *Yin H#,* ***Lu T**#, Liu L, Lu C**.* Preparation, characterization and application of a novel biodegradable macromolecule: carboxymethyl zein. *Int. J. Biol. Macromol. 2015*

8. *Sun Y, Zhang X,* ***Lu T**, Yuan Y, Ding Q, Lu C*,* A study on the PK and BA profiles in the mouse body for leonurine O/O microemulsion with

determination by the LC-MS/MS method. *Eur. J. Drug Metab. Pharmacokinet. 2016*

9. *Zhou A#,* ***Lu T****#, Wang L, Lu C*,Wang L, Wan M, Wu H**. Lymphatic transport of puerarin occurs after oral administration of different lipid-based formulations to unconscious lymph duct-cannulated rats. *Pharmaceut. Dev. Tech. 2013*

10. *Lin T, Lu C*, Zhu L,* ***Lu T***. The biodegradation of zein in vitro and in vivo and its application in implants. *AAPS PharmSciTech. 2011*

*# co-first author,*co-corresponding author*

PHD PORTFOLIO

Summary of PhD training and teaching

Name:	Tao Lu
Erasmus MC department:	Department of Surgery
Research School:	Molecular Medicine
PhD period:	Nov. 2013- Dec. 2018
Promotor:	Prof. Dr. Adriaan B. Houtsmuller
Co-promotor and supervisor:	Dr. Timo L.M. ten Hagen

Courses	**Year**	**ECTS**
Animal Experimentation (Article 9)	2014	3
Biomedical research Techniques	2015	1.5
Translational Imaging Workshop by AMIE	2015	1.4
English Biomedical Writing and Communication (10 weeks)	2017	3
Scientific Integrity	2014	0.3
Microscopic Image Analysis: From Theory to Practice	2014	0.8
Photoshop and Illustrator CS5 Workshop	2014	0.3
Research management for PhD-students	2014	1

Conferences	**Year**	**ECTS**
KWF Hyperthermia workshop, Amsterdam, NL	2013	0.2
Annual Meeting of the Society of Thermal Medicine, Orlando, US *Oral presentation*	2015	1

Liposome Advances: Progress in Drug and Vaccine Delivery, London, UK *2 Posters*	2015	1
ICONAN 2018 Nanomedicine and Nanobiotechnology, Rome, Italy *Oral presentation*	2018	1
Lab Science Day Meeting, Rotterdam, NL. *Oral presentation*	2013	0.2
Lab Science Day Meeting, Rotterdam, NL. *Oral presentation*	2014	0.2
Lab Science Day Meeting, Rotterdam, NL. *Oral presentation*	2015	0.2
Lab Science Day Meeting, Rotterdam, NL. *Oral presentation*	2016	0.2
Lab Science Day Meeting, Rotterdam, NL. *Oral presentation*	2017	0.2
JNI oncology lecture, Rotterdam, NL. *Oral presentation*	2015	1
Surgery Staff Dag, Rotterdam, NL	2014	0.2
Surgery Staff Dag, Rotterdam, NL	2015	0.2
Surgery Staff Dag, Rotterdam, NL	2016	0.2
Surgery Staff Dag, Rotterdam, NL *Oral presentation*	2017	1
Sophia Research Day, Rotterdam, NL *Oral presentation*	2017	1
MolMed day, Rotterdam, NL *Posters*	2015	0.3
MolMed day, Rotterdam, NL *Oral presentation*	2017	1
Journal Club	2013 - 2018	2

Teaching and supervision:	**Year**	**ECTS**
6 months internship and training: Prashna Bdhaggoe	2016	2
6 months internship and training: William Nijgh	2017	2
4-week internship for Nano-biology: 2 bachelor students	2015	2
4-week internship for Nano-biology: 2 bachelor students	2016	2

Curriculum Vitae

Education:

2007/09 – 2011/07
BSc in Pharmacy at Anhui Medical University, Hefei, China.
2011/09 – 2013/02
MSc in Industrial Pharmaceutical Sciences at University of Brighton, Brighton, UK.
2013/11 – 2018/04
PhD in Nanomedicine for tumor treatment at Department of Surgery, Erasmus MC, Rotterdam, the Netherlands.
2018/04 – 2018/12
Post doc in Nanomedicine for tumor treatment at Department of Surgery, Erasmus MC, Rotterdam, the Netherlands.
2019/01 – present
Post doc at Faulty of Sciences and Technology at Twente University, Enschede, the Netherlands.

Skills:

Biomaterial-based nanosized drug carrier development, optimization and characterization
Intravital imaging (CLSM), including 1) live animal drug delivery and release imaging, 2) live intracellular drug uptake and track
Animal handling (holding Dutch Article 9 animal license), including i.v./i.p./s.c. injection, tumor implantation, window chamber mouse model operation
UV-spectrophotometry & fluorospectrophotometry
High Performance Liquid Chromatography
Differential scanning calorimetry
Dynamic light scattering (Zetasizer)
Cell culture and cytotoxicity
Tissue section and staining

Awards:

1) Scholarship of Anhui Medical University, 2008 & 2010
2) Santander International Masters Scholarship and Huxley Scholarship, UK, 2012
3) New Investigator Award Winner at STM (Society for Thermal Medicine),Orlando,US, 2015
4) Best Oral Presentation Award Winner for ICONAN nanomedicine and nanobiotechnology,Rome,Italy, 2018

Memberships:

Student member of STM in 2015-2017

Junior Scholar in training member of RRS in 2015

Member of CRS BeNeLux & France Local Chapter from 2019

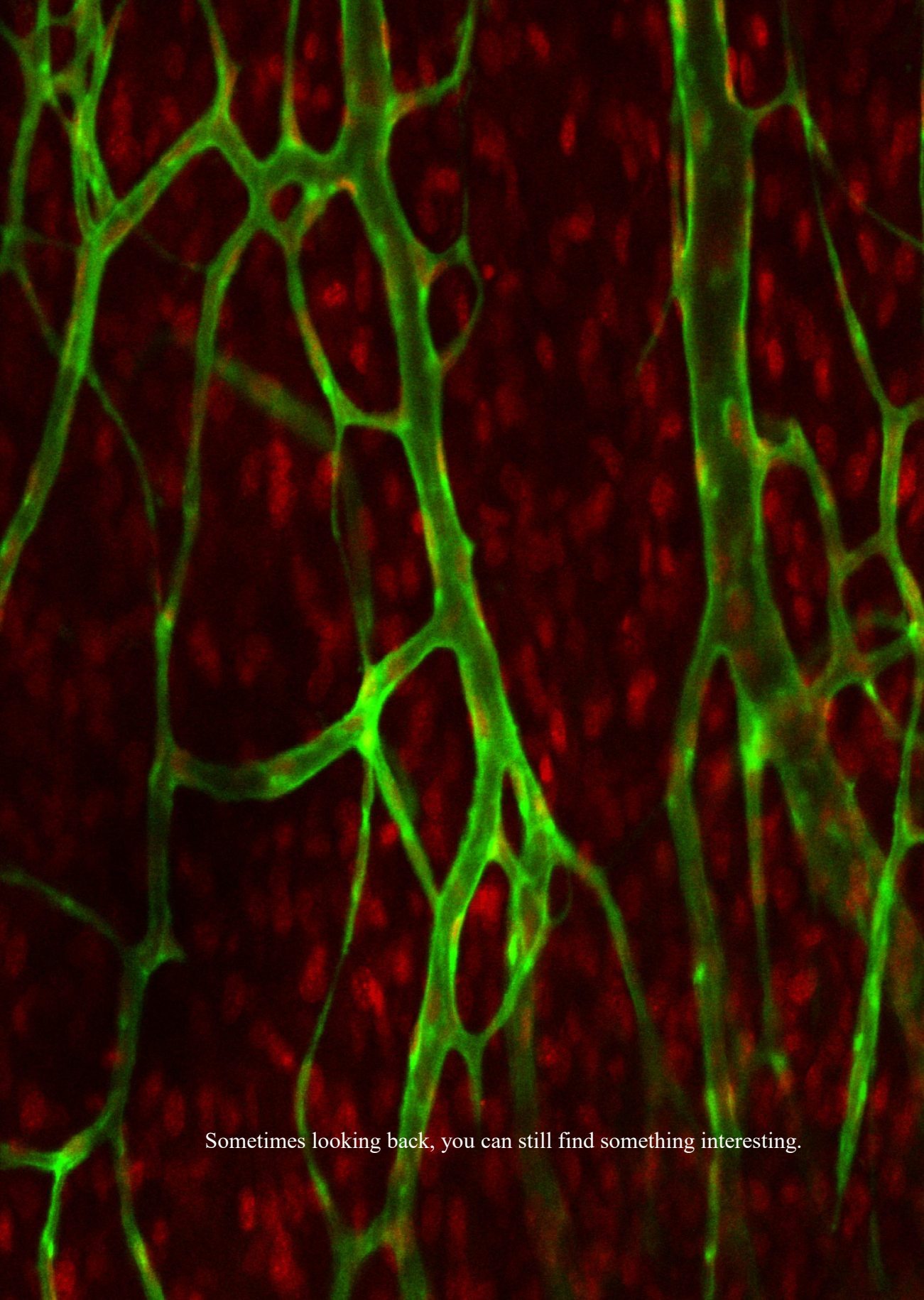
Sometimes looking back, you can still find something interesting.